



**PREPARATION OF HEMOGLOBIN IMPRINTED  
SURFACE PLASMON RESONANCE BIOSENSORS**

**HEMOGLOBİN BASKILANMIŞ YÜZEY PLAZMON  
REZONANS BİYOSENSÖRLERİN HAZIRLANMASI**

**YEŞEREN SAYLAN**

**Prof. Dr. ADİL DENİZLİ**

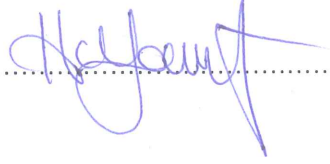
**Supervisor**

Submitted to Graduate School of Science and Engineering Hacettepe University as a  
Partial Fulfillment to the Requirements for the Award of the Degree of Doctor of  
Philosophy in Chemistry

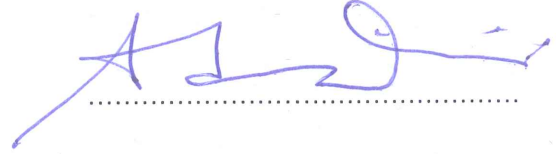
2017

This work named 'Preparation of Hemoglobin Imprinted Surface Plasmon Resonance Biosensors' by YEŞEREN SAYLAN has been approved as a thesis for Degree of **DOCTOR OF PHILOSOPHY IN CHEMISTRY** by the below mentioned Examining Committee Members.

Prof. Dr. Handan YAVUZ ALAGÖZ  
Head



Prof. Dr. Adil DENİZLİ  
Supervisor



Assoc.Prof. Dr. Bilgen OSMAN  
Member



Assoc. Prof. Dr. Nilay BERELİ  
Member



Assist. Prof. Dr. Fatma YILMAZ  
Member



This thesis has been approved as a thesis for the Degree of **DOCTOR OF PHILOSOPHY IN CHEMISTRY** by Board of Directors of the Institute for Graduate School of Science and Engineering.

Prof. Dr. Menemşe GÜMÜŞDERELİOĞLU  
Director of the Institute of  
Graduate School of Science and Engineering

## YAYINLAMA VE FİKRİ MÜLKİYET HAKLARI BEYANI

Enstitü tarafından onaylanan lisansüstü tezimin/raporumun tamamını veya herhangi bir kısmını, basılı (kağıt) ve elektronik formatta arşivleme ve aşağıda verilen koşullarla kullanıma açma iznini Hacettepe üniversitesine verdiğimi bildiririm. Bu izinle Üniversiteye verilen kullanım hakları dışındaki tüm fikri mülkiyet haklarım bende kalacak, tezimin tamamının ya da bir bölümünün gelecekteki çalışmalarda (makale, kitap, lisans ve patent vb.) kullanım hakları bana ait olacaktır.

Tezin kendi orijinal çalışmam olduğunu, başkalarının haklarını ihlal etmediğimi ve tezimin tek yetkili sahibi olduğumu beyan ve taahhüt ederim. Tezimde yer alan telif hakkı bulunan ve sahiplerinden yazılı izin alınarak kullanması zorunlu metinlerin yazılı izin alarak kullandığımı ve istenildiğinde suretlerini Üniversiteye teslim etmeyi taahhüt ederim.

- Tezimin/Raporumun tamamı dünya çapında erişime açılabilir ve bir kısmı veya tamamının fotokopisi alınabilir.**

(Bu seçenekle teziniz arama motorlarında indekslenebilecek, daha sonra tezinizin erişim statüsünün değiştirilmesini talep etmeniz ve kütüphane bu talebinizi yerine getirirse bile, tezinin arama motorlarının önbelleklerinde kalmaya devam edebilecektir.)

- Tezimin/Raporumun 20.06.2019 tarihine kadar erişime açılmasını ve fotokopi alınmasını (İç Kapak, Özet, İçindekiler ve Kaynakça hariç) istemiyorum.**

(Bu sürenin sonunda uzatma için başvuruda bulunmadığım takdirde, tezimin/raporumun tamamı her yerden erişime açılabilir, kaynak gösterilmek şartıyla bir kısmı ve ya tamamının fotokopisi alınabilir)

- Tezimin/Raporumun ..... tarihine kadar erişime açılmasını istemiyorum, ancak kaynak gösterilmek şartıyla bir kısmı veya tamamının fotokopisinin alınmasını onaylıyorum.**

- Serbest Seçenek/Yazarın Seçimi**

20 /06 /2017



Yeşeren Saylan

*“Hayatta en hakiki mürşit ilimdir.”*  
*“Science is the most reliable guide in a life.”*  
**Mustafa Kemal ATATÜRK**

## ETHICS


In this thesis study, prepared in accordance with the spelling rules of Institute of Graduate Studies in Science of Hacettepe University.

I declared that

- all the information and documents have been obtained in the base of the academic rules,
- all audio-visual and written information and results have been presented according to the rules of scientific ethics,
- in a case of using other works, related studies have been cited in accordance with the scientific standards,
- all cited studies have been fully referenced.

I did not do any distortion in the data set and any part of this thesis has not been presented as another thesis study at this or any other university.

20.06.2017

  
Yeşeren SAYLAN

## **ABSTRACT**

# **PREPARATION OF HEMOGLOBIN IMPRINTED SURFACE PLASMON RESONANCE BIOSENSORS**

**Yeşeren SAYLAN**

**Doctor of Philosophy, Department of Chemistry**

**Supervisor: Prof. Dr. Adil DENİZLİ**

**June 2017, 101 pages**

Proteins hold many pivotal structural, functional and organization features and closely associate with the other macromolecules such as lipids and carbohydrates to generate larger and more complex units in cellular machinery. Researchers have been focused on discovering fundamental properties of proteins, and realized that they are also one of the major indicators and predictors in disease stages, as well as recent studies pointed out that their structure, concentration, and even, orientation are crucial for facilitating cellular machinery. Due to their multiple roles in cell functionality and structure, one of the most attractive arena to investigate the significance of proteins is to detect small biological units for diagnosing diseases. For instance, hemoglobin --an iron carrying protein in red blood cells-- transports oxygen and carbon dioxide around the human body and also maintains the acid-base balance in the blood. In clinical practice, hemoglobin concentrations are closely correlated with several diseases and health status, including thalassemia, anemia, leukemia, heart disease, and excessive

loss of blood. Sensitive and accurate detection platforms will have potentially create new avenues to monitor the concentrations of such vital protein marker, hemoglobin, in the early detection and highly reliable prediction of disease.

Surface plasmon resonance technology has been considerably utilized to detect protein biomarkers, eukaryotic cells, bacteria, and viruses for diagnosis purposes. This sensing platform provides excellent optical modality to measure the changes in refractive index at the close vicinity of the metal surface. Compared with other sensitive biosensing modalities, the surface plasmon resonance biosensors holds multiple advantageous, including real-time and label-free analysis, high dual sensing modality (surface and bulk sensitivity), short assay time, independent of small changes in temperature and surface oscillations, low-cost assay, and multiplexing. Besides these prominent features, the surface plasmon resonance technology cannot only potentially be integrated with different surface sensitive tools, and it also enables versatile surface modifications that can easily be tailored to multiplexed detection.

Molecular imprinting method, one of a fascinating surface modification techniques, utilizes molecules as templates to create cavities for recognition of targets in the polymeric matrix. This method provides a broad range of versatility to imprint targets with different molecular size, three dimensional structure, and physicochemical properties. In contrast to the complex and time-consuming laboratory surface modification methods, this method offers a rapid, sensitive, inexpensive, easy-to-use, and selective approach for the diagnosis, screening and monitoring disorders. Owing to high selectivity, physical and chemical robustness, high stability, low-cost and reusability of this method, molecularly imprinted polymers have become very attractive and been applied in many fields, especially biosensors, diagnosis, and environmental monitoring.

In this study, a molecularly imprinted surface plasmon resonance biosensor was designed to detect hemoglobin as a model protein marker. First, hemoglobin:acrylamide pre-complex was prepared with template and monomer



mixture, and the cross-linker (methylenebis acrylamide) was applied to the pre-complex mixture to form a final mixture for polymerization. Followed by addition an initiator and activator (ammonium persulfate and tetramethyl ethylenediamine) pair to the final mixture, the monomer mixture was then used to decorate to the surface plasmon resonance biosensor surfaces. By employing spin coating technique, the monomer solution was uniformly distributed on the surface plasmon resonance biosensor surfaces. The polymerization was carried out under by photo-polymerization method. At the end of the polymerization, the unreacted monomers and impurities were removed and dried at room temperature. The hemoglobin imprinted surface plasmon resonance biosensor was characterized by Fourier transform infrared spectroscopy-attenuated total reflectance, atomic force microscope, an ellipsometer, and contact angle measurements. The hemoglobin imprinted surface plasmon resonance biosensor was tested for real-time detection of hemoglobin from hemoglobin solutions that have different hemoglobin concentrations. The selectivity and reusability performance of the hemoglobin imprinted surface plasmon resonance biosensor was also investigated.

In addition, the microfluidic-integrated surface plasmon resonance biosensors were also prepared for real-time hemoglobin detection by using different layers that are polymethyl methacrylate, double sided adhesive and gold coating substrate. After the different modification steps, the microfluidic-integrated surface plasmon resonance biosensors interacted with different hemoglobin concentration solutions. Finally, the equilibrium and adsorption isotherm models of interactions between hemoglobin solutions and two different surface plasmon resonance biosensors were determined.

**Keywords:** Biosensor, hemoglobin, molecular imprinting, surface plasmon resonance.

## ÖZET

# HEMOGLOBİN BASKILANMIŞ YÜZEY PLAZMON REZONANS BİYOSENSÖRLERİN HAZIRLANMASI

**Yeşeren SAYLAN**

**Doktora, Kimya Bölümü**

**Tez Danışmanı: Prof. Dr. Adil DENİZLİ**

**Haziran 2017, 101 sayfa**

Proteinler yapısal, işlevsel ve organizasyon olmak üzere birçok temel özelliklere sahiptirler ve hücrenel makinelerde daha büyük ve daha karmaşık birimler oluşturmak için lipidler ve karbonhidratlar gibi diğer makromoleküllerle yakından ilişkilidirler. Araştırmacılar, proteinlerin temel özelliklerini keşfetme üzerine yoğunlaşmış ve hastalıkların farklı aşamalarında önemli belirteçlerden biri olduklarını farkına varmışlardır. Son zamanlarda yapılan çalışmalarla yapılarının, derişimlerinin ve hatta yönelimlerinin hücrenel etkileşimleri kolaylaştırmada çok önemli oldukları keşfedilmiştir. Hücrenin işlevselliğinde ve yapısındaki çok sayıda rolünden dolayı, proteinlerin önemini araştıran en çekici alanlardan biri, hastalıkların teşhisi için biyolojik birimleri tespit etmektir. Örneğin, hemoglobın -kırmızı kan hücrelerinde demir taşıyan protein- insan vücudunda oksijen ve karbon dioksit taşır. Aynı zamanda kandaki asit-baz dengesini de muhafaza eder. Klinik uygulamalarda, hemoglobın derişimleri, talasemi, anemi, lösemi, kalp rahatsızlığı ve aşırı kan kaybı gibi çeşitli hastalıklar ve sağlık durumu ile yakından ilişkilidir. Hassas ve doğru algılama platformları, hastalıkların erken teşhisi ve

güvenilir bir şekilde öngörülmesinde böylesi hayati önemi olan protein belirteci hemoglobinin derişimlerini izlemek için yeni yollar yaratacaktır.

Yüzey plazmon rezonans teknolojisi, protein belirteçlerini, ökaryotik hücreleri, bakteri ve virüsleri tanısal amaçlı algılamak için oldukça yaygın kullanılan bir teknolojidir. Bu algılama platformu, metal yüzeyin yakınında meydana gelen kırılma indeksindeki deęişimleri ölçmek için mükemmel bir optik yöntem sağlar. Yüzey plazmon rezonans biyosensörler, dięer hassas algılama yöntemleri ile karşılaştırıldığında, sıcaklık ve yüzey salınımlarındaki küçük deęişikliklerden bağımsız olarak, gerçek zamanlı ve etiketsiz analiz, yüksek algılama alanı (yüzey ve hacim duyarlılığı), kısa analiz süresi ve düşük maliyetli analiz gibi bir çok avantaja sahiptir. Bu belirgin özelliklerin yanı sıra, yüzey plazmon rezonans teknolojisi sadece potansiyel olarak farklı yüzey hassas cihazları ile entegre olamaz. Ayrıca çoklu algılama için kolayca uyarlanabilen çok yönlü yüzey deęişikliklerine de olanak sağlar.

Mükemmel bir yüzey modifikasyon tekniklerinden biri olan moleküler baskılama yöntemi, polimerik matriksteki hedeflerin tanımlanması için boşluklar oluşturmak için molekülleri bir kalıp olarak kullanır. Bu yöntem, farklı yük, üç boyutlu yapı ve fizikokimyasal özelliklere sahip hedefleri baskılamak için geniş bir alan sunar. Bu yöntem, karmaşık ve zaman alıcı laboratuvar yüzey modifikasyon yöntemlerinin aksine, hastalıkların teşhis, tarama ve izleme için hızlı, hassas, ucuz, kullanımı kolay ve seçici bir yaklaşım sunar. Yüksek seçicilik, fiziksel ve kimyasal dayanıklılık, yüksek kararlılık, düşük maliyet ve tekrar kullanılabilirlik gibi özellikleri sayesinde, moleküler baskılanmış polimerler çok cazip hale gelmiştir ve birçok alanda, özellikle biyosensörlerde, teşhislerde ve çevresel izlemelerde uygulanır.

Bu çalışmada, hemoglobini tayini için moleküler baskılanmış yüzey plazmon rezonans biyosensörü tasarlanmıştır. İlk olarak, hemoglobin:akrilamid ön-kompleksi kalıp molekül ve monomer karışımı ile hazırlanmış ve daha sonra metilenbis akrilamid çapraz bağlayıcısı, ön-kompleks karışımına polimerizasyon için bir nihai karışım oluşturmak üzere eklenmiştir. Ek olarak, nihai karışıma bir başlatıcı ve aktiveleştirici çifti (amonyum

persülfat ve tetrametil etilendiamin) de eklenerek yüzey plazmon rezonans biyosensör yüzeylerini kaplamak için kullanılmıştır. Monomer çözeltisi, döndürmeli kaplama tekniği ile yüzey plazmon rezonans biyosensör yüzeylerine homojen olarak dağıtılmıştır. Polimerizasyon, foto-polimerizasyon yöntemiyle gerçekleştirilmiştir. Polimerizasyonun sonunda, reaksiyona girmemiş monomerler ve safsızlıklar uzaklaştırılmış ve biyosensör oda sıcaklığında kurutulmuştur. Hemoglobın baskılanmış yüzey plazmon rezonans biyosensörü, ilk olarak Fourier dönüşümlü infrared spektroskopi-zayıflatılmış toplam yansıma, atomik kuvvet mikroskobu, elipsometre ve temas açısı ölçümleri ile karakterize edilmiştir. Daha sonra, hemoglobın baskılanmış yüzey plazmon rezonans biyosensörü, farklı hemoglobın derişimlerine sahip hemoglobın çözeltilerinden gerçek zamanlı hemoglobın tayini için analizler yapılmıştır. Hemoglobın baskılanmış yüzey plazmon rezonans biyosensörünün seçicilik ve tekrar kullanılabilirlik performansı da araştırılmıştır.

Buna ek olarak, mikroakışkan entegreli yüzey plazmon rezonans biyosensörleri, poli metil metakrilat, çift taraflı yapışkan ve altın kaplı yüzey gibi farklı tabakalar kullanılarak gerçek zamanlı hemoglobın tespiti için hazırlanmıştır. Farklı modifikasyon basamaklarından sonra mikroakışkan entegreli yüzey plazmon rezonans biyosensörleri farklı hemoglobın derişimdeki çözeltilerle etkileştirilerek kinetik analizleri yapılmıştır. Son olarak, hemoglobın çözeltilerle ile iki farklı yüzey plazmon rezonans biyosensörleri arasındaki etkileşimin denge ve adsorpsiyon izoterm modelleri belirlenmiştir.

**Anahtar Kelimeler:** Biyosensör, hemoglobın, moleküler baskılama, yüzey plazmon rezonans.

## ACKNOWLEDGMENT

*Foremost, I would like to express my sincere gratitude to my dear supervisor Prof. Dr. Adil Denizli for his encouragement, guidance and enduring support throughout all period of my Ph.D. studies also for his patience, motivation, and immense knowledge. I am indebted his for giving me the chance in his research group, and he has truly helped me to have a scientific point of view in interdisciplinary concepts during my studies. His invaluable guidance, help and encouragement have allowed me to work in several scientific fields, and I actually believe that he has given me a chance to meet the fascinating world of science. I could not have imagined having a better supervisor for all my academic life. It has been a great honor for me to work with him.*

*I would also like to thank thesis committee, Prof. Dr. Handan Yavuz Alagöz, Assist. Prof. Dr. Fatma Yılmaz, Assoc. Prof. Dr. Nilay Bereli and Assoc. Prof. Dr. Bilgen Osman, for their insightful comments, intimate advice, unlimited guidance and support in my thesis.*

*I would like to give my very special thanks to Prof. Dr. Utkan Demirci and Dr. Fatih Inci for giving me an invaluable opportunity to work together for a year at Stanford University. It was unforgettable, full of experience and good memories that further my career remarkably.*

*I was very lucky by having friends, and would like to acknowledge Ilgım Göktürk Başal, Semra Akgönüllü, and Monireh Bakhshpour Yücel for their valuable friendship, support and encouragement throughout this study. In addition, my sincere thanks also go to my fellow labmates in BIOREG for their collaborating assisting and providing me a nice atmosphere to work in.*

*I gratefully acknowledge to The Scientific and Technical Research Council of Turkey (TUBITAK-2214-A) and Hacettepe University Scientific Research Projects Coordination Unit during my studies in the United States.*

*Lastly and more importantly, I owe my deepest gratitude to all my dearest family members for their endless love, patience, and support throughout my life and my stressful times. They are my real friends.*

*Thanks for all your encouragement!*

# CONTENTS

	<u>Page</u>
ABSTRACT .....	i
ÖZET .....	iv
ACKNOWLEDGMENT .....	vii
CONTENTS .....	viii
FIGURE LEGENDS .....	xi
TABLE LEGENDS .....	xv
SYMBOLS AND ABBREVIATIONS .....	xvi
1. INTRODUCTION .....	1
2. GENERAL INFORMATION .....	4
2.1. Hemoglobin.....	4
2.1.1. The Functional Class of Hemoglobin .....	4
2.1.2. Biological Function of Hemoglobin .....	5
2.1.3. Amino Acid Sequence of Hemoglobin .....	5
2.1.4. Molecular Characterization of Hemoglobin .....	6
2.1.5. Variants and Disorders of Hemoglobin .....	6
2.2. Molecular Imprinting Method .....	7
2.2.1. Types of Molecular Imprinting Methods .....	8
2.2.2. Synthesis Materials of Molecular Imprinting Polymers .....	12
2.2.3. Polymerization Types of Molecularly Imprinted Polymers .....	16
2.2.4. Applications of Molecularly Imprinted Polymers .....	17
2.3. Biosensors .....	20
2.3.1. Electrochemical Biosensors .....	21
2.3.2. Piezoelectric Biosensors .....	22
2.3.3. Optical Biosensors .....	22
2.4. Surface Plasmon Resonance Biosensors.....	23
2.4.1. The Background of Surface Plasmon Resonance .....	23
2.4.2. The Principle of Surface Plasmon Resonance .....	23

2.4.3. Application of Surface Plasmon Resonance .....	27
2.5. Microfluidics .....	28
2.5.1. Microfluidic-Integrated Biosensors .....	29
3. EXPERIMENTAL .....	30
3.1. Materials .....	30
3.2. Characterization of Acrylamide .....	30
3.3. Modification of SPR Surfaces.....	30
3.4. Preparation of Hemoglobin:Acrylamide Pre-Complex.....	31
3.5. Preparation of Hemoglobin Imprinted SPR Biosensor .....	31
3.6. Removal of Hemoglobin .....	32
3.7. Characterization of SPR Biosensors .....	32
3.7.1. FTIR-ATR Spectroscopy Analysis .....	32
3.7.2. Atomic Force Microscopy Analysis .....	33
3.7.3. Ellipsometry Analysis .....	34
3.7.4. Contact Angle Analysis .....	34
3.8. Surface Plasmon Resonance Analysis.....	35
3.9. Kinetic Analysis.....	37
3.10. Selectivity Analysis.....	38
3.11. Reusability Analysis .....	38
3.12. Preparation of Portable Microfluidic-Integrated SPR Biosensors .....	38
3.12.1. Fabrication of Gold Surfaces.....	38
3.12.2. Construction of Microfluidic Chips .....	39
3.12.3. Modification of Microfluidic-Integrated SPR Biosensors.....	41
4. RESULTS AND DISCUSSION.....	43
4.1. Characterization of Acrylamide.....	43
4.2. Preparation of Hemoglobin:Acrylamide Pre-Complex.....	43
4.3. Characterization of SPR Biosensors .....	44
4.3.1. FTIR-ATR Spectroscopy Analysis .....	44
4.3.2. Atomic Force Microscopy Analysis .....	46
4.3.3. Ellipsometry Analysis .....	48
4.3.4. Contact Angle Analysis .....	49
4.4. Surface Plasmon Resonance Measurements.....	51
4.4.1. Effect of pH .....	51

4.4.2. Effect of Hemoglobin Concentration .....	53
4.4.3. Kinetic Studies .....	60
4.4.4. Selectivity Analysis.....	66
4.4.5. Reusability Analysis .....	70
4.5. Portable Microfluidic-Integrated SPR Biosensors .....	74
4.5.1. Surface Chemistry Modification .....	74
4.5.2. SPR Measurements .....	74
4.5.3. Equilibrium Analysis .....	79
4.5.4. Adsorption Isotherm Models.....	80
5. CONCLUSION .....	84
6. REFERENCES .....	89
7. CURRICULUM VITAE .....	100



## FIGURE LEGENDS

	<u>Page</u>
Figure 2.1. The physiology of red blood cells.....	5
Figure 2.2. The representation of the covalent imprinting method.....	9
Figure 2.3. The representation of the non-covalent imprinting method.....	10
Figure 2.4. The representation of the semi-covalent imprinting method.....	11
Figure 2.5. The representation of the metal-mediated imprinting method.....	12
Figure 2.6. The schematic representation of the materials of the molecular imprinting method.....	13
Figure 2.7. The chemical structures of common functional monomers.....	14
Figure 2.8. The chemical structures of common cross-linkers.....	15
Figure 2.9. The chemical structures of common initiators.....	16
Figure 2.10. The number of publications in MIP (a) and Science Direct (b) databases for molecularly imprinted polymers.....	18
Figure 2.11. The number of publications in MIP (a) and Science Direct (b) databases for protein imprinted polymers.....	19
Figure 2.12. The number of publications in MIP (a) and Science Direct (b) databases for hemoglobin imprinted polymers.....	19
Figure 2.13. The basic set-up of components of biosensor for its construction.....	21
Figure 2.14. The excitation of surface plasmons in the Otto and Kretschmann configurations .....	24
Figure 2.15. The differences between gold and silver SPR curves.....	25
Figure 2.16. The schematic representation of the SPR sensorgram.....	26
Figure 2.17. The number of publications in MIP (a) and Science Direct (b) databases for molecular imprinting based surface plasmon resonance biosensors.....	27
Figure 2.18. The length scales for several biological and micro-fabrication structures.....	28
Figure 2.19. The chemical structures of common thermoplastics.....	29
Figure 3.1. Hand-made spin coater (a) and UV light (b) systems.....	31
Figure 3.2. FTIR-ATR spectroscopy system.....	32
Figure 3.3. Atomic force microscopy system.....	33

Figure 3.4. Ellipsometry system.....	34
Figure 3.5. Contact angle analysis system.....	35
Figure 3.6. Surface plasmon resonance system.....	36
Figure 3.7. The preparation steps of SPR system for analysis.....	37
Figure 3.8. The laser cutter system.....	39
Figure 3.9. All parts of the microfluidic chip (a) and portable SPR system (b).....	40
Figure 3.10. Schematic representation of the microfluidic-integrated SPR biosensor.....	42
Figure 3.11. The portable microfluidic-integrated SPR biosensor system.....	42
Figure 4.1. The FTIR spectrum of acrylamide monomer.....	43
Figure 4.2. The spectrophotometric measurements of hemoglobin:acrylamide pre-complex.....	44
Figure 4.3. The FTIR-ATR spectrum of non-imprinted SPR biosensor.....	45
Figure 4.4. The FTIR-ATR spectrum of hemoglobin imprinted SPR biosensor.....	45
Figure 4.5. The AFM image of bare SPR biosensor.....	46
Figure 4.6. The AFM image of non-imprinted SPR biosensor.....	47
Figure 4.7. The AFM image of hemoglobin imprinted SPR biosensor.....	47
Figure 4.8. The ellipsometer image of non-imprinted SPR biosensor.....	48
Figure 4.9. The ellipsometer image of hemoglobin imprinted SPR biosensor.....	49
Figure 4.10. The contact angle image of bare SPR biosensor.....	50
Figure 4.11. The contact angle image of non-imprinted SPR biosensor.....	50
Figure 4.12. The contact angle image of hemoglobin imprinted SPR biosensor.....	51
Figure 4.13. The real-time hemoglobin detection with hemoglobin imprinted SPR biosensor at different pH in terms of a sensorgram (a) and a bar graph (b). Experiment condition: $C_{Hb}=0.1$ mg/mL, $T=25^{\circ}C$ .....	52
Figure 4.14. The real-time hemoglobin detection with hemoglobin imprinted SPR biosensor. Experiment condition: $C_{Hb}=0.0005$ mg/mL, $T=25^{\circ}C$ , pH 6.0.....	53
Figure 4.15. The real-time hemoglobin detection with hemoglobin imprinted SPR biosensor. Experiment condition: $C_{Hb}=0.0015$ mg/mL, $T=25^{\circ}C$ , pH 6.0.....	54
Figure 4.16. The real-time hemoglobin detection with hemoglobin imprinted SPR biosensor. Experiment condition: $C_{Hb}=0.0035$ mg/mL, $T=25^{\circ}C$ , pH 6.0.....	54

Figure 4.17. The real-time hemoglobin detection with hemoglobin imprinted SPR biosensor. Experiment condition: $c_{\text{Hb}}=0.025$ mg/mL, $T=25^{\circ}\text{C}$ , pH 6.0.....	55
Figure 4.18. The real-time hemoglobin detection with hemoglobin imprinted SPR biosensor. Experiment condition: $c_{\text{Hb}}=0.05$ mg/mL, $T=25^{\circ}\text{C}$ , pH 6.0.....	55
Figure 4.19. The real-time hemoglobin detection with hemoglobin imprinted SPR biosensor. Experiment condition: $c_{\text{Hb}}=0.1$ mg/mL, $T=25^{\circ}\text{C}$ , pH 6.0.....	56
Figure 4.20. The real-time hemoglobin detection with hemoglobin imprinted SPR biosensor. Experiment condition: $c_{\text{Hb}}=0.25$ mg/mL, $T=25^{\circ}\text{C}$ , pH 6.0.....	56
Figure 4.21. The real-time hemoglobin detection with hemoglobin imprinted SPR biosensor. Experiment condition: $c_{\text{Hb}}=0.5$ mg/mL, $T=25^{\circ}\text{C}$ , pH 6.0.....	57
Figure 4.22. The real-time hemoglobin detection with hemoglobin imprinted SPR biosensor. Experiment condition: $c_{\text{Hb}}=1.0$ mg/mL, $T=25^{\circ}\text{C}$ , pH 6.0.....	57
Figure 4.23. The combination of real-time responses of hemoglobin imprinted SPR biosensor. Experiment condition: $c_{\text{Hb}}=0.0005-1.0$ mg/mL, $T=25^{\circ}\text{C}$ , pH 6.0.....	58
Figure 4.24. The calibration curve of hemoglobin imprinted SPR biosensor response to hemoglobin solutions between 0.0005 mg/mL and 1.0 mg/mL.....	58
Figure 4.25. The calibration curves of hemoglobin imprinted SPR biosensor response to hemoglobin solutions between 0.0005-0.05 mg/mL (a) and 0.1-1.0 mg/mL (b)....	59
Figure 4.26. Determination of kinetic rate constants: Association kinetics analysis....	61
Figure 4.27. Determination of kinetic rate constants: Equilibrium analysis.....	62
Figure 4.28. Langmuir adsorption isotherm model.....	64
Figure 4.29. Freundlich adsorption isotherm model.....	65
Figure 4.30. Langmuir-Freundlich adsorption isotherm model.....	65
Figure 4.31. The selectivity combination of real-time responses of hemoglobin imprinted SPR biosensor. Experiment condition: $c_{\text{protein}}=0.1$ mg/mL, $T=25^{\circ}\text{C}$ , pH 6.0.....	68
Figure 4.32. The selectivity combination of real-time responses of non-imprinted SPR biosensor. Experiment condition: $c_{\text{protein}}=0.1$ mg/mL, $T=25^{\circ}\text{C}$ , pH 6.0.....	68
Figure 4.33. The selectivity comparison of hemoglobin imprinted (MIP) and non-imprinted (NIP) SPR biosensors. Experiment condition: $c_{\text{protein}}=0.1$ mg/mL, $T=25^{\circ}\text{C}$ , pH 6.0.....	69

Figure 4.34. The selectivity comparison of hemoglobin imprinted (MIP) and non-imprinted (NIP) SPR biosensors. Experiment condition: $C_{\text{protein}}=0.1$ mg/mL, $T=25^{\circ}\text{C}$ , pH 6.0.....	70
Figure 4.35. The reusability of hemoglobin imprinted SPR biosensor. Experiment condition: $C_{\text{Hb}}=0.05-1.0$ mg/mL, $T=25^{\circ}\text{C}$ , pH 6.0.....	71
Figure 4.36. The storage stability of hemoglobin imprinted SPR biosensor. Experiment condition: $C_{\text{Hb}}=0.1$ mg/mL, $T=25^{\circ}\text{C}$ , pH 6.0.....	72
Figure 4.37. The evaluation of surface chemistry steps via real-time monitoring SPR angle changes.....	74
Figure 4.38. The plot of SPR angle shift after the application of 5 $\mu\text{g/mL}$ hemoglobin to the microfluidic-integrated SPR biosensor.....	75
Figure 4.39. The plot of SPR angle shift after the application of 10 $\mu\text{g/mL}$ hemoglobin to the microfluidic-integrated SPR biosensor.....	76
Figure 4.40. The plot of SPR angle shift after the application of 25 $\mu\text{g/mL}$ hemoglobin to the microfluidic-integrated SPR biosensor.....	76
Figure 4.41. The plot of SPR angle shift after the application of 50 $\mu\text{g/mL}$ hemoglobin to the microfluidic-integrated SPR biosensor.....	77
Figure 4.42. The plot of SPR angle shift after the application of 100 $\mu\text{g/mL}$ hemoglobin to the microfluidic-integrated SPR biosensor.....	77
Figure 4.43. The plot of SPR angle shift after the application of 200 $\mu\text{g/mL}$ hemoglobin to the microfluidic-integrated SPR biosensor.....	78
Figure 4.44. The plot of SPR angle shift after the application of 250 $\mu\text{g/mL}$ hemoglobin to the microfluidic-integrated SPR biosensor.....	78
Figure 4.45. The calibration curve for hemoglobin detection onto the microfluidic-integrated SPR biosensor.....	79
Figure 4.46. Determination of kinetic rate constants: Equilibrium analysis.....	80
Figure 4.47. Langmuir adsorption isotherm model.....	81
Figure 4.48. Freundlich adsorption isotherm model.....	81
Figure 4.49. Langmuir-Freundlich adsorption isotherm model.....	82

## TABLE LEGENDS

	<u>Page</u>
Table 2.1. The pre-valences of carriers of hemoglobin gene variants and affected conceptions.....	7
Table 2.2. The comparison of natural biomolecules and molecularly imprinted polymers.....	8
Table 2.3. The comparison of the different polymerization types.....	17
Table 2.4. The main advantages and disadvantages of surface plasmon resonance system.....	26
Table 3.1. The specifications of the SPR system used in this study according to manufacturer.....	36
Table 4.1. Equilibrium and association kinetics constants.....	63
Table 4.2. The comparison of adsorption isotherm models.....	66
Table 4.3. The selectivity and relative selectivity coefficients of hemoglobin imprinted (MIP) and non-imprinted (NIP) SPR biosensors.....	69
Table 4.4. The comparison of different systems for hemoglobin detection.....	73
Table 4.5. The comparison of adsorption isotherm models.....	82
Table 4.6. The comparison of different systems for hemoglobin detection.....	83

## SYMBOLS AND ABBREVIATIONS

### Symbols

$\alpha$	Alpha
$\beta$	Beta
$\gamma$	Gamma

### Abbreviations

AAm	Acrylamide
AFM	Atomic Force Microscope
APS	Ammonium Persulfate
BSA	Bovine Serum Albumin
DSA	Double Sided Adhesive
EDC	N-(3-Dimethylaminopropyl)-N'-Ethylcarbodiimide Hydrochloride
FTIR-ATR	Fourier Transform Infrared-Attenuated Total Reflectance
Hb	Hemoglobin
Lyz	Lysozyme
MBAAm	Methylene Bisacrylamide
Myb	Myoglobin
MIP	Molecularly Imprinted Polymer
MUA	Mercapto Undecanoic Acid
NIP	Non-Imprinted
NHS	N-Hydroxy Succinimide
PMMA	Polymethyl Methacrylate
RI	Refractive Index
RMS	Root Mean Square
SPR	Surface Plasmon Resonance
TEMED	Tetramethyl Ethylenediamine
Trf	Transferrin
UV	Ultra Violet
WHO	World Health Organization

## 1. INTRODUCTION

Proteins are one of the essential molecules in living organisms that denote multiple functional and structural features in cellular machinery. From a biological perspective, any abnormality in protein structure and function can potentially cause to deficiencies in cells, leading to diseases. Therefore, researches around evaluating these parameters are still essential to understand most diseases [1]. In particular, protein recognition and detection studies have presented new horizons for researchers to differentiate health and disease-status. Recent efforts significantly impact on the development of selective and reliable bio-analytical modalities and tools in protein research realm. Such an example, hemoglobin (Hb), a tetrameric protein in the red blood cells, formed with two dimer subunits with an iron-carrying oxygen transport protein. Any structural changes in these 4 subunits of Hb lead to serious disorders, mostly genetic diseases, including hemoglobinopathies, thalassaemia and sickle cell anemia [2]. Due to its high frequency in unusual genetic status, hemoglobin-based diseases are uncommon among genetic conditions, the survey results are convenient for most parts of the world and frequency determines can be made for several nationalities [3].

There are several clinical and analytical tool that are currently utilized to recognize proteins. However, considerable limitations including high-cost, assay time, need for skilled personnel, and poor stability is major bottlenecks to develop an effective method possessing favorable specificity in this field [4]. Among both current commercially available and laboratory-based analytical methods, molecular imprinting method has been ably applied to distinguish and recognize proteins [5]. Briefly, molecular imprinting offers a promising method to construct three-dimensional signature of proteins via molecularly imprinted polymers (MIPs), which form recognition cavities completing to the shape, conformation, and size of the template molecule [6]. The procedure consists of subsequent crosslinking of the monomers and template molecules to produce a polymeric material, which is also complementary for target molecules [7]. In oppose to biological molecules MIPs offer notable advantages, such as reusability, stability in high

pressure and temperature, ease-of-preparation, versatility, inexpensive production, and high sensitivity capability to the target protein. Therefore, they have been utilized in multiple operations such as chromatography [8], biosensing [9], bioseparation [10], drug delivery [11], and environmental safety studies [12]. On the other hand, biosensors utilize biological moieties to selectively detect one compound in heterogeneous conditions. They can be sorted by their type of bio-receptor or transducer. For instance, a bio-receptor can be a biological moiety such as an antibody, enzyme, protein, and nucleic acid or a whole living organism/network such as cells, tissue, or whole organism to monitor biochemical reaction/recognition. Particularly, recent literature has clearly demonstrated the impact of surface plasmon resonance (SPR)-based platforms on the biotargets detection [13]. This modality simply examines binding properties by recording the change of refractive index at the close vicinity of a layer (e.g., gold and silver). To produce surface plasmons, the modality requires a coupling element such as a prism or fiber optic cable, and convert changes in dip-angle of reflection into a real-time binding data [14]. This provides highly sensitive and also rapid detection of biotargets when compared to the other existing detection strategies such as ELISA, which require time-consuming washes and day-long incubations. In addition, the detection does not require any labeling, thus significantly reducing the assay cost, procedure steps, complexity, and laboring. As demonstrated in the literature, SPR is able to directly detect a variety of biological targets, including proteins, lipids, nucleic acids, and carbohydrates. Although there are multiple encouraging features of SPR in clinical testing, the device size and chip cost in commercialized SPR tools are still hindering their utilization in medical diagnosis at daily basis.

Microfluidics is an emerging technology, which manipulates and analyzes minute volumes of fluid. Recent efforts successfully demonstrate the integration of this technology with biological and medical sciences [15]. Particularly, the integration of microfluidics with SPR biosensors have a significant impact on the development of reliable, accurate, and easy-to-use platforms for medical diagnostics by reducing sample volume and increasing interactions of target molecules with the sensor surface. Among these detection parameters, microfluidics also enables to miniaturize such



surface sensitive platforms to a hand-held size, thus leveraging their applicability at the bed-side, point-of-care, and primary clinics.

## **2. GENERAL INFORMATION**

### **2.1. Hemoglobin**

Proteins hold much crucial structural, and functional properties and intimately associate with the other macromolecules such as lipids and carbohydrates to produce larger and more complex units. Scientists have been focused on discovering fundamental and important properties of proteins, and recognized that they are also one of the major indicators and markers in most disease, as well as recent studies showed that their size, structure, concentration, and even, orientation are essential for facilitating cellular machinery. Due to their multiple and necessary roles in cell functionality and structure, one of the most attractive area to investigate the significance of proteins is to detect biological molecules for clinical studies [16].

For instance, hemoglobin (Hb) is the primary protein of a life for a diversity of activities. It has crucial functions in the transportation of oxygen and carbon dioxide and the maintenance of the balance of pH in the red blood cells. Sensitive and accurate detection platforms will have potentially create new avenues to monitor the concentrations of such vital protein marker, hemoglobin, in the early detection and highly reliable prediction of disease [17]. Because especially in clinical practice, hemoglobin concentrations are closely correlated with several diseases and health status and the abnormality of the hemoglobin levels can result in various kinds of genetic diseases, including thalassemia, leukemia, sickle cell anemia, heart disease, and excessive loss of blood [18].

#### **2.1.1. The Functional Class of Hemoglobin**

Hemoglobin is heme-carrying and oxygen transport protein in the red blood. It may be found in various types. Their existence can be like monomers, dimmers, or tetramers. The chains of polypeptide, which consist of identical globin domains, are also existed in hemoglobin molecule. The hemoglobin oligomerization is an essential movement in evolution, which is essential for efficient oxygen transport [19].

### 2.1.2. Biological Function of Hemoglobin

The red blood cells are continuously manufactured in the red bone marrow of the skull, the ribs, the vertebrae, and the ends of the long bones. There are 4-6 million red blood cells per  $\text{mm}^3$  of whole blood in normal status. They are biconcave disks. Their shape causes the increase in their flexibility for movement in the capillary and their surface area for the gas diffusion. Figure 2.1 shows that the movement of red blood cells through the capillary and each red blood cell is a biconcave disk that includes several hemoglobin molecules. Hemoglobin contains 4 polypeptide chains that are shown as blue. There is a heme group that contains iron in the middle of each chain. When the hemoglobin molecule is oxygenated, oxygen gets together with iron. The color of oxyhemoglobin is bright red, and deoxyhemoglobin is a dark maroon. The iron part of hemoglobin obtains oxygen in the lungs and gives it up to the tissues. The whole blood carries 20 mL of oxygen per 100 mL of blood. This exhibits that hemoglobin increases the oxygen-carrying capacity of blood more than 60 times [20].

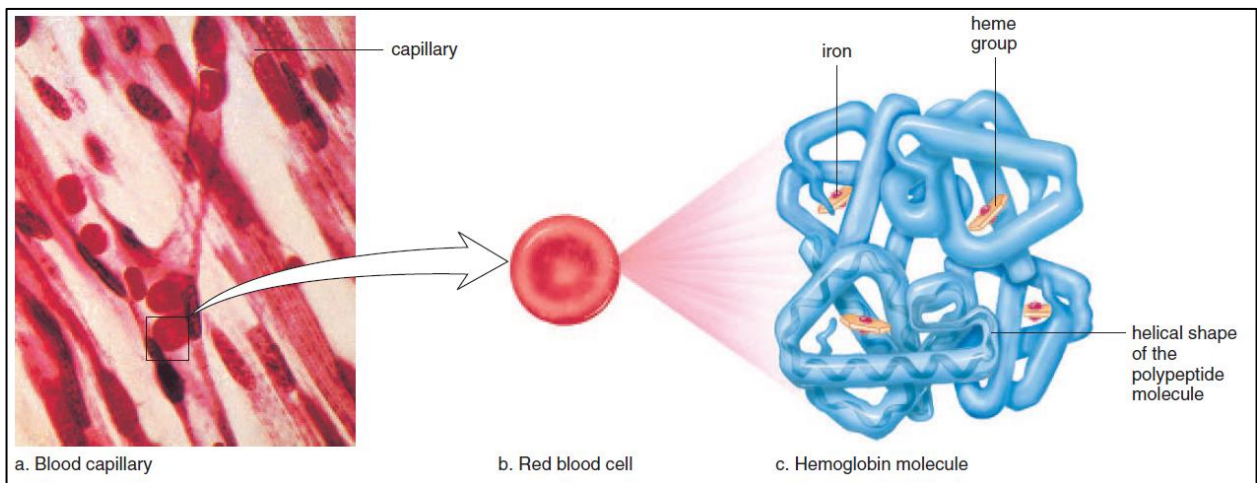


Figure 2.1. The physiology of red blood cells [20].

### 2.1.3. Amino Acid Sequence of Hemoglobin

Hemoglobin genes are found in a number of craniate species that are sequenced. It is a significant perception into the proteins evolution [21]. The first cDNA to be cloned and sequenced as human alpha ( $\alpha$ ) and beta ( $\beta$ ) chains [22]. Hemoglobin is

post-translationally modified in some species. The most common modification is the acetylation of the N-terminus. Human blood involves minor glycosylated components.

#### **2.1.4. Molecular Characterization of Hemoglobin**

Hemoglobin is generally produced by the vertebrate blood. The fresh blood is instantly incorporate with citrate or heparin in order for coagulation prevention. The red and white blood cells can be collected from plasma by centrifugation. The cell debris can be taken out via centrifugation. Higher hemoglobin level (98%) is observed in the hemolysate status and no further decontamination is needed [23].

#### **2.1.5. Variants and Disorders of Hemoglobin**

As mentioned before, the hemoglobin molecule consists of the 4 globin chains that are fetal hemoglobin (Hb F) has 2 $\alpha$  and 2 gamma ( $\gamma$ ) and adult hemoglobin (Hb A) has 2 $\alpha$  and 2 $\beta$  chains. Due to self-generated mutation, hemoglobin gene variants are present at low prevalence [24]. The most hemoglobin gene variants are uncommon and the others are benign, but some are common because carriers are less likely than the others to die from malaria. The most common variant,  $\alpha$  plus thalassaemia, is generally benign. However, people who come into the combinations of hemoglobins S, C, E, D,  $\beta$  thalassaemia, or  $\alpha$  zero thalassaemia may have a serious hemoglobin disorder [25].

Table 2.1. The pre-valences of carriers of hemoglobin gene variants [25].

WHO region	Demography 2003				% of the population carrying			Affected conceptions (per 1000)			Affected births (% of under-5 mortality)
	Population (millions)	Crude birth rate	Annual births (1000s)	Under-5 mortality rate	Significant variant <sup>a</sup>	$\alpha^+$ thalassaemia <sup>b</sup>	Any variant <sup>c</sup>	Sickle-cell disorders <sup>d</sup>	Thalassaemias <sup>e</sup>	Total	
African	586	39.0	22 895	168	18.2	41.2	44.4	10.68	0.07	10.74	6.4
American	853	19.5	16 609	27	3.0	4.8	7.5	0.49	0.06	0.54	2.0
Eastern Mediterranean	573	29.3	16 798	108	4.4	19.0	21.7	0.84	0.70	1.54	1.4
European	879	11.9	10 459	25	1.1	2.3	3.3	0.07	0.13	0.20	0.8
South-east Asian	1 564	24.4	38 139	83	6.6	44.6	45.5	0.68	0.66	1.34	1.6
Western Pacific	1 761	13.6	23 914	38	3.2	10.3	13.2	0.00	0.76	0.76	2.0
<b>World</b>	<b>6 217</b>	<b>20.7</b>	<b>128 814</b>	<b>81</b>	<b>5.2</b>	<b>20.7</b>	<b>24.0</b>	<b>2.28</b>	<b>0.46</b>	<b>2.73</b>	<b>3.4</b>

Hemoglobin diseases show an important health issue in 71% of 229 countries, and this 71% of countries comprise 89% of births all over the world (Table 2.1). More than 330 thousands effected babies are born yearly. According to the statistics, the pregnant women carry b or zero thalasseмииs, or hemoglobin S, C, D or E, around 7% and more than 1% of couples are at risk. Detection of hemoglobin diseases should be formed the part of main health services in the countries [25].

## 2.2. Molecular Imprinting Method

The selective biomolecules detection acts a significant function in several basic procedures in many systems [26]. However, natural recognition elements have high biological interest to their targets, they do cannot require the practical application because of the sensitive properties such as low durability at high pressure, temperature and organic solvents, and also low stability in different pH. Recently, one of the super-molecular chemistry type, molecular imprinting method, has been proposed to defeat the most of the disadvantages [27].

Molecular imprinting method was first reported by Wulff and Sarhan in the early 1970s [28]. After then, many of the scientists from all over the world observed the prospering

of this method. This method principally relies on the molecular identification reaction that occurs at the surrounding of the target molecule called as a template [29].

Molecularly imprinted polymers (MIPs) can be produced by the different kinds of cross-linkers, functional monomers and solvents combinations [30-32]. The quality and feature of the MIPs can be changed the combination of the monomer mixture, the experimental circumstances, the interaction mechanisms, and so on [33-36]. MIPs have multiple improvements including easy preparation, cost-friendly, high stability, affinity and selectivity toward template molecule. Furthermore, MIPs can be used in variable areas, such as biosensors, enzyme mimics, and solid phase extraction [37, 38]. The advantages of molecularly imprinted polymers compared to natural biomolecules are exhibited in Table 2.2.

Table 2.2. The comparison of natural biomolecules and molecularly imprinted polymers [38].

Natural Biomolecules	Molecularly Imprinted Polymers
<ul style="list-style-type: none"> <li>• Not stable</li> <li>• Expensive</li> <li>• Poor performance in organic solvents</li> <li>• Needed more operational systems</li> <li>• Working limited analytes</li> <li>• Low compatible with other technology</li> </ul>	<ul style="list-style-type: none"> <li>• High stability at harsh conditions</li> <li>• Cost-friendly</li> <li>• High performance in organic solvents</li> <li>• Needed minimum systems</li> <li>• Working any analytes</li> <li>• High compatible with other technology</li> </ul>

### 2.2.1. Types of Molecular Imprinting Methods

Molecularly imprinted polymers can be synthesized via mixing the functional monomers and template molecule in the presence of suitable cross-linkers. The fitted cavities that have size, shape, chemical and physical functionality are obtained when the template removed from the polymeric matrix. The selectivity of a MIP results from the presence of specific cavities designed for the target analytes. It is possible to prepare MIPs by

using covalent [39], non-covalent [40], semi-covalent [41] and metal-mediated molecular imprinting methods [42].

### 2.2.1.1. The Covalent Imprinting Method

This method is distinguished by the combination of binding the templates and functional monomers as covalently. Homogeneous binding sites occur in the polymeric matrix. The benefit of this method is the functional groups are only connected with the template molecule (Figure 2.2). In addition, the disadvantage of this method is that the limited number of compounds can be imprinted by this method [39].

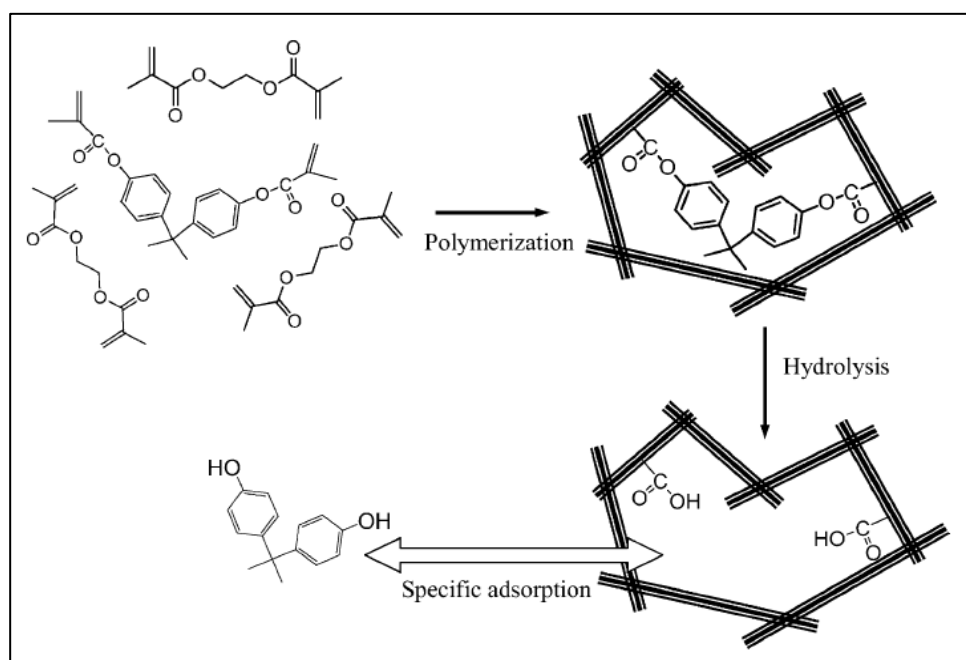


Figure 2.2. The representation of the covalent imprinting method [39].

### 2.2.1.2. The Non-Covalent Imprinting Method

This method bases on the interactions between functional monomer and template molecule while polymerization is the same as the between polymeric matrix and template molecule at rebinding part. Because of the simplicity of the non-covalent imprinting method is the most extensively applied [43]. As shown in Figure 2.3, the

materials show in the pre-polymerization position. Then, the template molecule has three binding sites to interact with the functional monomer.

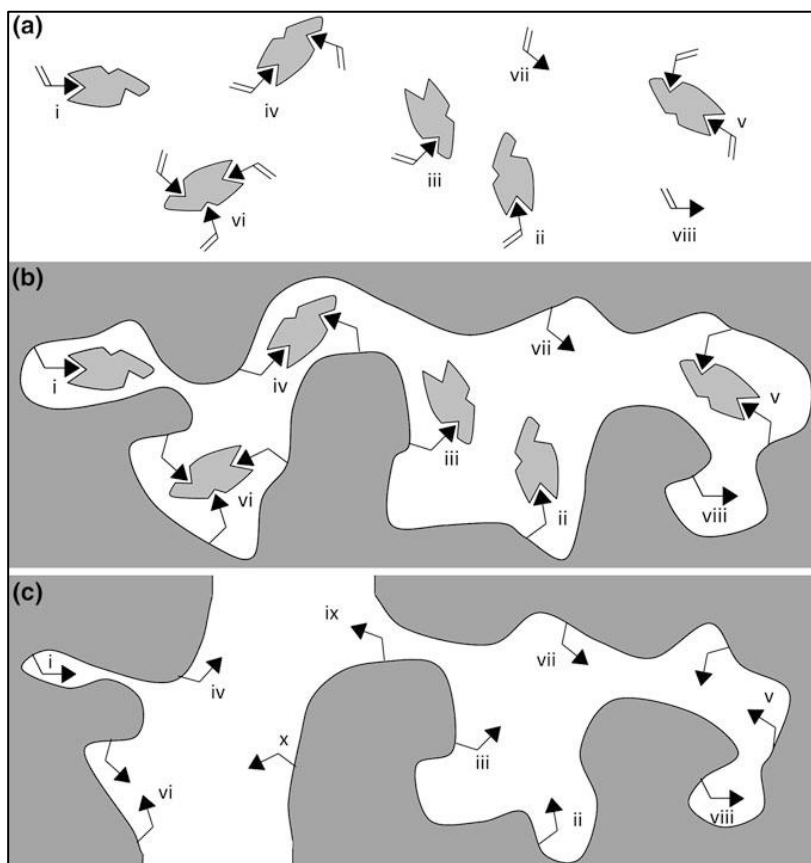


Figure 2.3. The representation of the non-covalent imprinting method [43].

### 2.2.1.3. The Semi-Covalent Imprinting Method

This method depends on the combination of the covalent and the non-covalent methods. The template molecules bind covalently functional groups that cause the improvement after cleavage of this molecule. More homogeneous distribution in binding sites (Figure 2.4). The rebinding, which occurs by using non-covalent interactions, has no kinetic limitations with the exception of diffusion [41].



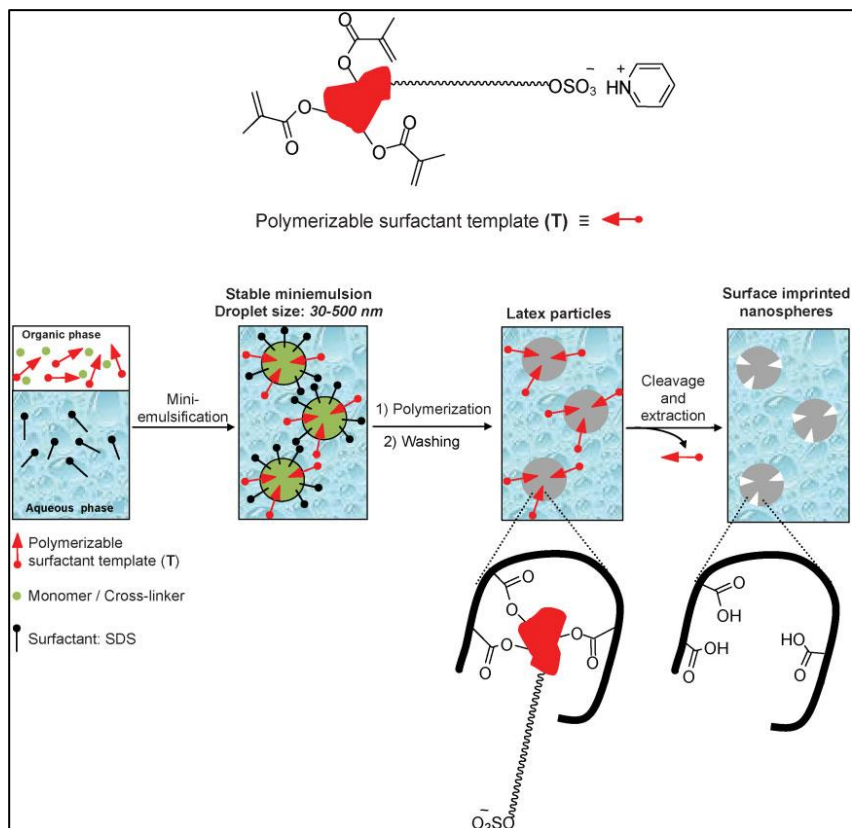


Figure 2.4. The representation of the semi-covalent imprinting method [41].

#### 2.2.1.4. The Metal-Mediated Imprinting Method

The metal coordination employs as an alternative method that means of binding between the template molecule and functional monomer in the fabrication of polymeric matrix. The matrix comprises of polymerizable ligands to complex the metals which in turn coordinates to the template molecule [42]. The representation of the metal-mediated imprinting method is demonstrated in Figure 2.5.

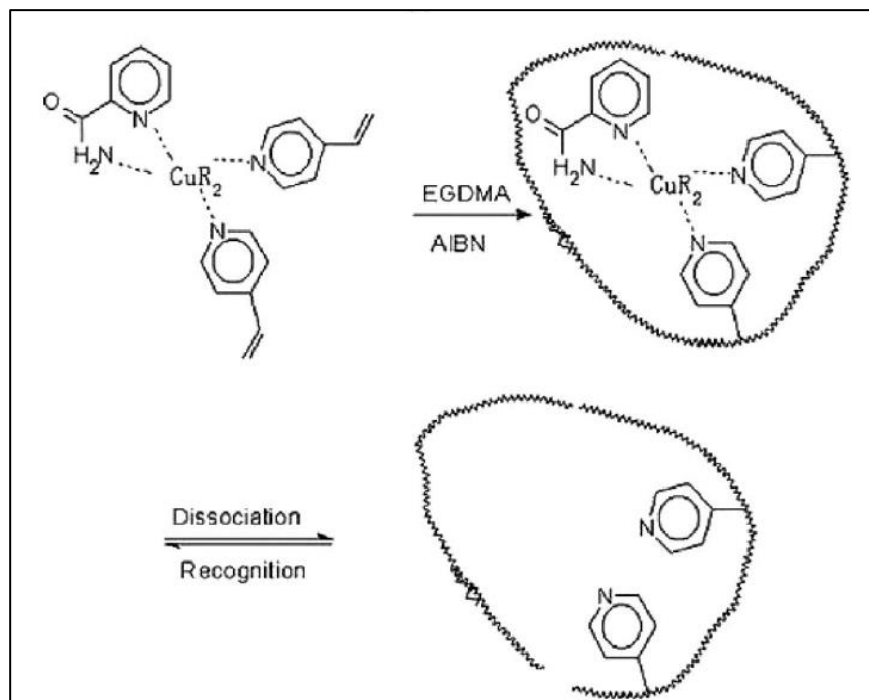


Figure 2.5. The representation of the metal-mediated imprinting method [42].

### 2.2.2. Synthesis Materials of Molecular Imprinting Polymers

The template molecules, functional monomers, cross-linkers and initiators are necessary for the polymerization. During the polymerization, the template molecule binds to the functional monomer to produce a pre-complex. The pre-complex is copolymerized in a presence of cross-linker that prepares a polymeric matrix around the monomer–template complex. After the template molecule removal, a template-specific recognition cavity is formed in the polymeric matrix (Figure 2.6).

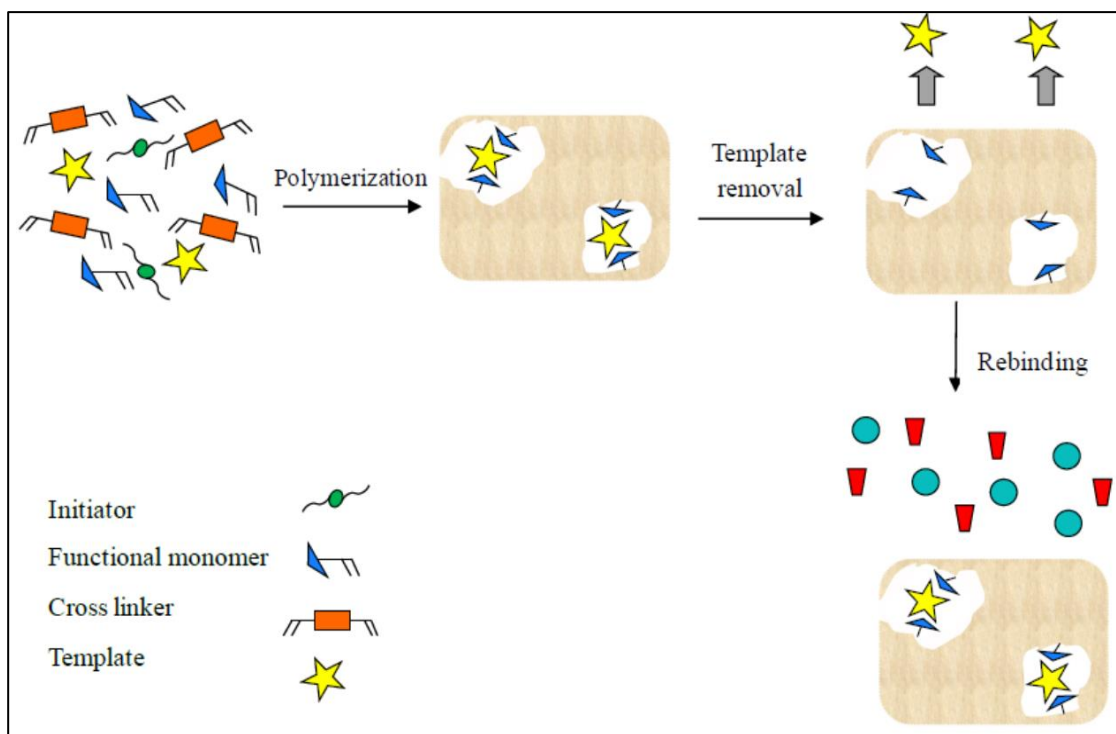


Figure 2.6. The schematic representation of the materials of the molecular imprinting method [44].

### 2.2.2.1. Templates

The templates have the most importance materials in all molecular imprinting processes. The procedure includes crosslinking functional monomers around the selected template. After the polymerization, the template is removed from the polymeric matrix. The final product has template binding sites and is ready to rebind template molecule over and over [45].

### 2.2.2.2. Functional monomers

The functional monomers are one of the main reasons for the specific recognition of the template in the binding site. Thus, it is a crucial step to prepare the combination of the template and functional monomer. It is also significant to figure out the optimum ratios of the monomers otherwise it only increase the complexity of the chemical environment and may results disruptions [46]. The most common functional monomers are shown in Figure 2.7.

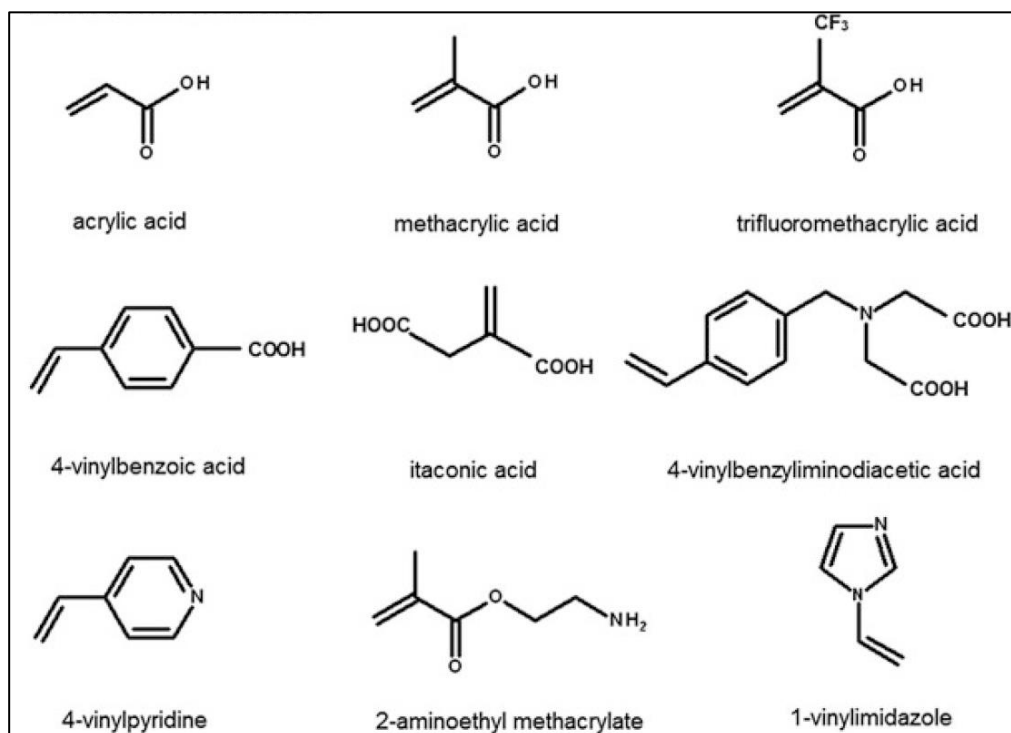


Figure 2.7. The chemical structures of common functional monomers [45].

### 2.2.2.3. Cross-linkers

The cross-linkers make the polymer chain bind to another. They act critical functions to determine the features of polymers. The high percentages of cross-linkers are needed to obtain the structural integrity of the imprinted binding sites. The main function of the cross-linker is to produce a rigid polymeric matrix and also comprise recognition groups [47]. The most common cross-linkers are shown in Figure 2.8.

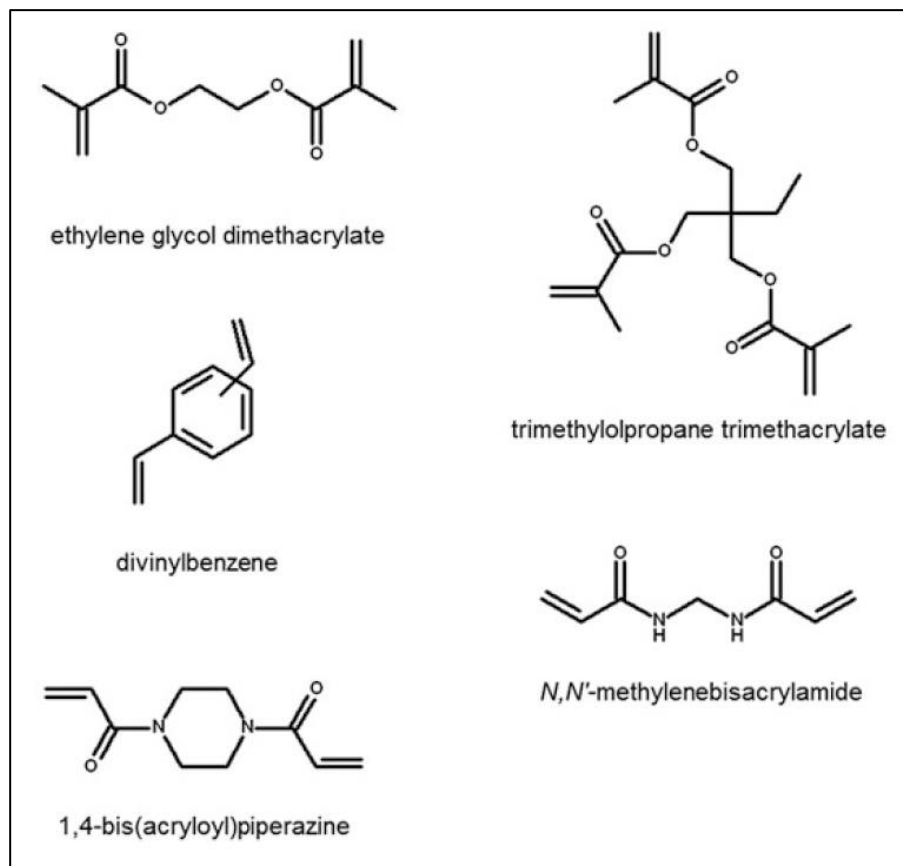


Figure 2.8. The chemical structures of common cross-linkers [45].

#### 2.2.2.4. Initiators

The initiators are chemical species which effects the monomer to produce an intermediate compound that able to link with a large number of other monomers into a polymeric matrix. Initiators should be selected according to the polymerization type and template molecule. The template may photo-chemically or thermally unstable then triggering methods and initiators have to be selected according to template stability [48]. The most common initiators are represented in Figure 2.9.

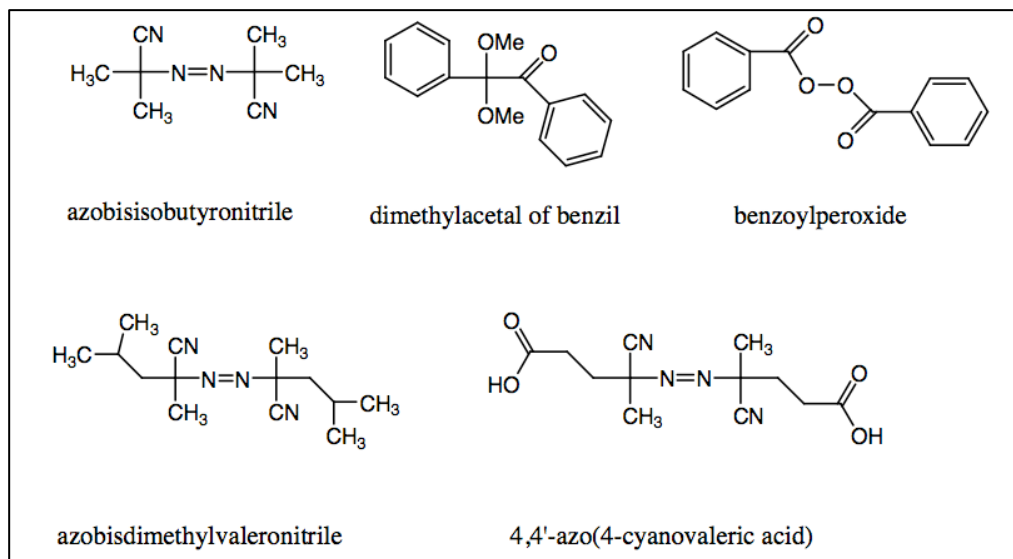


Figure 2.9. The chemical structures of common initiators [48].

### 2.2.2.5. Solvents/Porogens

According to the type of solvent polymer chains may become more expanded or the chains stay close to each other. These effects cause collapsing the polymer chains to form a hard sphere, or swelling in order to maximize the number of polymer-fluid contacts. The critical function is that the solvent attends as a porogen maker that checks the morphology and porosity of the polymeric matrix. Because of porogens a macroporous polymer structure may have enormous surface areas [49].

### 2.2.3. Polymerization Types of Molecularly Imprinted Polymers

The polymerization can be carried out homogeneous or heterogeneous medium. This classification is generally depended on the initial reaction mixture. Some homogeneous polymerization systems may change heterogeneous while polymerization continues because of the insolubility of the polymer. The comparison of the different polymerization types of molecular imprinting method is demonstrated in Table 2.3.

Table 2.3. The comparison of the different polymerization types [50].

<b>Polymerization Type</b>	<b>Advantages</b>	<b>Disadvantages</b>
<b>Bulk</b>	<ul style="list-style-type: none"> <li>• Simple and universal; no need a particular ability or sophisticated instrumentation.</li> </ul>	<ul style="list-style-type: none"> <li>• Over-long procedures; irregularity of size and shape; low performance.</li> </ul>
<b>Suspension</b>	<ul style="list-style-type: none"> <li>• Spherical particles; highly reproducible results; large scale possible.</li> </ul>	<ul style="list-style-type: none"> <li>• Phase partitioning of a complex system; specialist surfactant polymers needed.</li> </ul>
<b>Multi-step swelling</b>	<ul style="list-style-type: none"> <li>• Mono-disperse beads of controlled diameter; outstanding particle for HPLC.</li> </ul>	<ul style="list-style-type: none"> <li>• Complex process conditions; the require for aqueous emulsions.</li> </ul>
<b>Precipitation</b>	<ul style="list-style-type: none"> <li>• Imprinted microspheres; uniform size and high yields.</li> </ul>	<ul style="list-style-type: none"> <li>• A huge amount of template; high dilution factor.</li> </ul>
<b>In-situ</b>	<ul style="list-style-type: none"> <li>• Single-step preparation; cost-friendly, well porosity.</li> </ul>	<ul style="list-style-type: none"> <li>• Wide optimization needed for every template system.</li> </ul>
<b>Surface</b>	<ul style="list-style-type: none"> <li>• Mono-disperse product; thin imprinted layers.</li> </ul>	<ul style="list-style-type: none"> <li>• Complicated system; time consuming.</li> </ul>

#### 2.2.4. Applications of Molecularly Imprinted Polymers

The molecular imprinting can be employed in a variety of applications such as chromatography [51], solid phase extraction [52], permeable membranes [53], drug delivery [54], adsorbent [55], microfluidic device [56], biosensor [57] and so on.

In the literature, there are numerous publications and ongoing researches around molecular imprinting method (Figure 2.10). During this statistics, “imprint” was selected

as a keyword to classify the number of the publication in the MIP database. On the other hand, “imprint” was also chosen as keywords to count the number of publications in the Science Direct database [58, 59]. According to results, the total publication numbers are calculated as 6955 (a) and 55417 (b) for MIP and Science Direct databases since 2007. It can be seen that the number of publications for molecularly imprinted polymers is increasing almost every year and changing with different databases. The growth in molecularly imprinted polymers that use for several templates has increased rapidly over the last ten years.

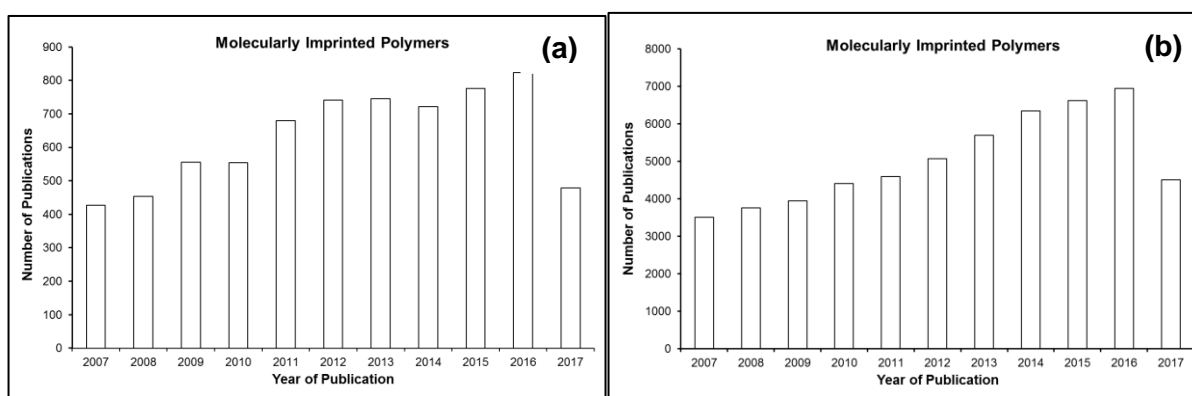


Figure 2.10. The number of publications in MIP (a) and Science Direct (b) databases for molecularly imprinted polymers.

In addition, Figure 2.11 displays the publication numbers for all proteins in molecular imprinting method. The template is selected as “protein” in order to classify the number of publications in the MIP database [58] and the keywords are selected as “imprint” with “protein” in order to identify the publication numbers in the Science Direct database [59]. According to results, the total publication numbers are calculated as 783 (a) and 16519 (b) for MIP and Science Direct databases since 2007. It can be also seen that the number of publications for protein imprinted polymers is increasing almost every year and changing with different databases.



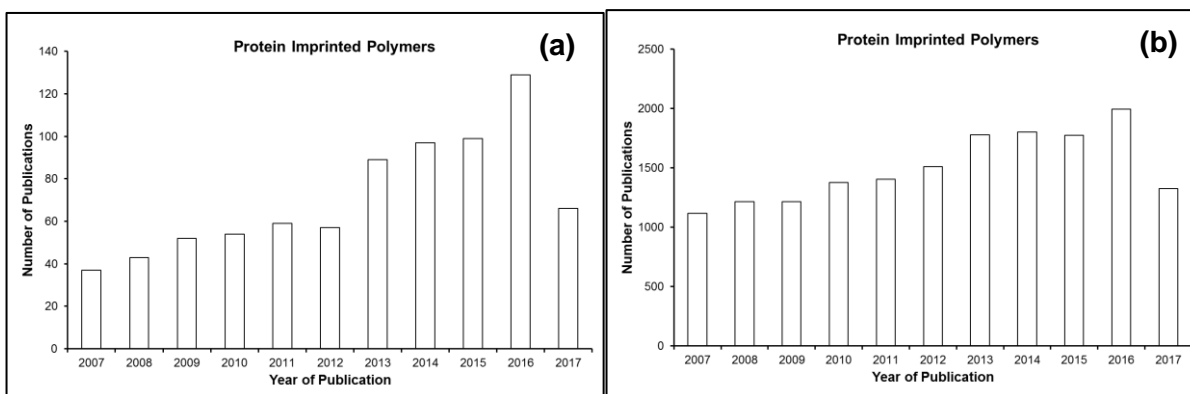


Figure 2.11. The number of publications in MIP (a) and Science Direct (b) databases for protein imprinted polymers.

Figure 2.12 also displays the publication numbers for only hemoglobin in molecular imprinting method. The template is selected as “hemoglobin” in order to classify the publication numbers in the MIP database [58] and the keywords are selected as “imprint” with “hemoglobin” in order to classify the number of publications in the Science Direct database [59]. According to results, the total numbers of publication are calculated as 96 (a) and 1274 (b) for MIP and Science Direct databases since 2007. It can be observed that the different number of publications for hemoglobin imprinted polymers is published for each year and changing with different databases.

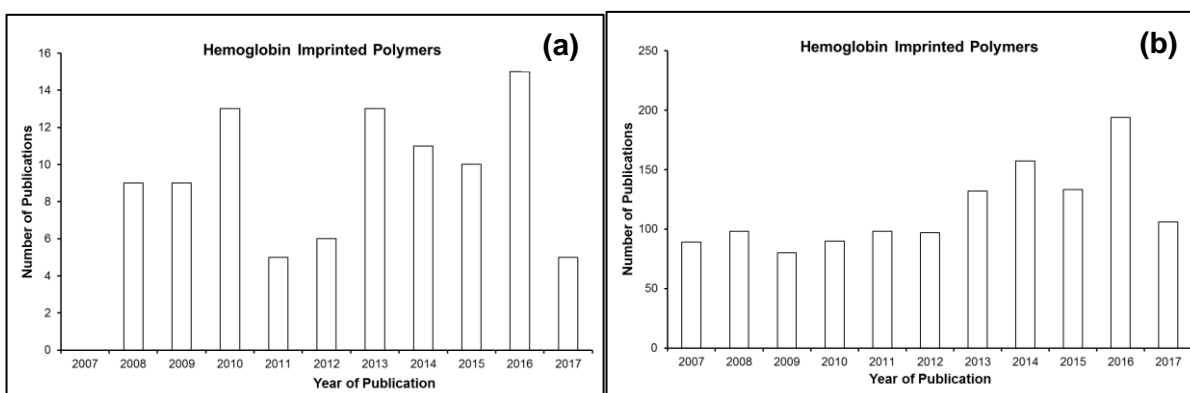


Figure 2.12. The number of publications in MIP (a) and Science Direct (b) databases for hemoglobin imprinted polymers.

### **2.3. Biosensors**

A biosensor is an analytical device with three major modules: (i) a sensing bioreceptor, (ii) a transducer, and (iii) a detector with a digital output. Principally, target molecule interacts with bioreceptor [60], and the biological sensing element selectively recognizes a particular biological molecule through a reaction, specific adsorption, or another process as physical/chemical. Then, the transducer translates molecular changes (*e.g.*, chemical or physical changes) to a quantifiable signal measured by the digital detector module (Figure 2.13) [61-62]. The detector, termed as a transducer, can be electrochemical, piezoelectric or optical.

Biosensors provide multiple capabilities, including exceptional performance, user-friendly operation, rapid response, high sensitivity and specificity, portability, relatively compact size, and real-time analysis [61]. Over the last decade, efforts in biosensor realm have expanded rapidly, and it has already denoted a broad range of applications in the fields of clinical analysis, environmental, food safety, and homeland security. Nowadays, researchers aim to improve the sensitivity and specificity of the methods by focusing on the biosensor fabrication and production quality, developing advanced surface chemistries, increasing the affinity between the surface ligands and target biomarkers, and using nanomaterials such as nanofilms, gold nanoparticles or quantum dots for signal amplification studies.

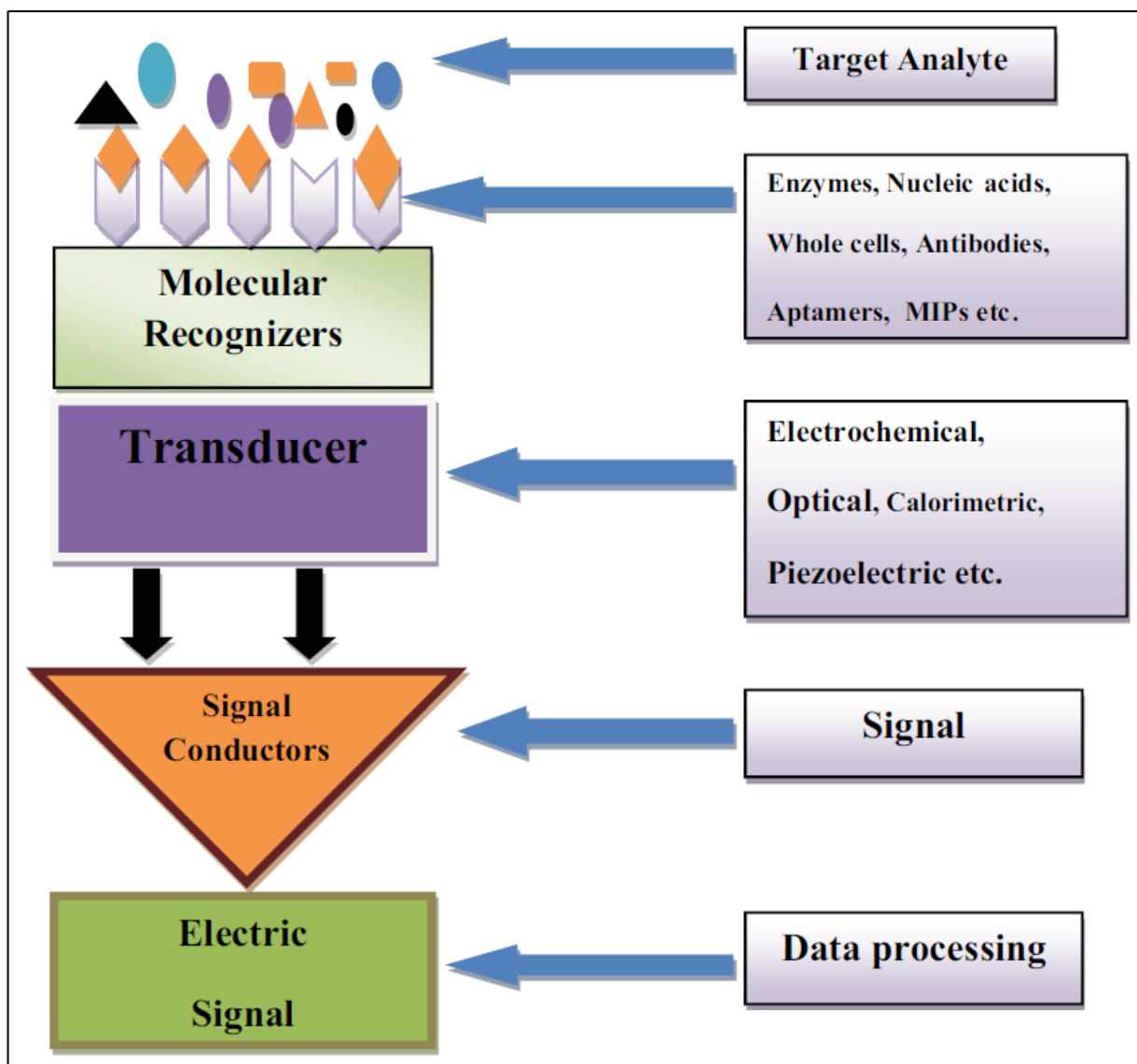


Figure 2.13. The basic set-up of components of the biosensor for its construction [61].

### 2.3.1. Electrochemical Biosensors

Electrochemical biosensors have been utilized for a long time to reach a wide range of applications in various areas. These sensors represent a typical platform for the construction of biosensors, which include semiconductors (transducers) and screen-printed electrodes. Briefly, these biosensors monitor any alterations in dielectric properties, dimension, shape and charge distribution while antibody–antigen complex is formed on the electrode surface. They can be classified into three major groups: (i) potentiometric, (ii) amperometric, and (iii) impedimetric transducers. These biosensors

have been employed to detect a variety of biological targets, including proteins, antigen, deoxyribonucleic acid, antibody, and heavy metal ions [63-65].

### **2.3.2. Piezoelectric Biosensors**

One of the most common piezoelectric biosensors is quartz crystal microbalance biosensor, which measures any mass change (i.e., load or unload) and viscoelasticity of materials by recording frequency and damping change of a quartz crystal resonator. Due to high sensitivity to environmental conditions, the sensing mechanism significantly requires an isolation equipment that minimizes/eliminates any hindrance factors such as vibration. These biosensors have been used in a wide variety of applications, including biotargets with low molecular weights, carbohydrates, proteins, nucleic acids, viruses, bacteria, cells, and lipid-polymeric interfaces [66, 67].

### **2.3.3. Optical Biosensors**

Optical biosensors focus on the measurement of a change in the optical characteristics of the transducer surface when biotarget and recognition element form a complex. These biosensors can be divide into two groups: (i) direct and (ii) indirect. In the direct optical biosensors, signal generation depends on the formation of a complex on the transducer surface. The indirect optical biosensors are mostly designed with various labels such as fluorophores or chromophores to detect the binding events and amplify the signal. Although indirect biosensing methods can produce higher signal levels, they suffer from non-specific binding and high reagent cost of labelling step [68]. In the literature and the market, there are multiple optical biosensors, including optrode-based fibre optic biosensors, evanescent wave fibre optic biosensors, time-resolved fluorescence, the resonant mirror optical biosensor, interferometric biosensors and surface plasmon resonance biosensors [56]. Their detection window is so versatile and they sense multiple types of biomolecules from physiological and biological specimens [69-71].

## **2.4. Surface Plasmon Resonance Biosensors**

### **2.4.1. The Background of Surface Plasmon Resonance**

Surface plasmon resonance (SPR), an evanescent wave-based refractive index (RI) technique, monitors real-time biomolecular interactions. Historically, the first observation of this phenomenon was reported by Wood in 1902 [72]. Later on, the excitation of surface plasmons was independently presented by Kretschmann [73] and Otto [74]. Fifteen years later, Liedberg utilized this modality as gas detection [75]. However, until the 1990s, SPR was not commercially available to detect biomolecular interactions, and after that, the first SPR biosensing instrument was released to the market [76, 77].

### **2.4.2. The Principle of Surface Plasmon Resonance**

The first configurations (Kretschmann and Otto configurations) are still the most common approaches modalities to excitation of surface plasmons (Figure 2.14). This technique utilizes a metal film, typically gold or silver and two different media with a different refractive index like a prism and a sample to act as an optical biosensor. The interaction of a wave with free electrons at the metal film will induce the excitation of surface plasmons, result in reducing in the reflected light intensity. This calls as surface plasmon resonance (SPR) and happens only at a resonance angle. This SPR angle is adapted by adding the analyte onto the metal film to allow the detecting of binding.

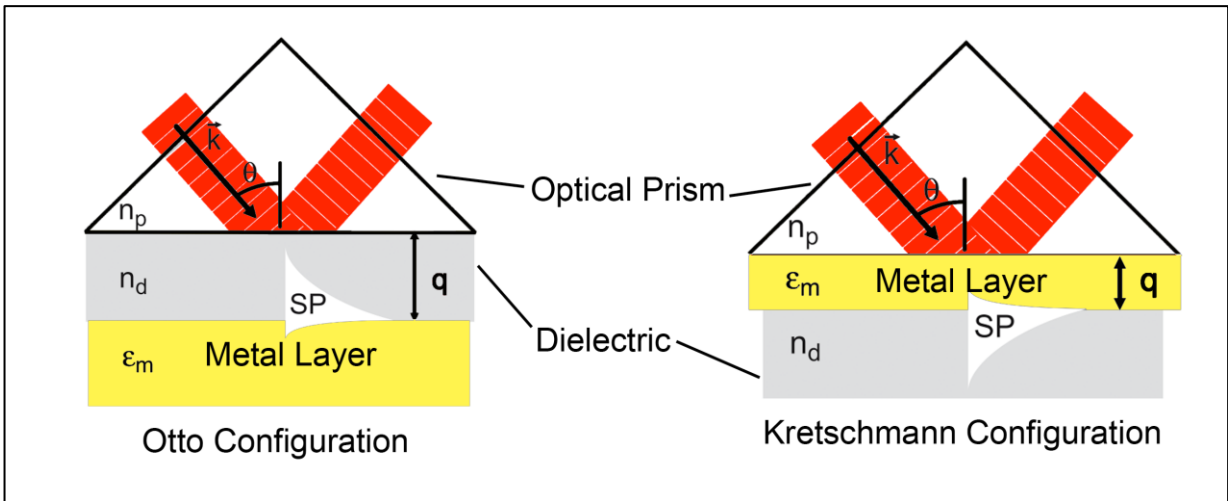


Figure 2.14. The excitation of surface plasmons in the Otto and Kretschmann configurations [50].

The SPR profile is affected by the choice of metal due to its inherent optical properties, such as dielectric permittivity. Figure 2.15 compares the SPR curve, a plot of reflected light intensity vs the incident angle for gold and silver films in the air [78]. The sharper resonance peak of silver is obvious and can be attributed to the intrinsic dampening of the surface plasmon oscillations on the metal film. All surface plasmon metals will tend to dampen these oscillations due to scattering of the electric field of the excitation light. A variety of metals will produce SPR. Metals with high free electron density such as gold and silver are mostly utilized to produce strong surface plasmons on the surface. Especially, gold is the preferred metal as other metals are not as practical. For example, some are too expensive (In), violently reactive (sodium), too broad in their SPR response (copper, aluminum), or too susceptible to oxidation (silver). Due to high resistance to oxidation and easy-to-functionalize surfaces, the gold material holds great potential and it is the most widely used metal material in SPR approaches [79].

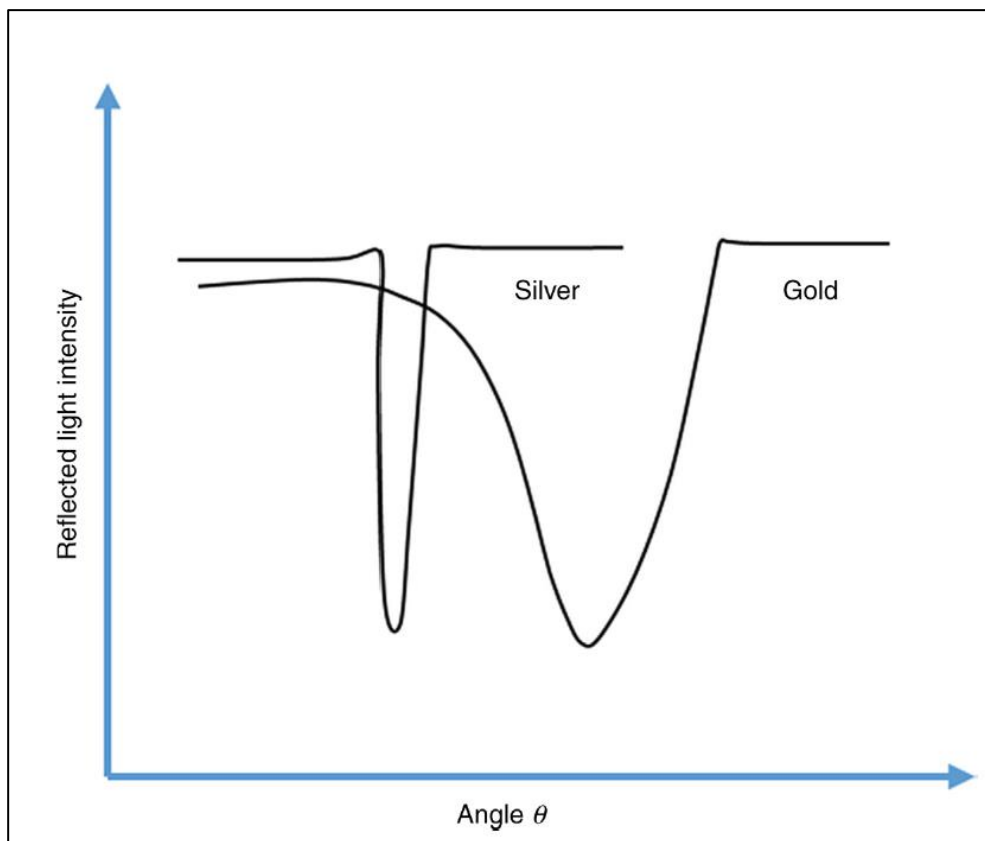


Figure 2.15. The differences between gold and silver SPR curves [78].

As shown in Figure 2.16, a typical SPR sensorgram that obtains from an experiment is composed of multiple analyte injection cycles using the SPR biosensor (1). Injection of analyte solution complementary to the ligand results in a population of the surface active sites (2) leading to saturation (3) and a corresponding increase in the SPR response. Upon completion of the injection, the bound analyte will dissociate from the surface (4) reducing the SPR response, until an injection of a regeneration buffer removes any remaining bound analyte (5) to regenerate the ligand-immobilized surface (6) in preparation for the next analyte sample [80]. The major advantages and disadvantages are demonstrated in Table 2.4.

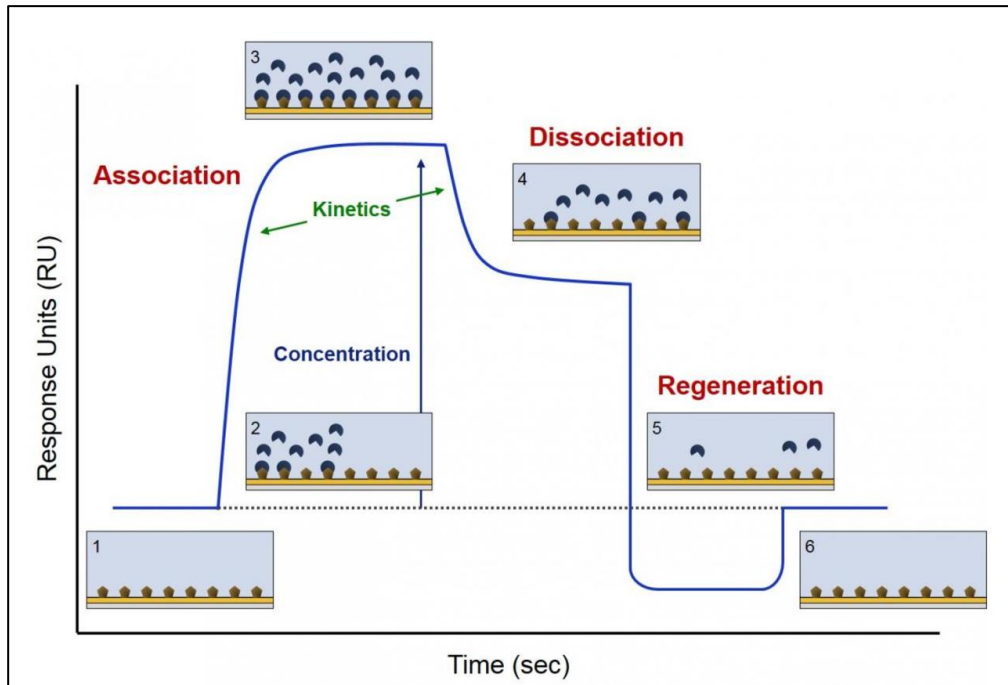


Figure 2.16. The schematic representation of the SPR sensorgram [80].

Table 2.4. The main advantages and disadvantages of surface plasmon resonance system.

Advantages	Disadvantages
<ul style="list-style-type: none"> <li>• Label-free environment</li> <li>• Real-time, continuous measurements</li> <li>• Generic methods for diverse molecule sets</li> <li>• Quik testing</li> <li>• Highly sensitive</li> <li>• Small sample amounts and volumes</li> <li>• Specific to binding event</li> </ul>	<ul style="list-style-type: none"> <li>• Immobilization effects</li> <li>• Steric hindrance with binding events</li> <li>• Non-specific binding</li> <li>• Limited mass transport</li> <li>• Control experiment needed</li> <li>• Misinterpretation of data common</li> <li>• Expense of biosensor chips and instrumentation</li> </ul>



### 2.4.3. Application of Surface Plasmon Resonance

To date, SPR has been one of the most popular core technology, and it has integrated into several research-based biosensing devices due to its rapid response ultra-sensitivity, and lower instrumentation cost as compared to the other optical technologies such as liquid chromatography, mass spectrometry, Raman/IR spectroscopy, fluorescence labeling enzyme assay, and so on. These biosensing surfaces can be decorated with different chemical approaches.

In the literature, there are numerous publications and ongoing researches around surface plasmon resonance integrated with molecular imprinting method (Figure 2.17). During this statistics, “surface plasmon resonance” was selected as a keyword to classify the publication numbers in the MIP database [58]. On the other hand, “imprint” with “surface plasmon resonance” was chosen as keywords to count the publication numbers in the Science Direct database [59]. According to results, the total publication numbers are calculated as 70 (a) and 1259 (b) for MIP and Science Direct databases since 2007. It can be observed that the different publication numbers for molecular imprinting based surface plasmon resonance are published for each year and changing with different databases.

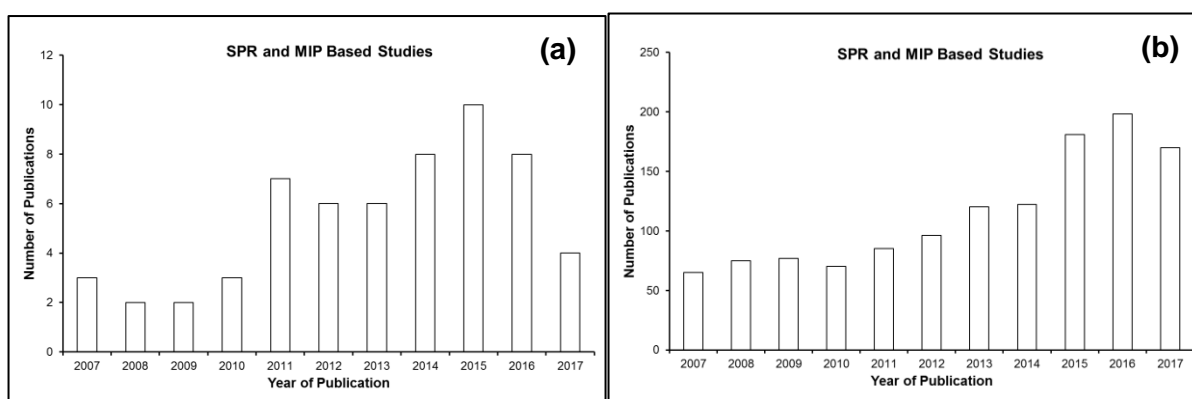


Figure 2.17. The number of publications in MIP (a) and Science Direct (b) databases for molecular imprinting based surface plasmon resonance biosensors.

## 2.5. Microfluidics

Microfluidics provides the high capability to manipulate and analyze minute volumes of fluid. This technology is an emerging approach with several applications in the different disciplines. Modern microfluidics [101] can be followed back to the evolution of a silicon chip-based gas chromatography at Stanford University [102] and the ink-jet printer at International Business Machines [103] in the end of 1970s. Although these systems were very extraordinary, the conception of the integrated microfluidic system was not advanced until the early 1990s [104].

Microfluidic techniques have been utilized in the fields of biology, chemistry, proteomics, genomics, biodefense, pharmaceuticals, and other related areas. From a biological perspective, microfluidics especially mimicks the limits of volume in cellular systems, where biological processes include small amount fluidic transport. Such an example, molecular transfer occurs across cellular membranes, to oxygen diffusivity through the lungs, to blood flow through micro-scale arterial networks. Furthermore, microfluidics can potentially enable more realistic in vitro conditions for small-scale biological molecules. Several biological entities and structures were here demonstrated with common micro-fabrication forms utilized in microfluidic approach (Figure 2.18) [14].

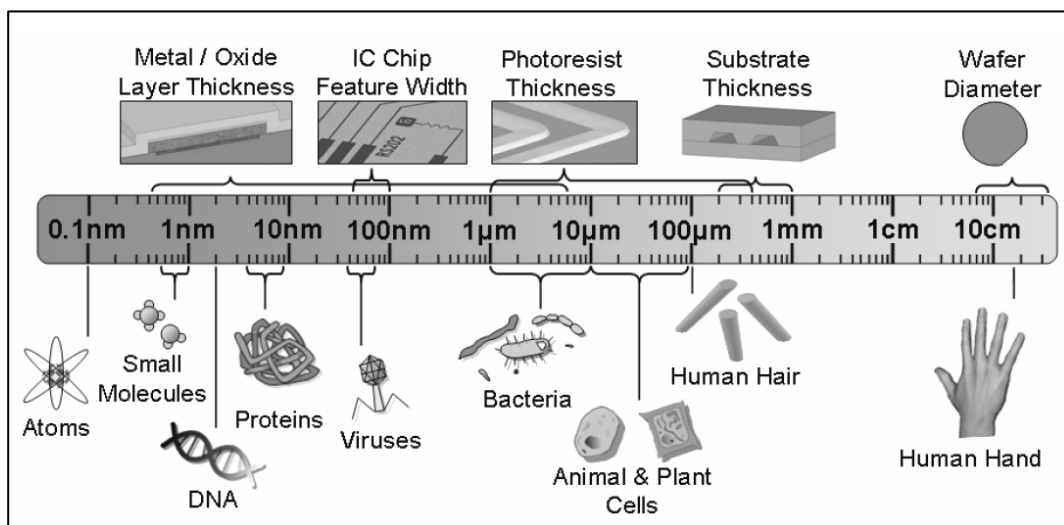


Figure 2.18. The length scales for several structures [14].

### 2.5.1. Microfluidic-Integrated Biosensors

Since microfluidics requires low sample volume, decreased processing time, low cost analysis and low reagent consumption, there is a growing demand in the integration biosensors with microfluidics. These hybrid platforms would also have multiple advantages, such as multiplexing, minimal handling of hazardous materials, portability, and versatility in design. Furthermore, these integrated platforms will improve the current sensing technologies in terms of analytical capability and widen potential applications in medical diagnostics. By further miniaturization and improvements, these hybrid platforms have been adopted to point-of-care diagnostics [105].

In regard to cost, microfluidic chips need plastic components, which are really inexpensive and also can be simply fabricated. An only key factor in choosing suitable polymers for microfluidic chips is to use transparent area on spectral regions of interest for available detectors. As a result of this criterion, acrylates such as polymethyl methacrylate, polydimethylsiloxane, cyclic olefin copolymer, and polycarbonate are one of the best candidates as chip base material (Figure 2.19). Further, polymethyl methacrylate (PMMA) is the most widely-used thermoplastic polymer, and it provides a transparent plastic like plexi-glass at its solid state. In addition, high thermal stability, high chemical resistances, and low cost are the other encouraging factors for the use of PMMA [106].

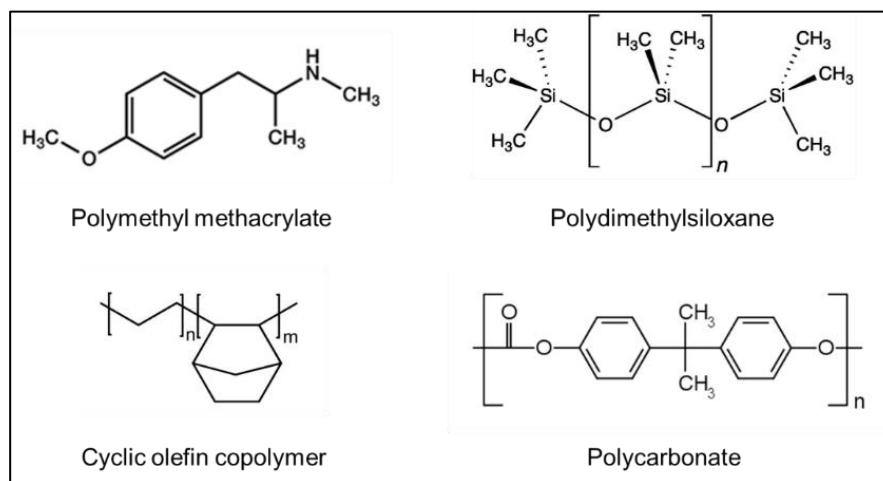


Figure 2.19. The chemical structures of common thermoplastics.

### 3. EXPERIMENTAL

#### 3.1. Materials

Acrylamide (AAm, A3553, Sigma), N,N-methylenebis acrylamide (MBAAm, M7279, Sigma), ammonium persulfate (APS, A3678, Sigma), N,N,N',N'-tetramethylethylenediamine (TEMED, T9281, Sigma), bovine hemoglobin (Hb, H3760, Sigma), bovine serum albumin (BSA, A2153, Sigma-Aldrich), lysozyme (Lyz, 62971, Fluka), transferrin (Trf, T8158, Sigma-Aldrich), myoglobin (Myb, M0640, Sigma), 2-propene-1-thiol (Allyl mercaptan, 06030, Sigma-Aldrich), dipotassium hydrogen phosphate ( $K_2HPO_4$ , 60356, Sigma-Aldrich), potassium dihydrogen phosphate ( $KH_2PO_4$ , 04243, Sigma-Aldrich), gold surfaces (GWC-1000-050, GWC Technologies, Madison, Wisconsin), 11-mercaptoundecanoic acid (MUA, 450561, Aldrich, Sigma Aldrich), N-(3-dimethylaminopropyl)-N'-ethyl carbodiimide hydrochloride (EDC, 03450, Fluka, Sigma Aldrich), MES (M3671, Sigma, Sigma Aldrich), N-hydroxy succinimide (NHS, 130672, Aldrich, Sigma Aldrich), protein G (21193, Thermo Scientific), human hemoglobin antibody (MA5-14708, Thermo Fisher Scientific), human hemoglobin (MBS173108, MyBioSource), poly methyl methacrylate (PMMA, McMaster Carr, Atlanta, GA), double sided adhesive (DSA, iTapestore, Scotch Plains, NJ) were purchased for all experiments.

#### 3.2. Characterization of Acrylamide

Acrylamide monomer sample was placed in a Fourier transform infrared (FTIR) spectroscopy (Thermo Fisher Scientific, Nicolet iS10, Waltham, MA, USA) and total light reflection was quantified in the wavenumber range  $500\text{--}4000\text{ cm}^{-1}$  at  $2\text{ cm}^{-1}$  resolution and scanned by pellets consisting of 2.0 mg microspheres and 98.0 mg KBr (IR grade Merck, Germany).

#### 3.3. Modification of SPR Surfaces

The modification of the gold SPR surfaces was carried out with allyl mercaptan ( $CH_2CHCH_2SH$ ). 5.0  $\mu\text{L}$  of allyl mercaptan was dropped and incubated overnight to

present allyl groups onto the gold surface of SPR. After the modification, the gold SPR surfaces were washed with alcohol and dried to be ready for imprinting steps.

### 3.4. Preparation of Hemoglobin:Acrylamide Pre-Complex

The hemoglobin:acrylamide pre-complex was prepared with Hb (1  $\mu\text{mol}$ ) and different amounts of AAm (1, 2, 3, 4, 5 mmol) dissolved in 1.0 mL water, was stirred 30 min with the help of magnetic stirrer. The ratio of monomer to the template was evaluated by UV-visible spectrophotometer (Shimadzu, Model 1601, Japan). Spectrum measurements were continued until no increment of absorbance belongs to the formed pre-complex between hemoglobin template and AAm monomer could be seen.

### 3.5. Preparation of Hemoglobin Imprinted SPR Biosensor

Hemoglobin imprinted SPR biosensor was prepared by using Hb:AAm pre-complex and MBAAm (6.0 mg) as a cross-linker. To obtain hemoglobin imprinted thin film, 10  $\mu\text{L}$  APS (%10) and 10  $\mu\text{L}$  TEMED (%5) as an initiator/activator pair was added to the modified gold SPR surface was coated uniformly by spin coating (Figure 3.1 (a)). The polymerization was carried out under UV light (100 W, 365 nm) by photo-polymerization method for 30 min (Figure 3.1 (b)). At the end of polymerization, the unreacted monomer and impurities were removed by washing ethyl alcohol and dried.

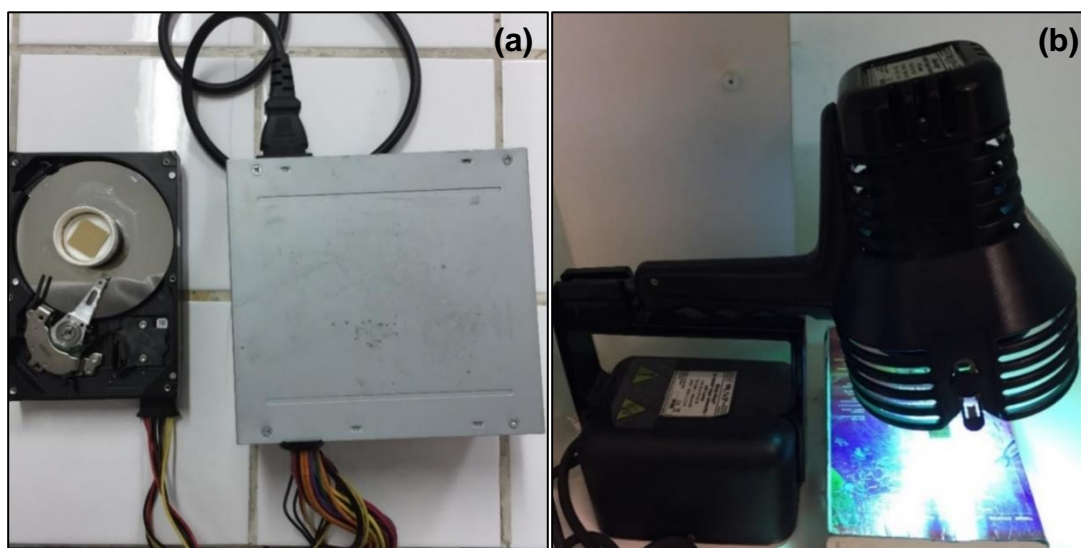


Figure 3.1. Hand-made spin coater (a) and UV light (b) systems.

### 3.6. Removal of Hemoglobin

Hemoglobin imprinted SPR biosensor was washed with 0.01 M NaCl in an hour to remove the template from hemoglobin imprinted SPR biosensor. This process was repeated several times until not determination at 406 nm with a UV-visible spectrophotometer.

### 3.7. Characterization of SPR Biosensors

Characterization studies of hemoglobin imprinted and non-imprinted SPR biosensors were done via Fourier transform infrared-attenuated total reflectance (FTIR-ATR) spectroscopy, atomic force microscopy (AFM), ellipsometry and contact angle analysis.

#### 3.7.1. FTIR-ATR Spectroscopy Analysis

The hemoglobin imprinted and non-imprinted SPR biosensors were placed one by one in an FTIR-ATR spectroscopy system (Figure 3.2).



Figure 3.2. FTIR-ATR spectroscopy system.

### 3.7.2. Atomic Force Microscopy Analysis

The atomic force microscope (AFM) was employed in tapping mode (Nanomagnetics Instruments, Oxford, UK) to characterize the surfaces of the bare, non-imprinted and hemoglobin imprinted SPR biosensors. The AFM system could perform measurements in high resolution due to the cantilever interferometer (Figure 3.3). The bare, non-imprinted and hemoglobin imprinted SPR biosensors were placed to the AFM system and images were obtained with definite conditions.



Figure 3.3. Atomic force microscopy system.

### 3.7.3. Ellipsometry Analysis

Ellipsometry measurements of the non-imprinted and hemoglobin imprinted SPR biosensors were accomplished via using an ellipsometry system (Nanofilm EP3, Germany) with definite conditions (Figure 3.4).

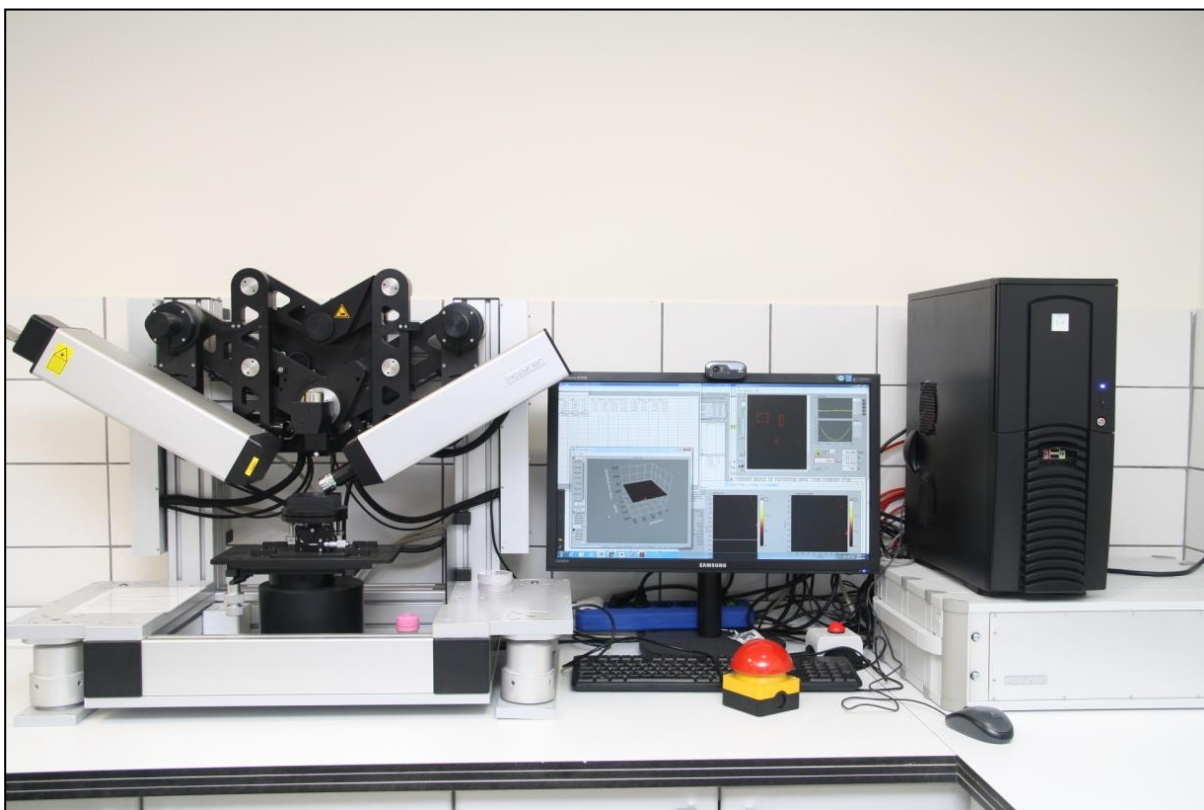


Figure 3.4. Ellipsometry system.

### 3.7.4. Contact Angle Analysis

The contact angle values of biosensor surfaces were measured by KRUSS DSA100 system (Hamburg, Germany). A sessile drop method was used to obtain contact angle values of the bare, non-imprinted and hemoglobin imprinted SPR biosensors. They were calculated as the average of the contact angles of different drops (Figure 3.5).



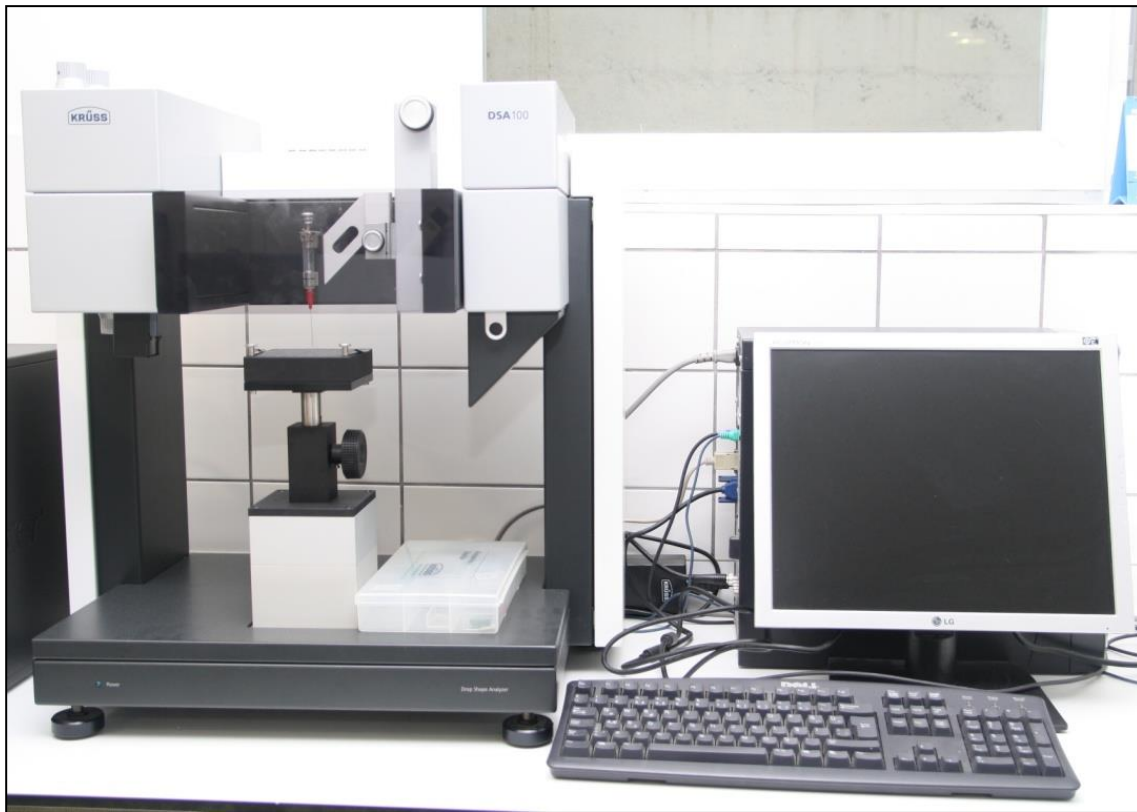


Figure 3.5. Contact angle analysis system.

### **3.8. Surface Plasmon Resonance Analysis**

Kinetic studies with hemoglobin imprinted and non-imprinted SPR biosensors done by using SPRImager II (GWC Technologies, Madison, USA) (Figure 3.6 and Table 3.1). The sensorgram data are obtained by Digital Optics V++ software and Microsoft Excel software. The optic images of preparation steps of SPR system for analysis in Figure 3.7.



Figure 3.6. Surface plasmon resonance system.

Table 3.1. The specifications of the SPR system used in this study according to the manufacturer.

	<b>SPR-IMG-802-240</b>
Electrical supply	230/240V 50-60Hz
Power consumption	70W
Ambient operating temperature	15 - 35°C
Sample operating temperature	Ambient – 60°C
Sensitivity, SPRchip™ samples	8pg mm <sup>-2</sup>
Fluid flow rate min-max speed	30-600 ml/min (.031" ID tubing)
Standard flow cell volume	17 µL
Operating wavelength	800 nm
Incident light angle range	40-70°
Benchtop footprint	25" x 18" (63cm x 45cm)
Net weight	24 kg
CCD camera	1/2" format, 768x494 pixels
Prism material	SF10 prism (n=1,720)

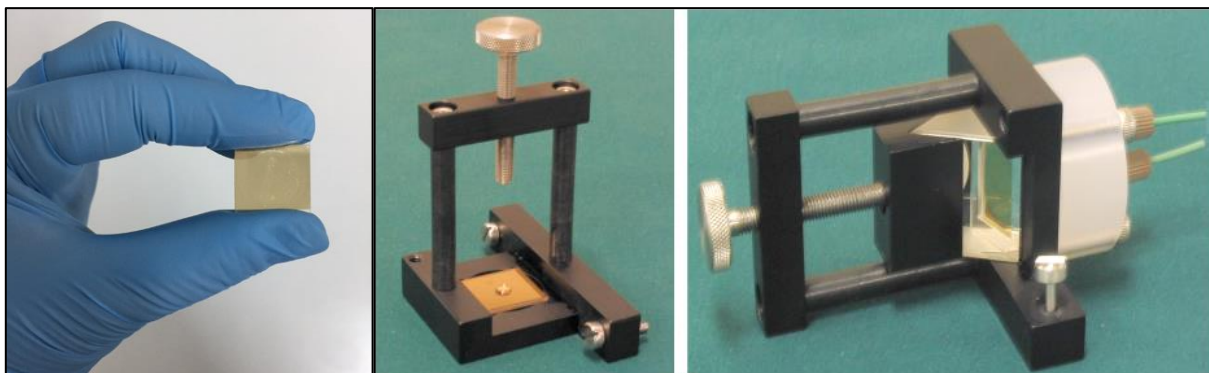


Figure 3.7. Preparation steps of SPR system for analysis.

All studies were done at room temperature. Incidence angle set to one third of the difference between the minimum and maximum reflectivities. Because of slow flow rates are better to increase the chance for the ligand to adsorb to the surface SPR measurements are done at 150  $\mu\text{L}/\text{min}$  flow rate. Flow rate calculated by water mass weighting against time.

### 3.9. Kinetic Analysis

Kinetic analysis were first performed in different pH solutions that range from 4.0-8.0 with same hemoglobin concentration (0.1 mg/mL) and then different hemoglobin concentrations from 0.0005 mg/mL to 1.0 mg/mL. After obtaining pH that response maximum reflectivity change and adjusting the plasmon curves and resonance angle, adsorption buffer solution, pH 6.0, was passed from the SPR system. Then, hemoglobin solutions with different concentrations were pumped at the SPR system individually. The value of reflectivity change ( $\% \Delta R$ ) was observed instantly and desorption agent, 0.01 M NaCl, was provided when the system was in an equilibrium condition. After the desorption process, SPR biosensor was regenerated with water and adsorption buffer was re-equilibrated. Adsorption-desorption-regeneration steps were repeated in each sample solution. The signal changes for each concentration are then calculated from a series of difference images obtained by subtracting the reference image from the image

obtained at each concentration of the analyte. Reflectivity changes are then plotted versus concentration of the analyte.

### **3.10. Selectivity Analysis**

The selectivity of non-imprinted and hemoglobin imprinted SPR biosensors was investigated by using lysozyme (Lyz), transferrin (Trf), bovine serum albumin (BSA), and myoglobin (Myb), solutions as competing proteins in same concentrations (0.1 mg/mL). In addition, the selectivity studies were done with a mixture of these competing proteins and hemoglobin in the same concentration (0.1 mg/mL).

### **3.11. Reusability Analysis**

To demonstrate the reusability of hemoglobin imprinted SPR biosensor, the same hemoglobin solution was given to SPR system for four times. In addition, the different concentrations of hemoglobin solutions that range from 0.1 mg/mL to 1.0 mg/mL were also performed for reusability studies.

### **3.12. Preparation of Portable Microfluidic-Integrated SPR Biosensors**

#### **3.12.1. Fabrication of Gold Surfaces**

The gold surfaces were fabricated in optimum condition. They washed with solvents to remove impurities before microfluidic chip assembly. In the first step of the cleaning, the gold chips were submerged in an isopropanol and ethanol (1:1) bath and heated 60°C for 5 min. They were then cleaned with deionized water and dried under N<sub>2</sub> atmosphere. Followed by drying step, the surfaces were submerged piranha solution (H<sub>2</sub>O:H<sub>2</sub>O<sub>2</sub>:NH<sub>4</sub>OH, 5:1:1) for 5 min, and they were rinsed with ethanol and dried under either ambient conditions or N<sub>2</sub> atmosphere.

### 3.12.2. Construction of Microfluidic Chips

As seen in Figure 3.8, a laser cutter (Versa Laser TM, Scottsdale, AZ) was used to cut the PMMA and DSA and construct the microfluidic chip. The microfluidic chip dimensions set as 31x57x3 mm. Two PMMA (3.0 mm) layers were combined by employing a layer of DSA (50 nm). Other DSA layer and a gold coated surface fabricated a microchannel. The microchannel (12x37x50 nm) was placed in the middle of the microfluidic chip. The PMMA-DSA-PMMA-DSA-gold surface was combined with a one use. Two holes were cut into the PMMA layer with a diameter as 0.7 mm that used as the inlet and outlet. The other DSA layer produced a microchannel with a channel volume of 4.0  $\mu$ L. The last step, a gold surface of dimensions 1.4x1.4 cm was mounted onto the microfluidic chip. All parts of the microfluidic chip and portable SPR system was represented in Figure 3.9 (a) and Figure 3.9 (b).

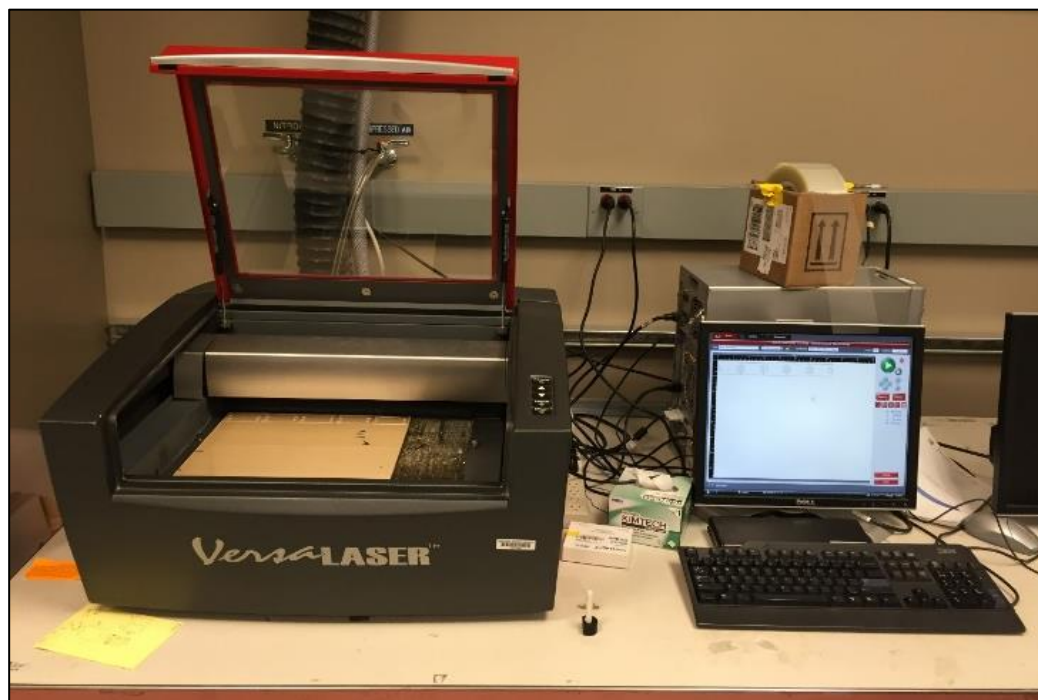


Figure 3.8. The laser cutter system.

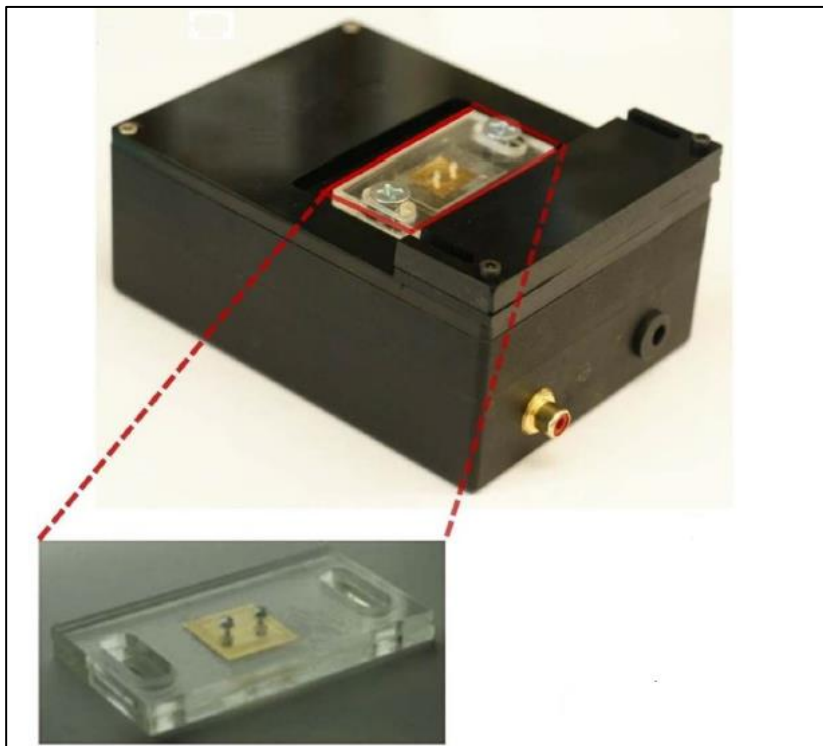
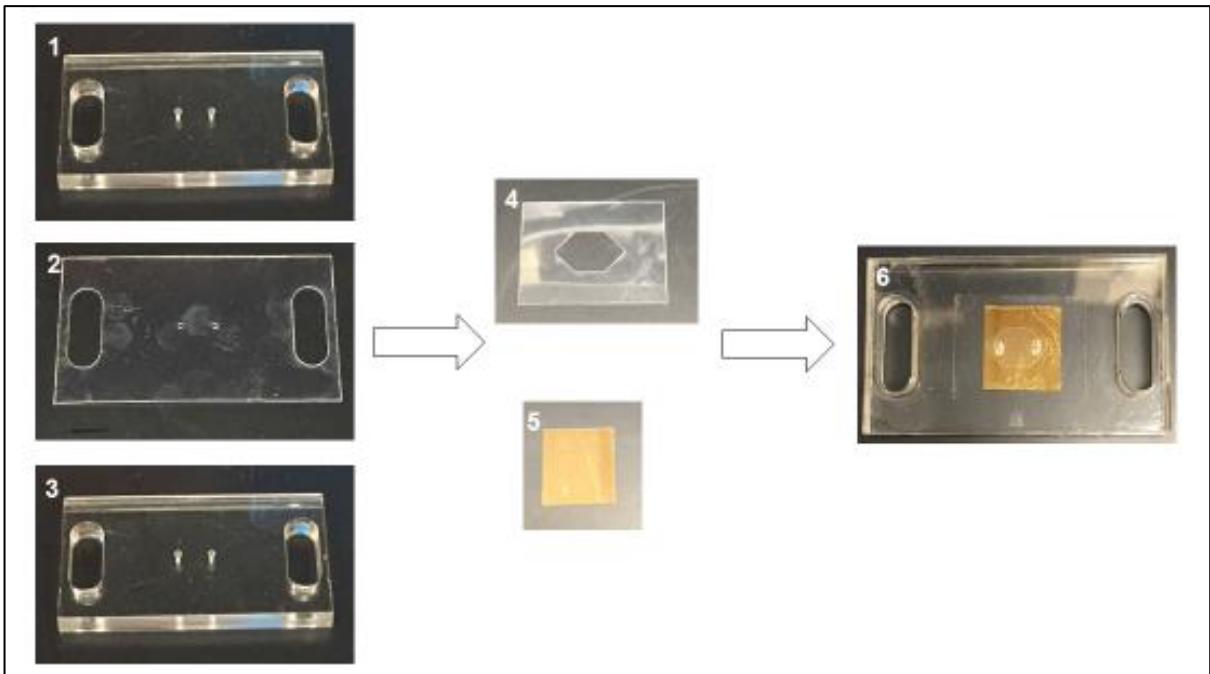


Figure 3.9. All parts of the microfluidic chip (a) and portable SPR system (b) [15].

### 3.12.3. Modification of Microfluidic-Integrated SPR Biosensors

After cleaning, the gold surfaces were modified with a layer-by-layer surface chemistry approach. Briefly, the gold surfaces were incubated with 11-mercaptoundecanoic acid (MUA, 10 mM) prepared in ethanol overnight at room temperature, and carboxyl groups were originated onto the gold surface. Then, the gold surface was integrated with the microfluidic chip, and the tubings were attached to the inlets and outlets using epoxy. The gold surfaces were then washed with 300  $\mu$ L of phosphate buffer saline buffer (PBS, pH 7.4), and then, 100  $\mu$ L of N-(3-dimethylaminopropyl)-N'-ethyl carbodiimide hydrochloride (EDC, 100 mM)/N-hydroxy succinimide (NHS, 50 mM) mixture was introduced into the channel via a syringe through the inlet. EDC/NHS was incubated for 30 min at room temperature. Basically, EDC reacts with carboxyl groups to form amine reactive groups that are stabilized by NHS addition. The succinimide group is produced and this group reacts with amine groups of the protein. The microfluidic-integrated SPR biosensor surfaces were then washed with 300  $\mu$ L of PBS. After that 100  $\mu$ L of protein G (0.1 mg/mL) was added to the microfluidic chip for an hour incubation at room temperature. After the protein G modification, the microfluidic-integrated SPR surfaces were then washed with 300  $\mu$ L of PBS. To detect hemoglobin on the chip surface, we immobilized anti-hemoglobin antibody (100  $\mu$ L, 5  $\mu$ g/mL in PBS) by incubating for an hour at room temperature. Finally, after washing the microfluidic-integrated SPR biosensor, it can be ready for real-time hemoglobin detection. Figure 3.10 is demonstrated the schematic representation of the microfluidic-integrated SPR biosensor. In addition, Figure 3.11 is also showed that the parts of the portable microfluidic-integrated SPR biosensor system.



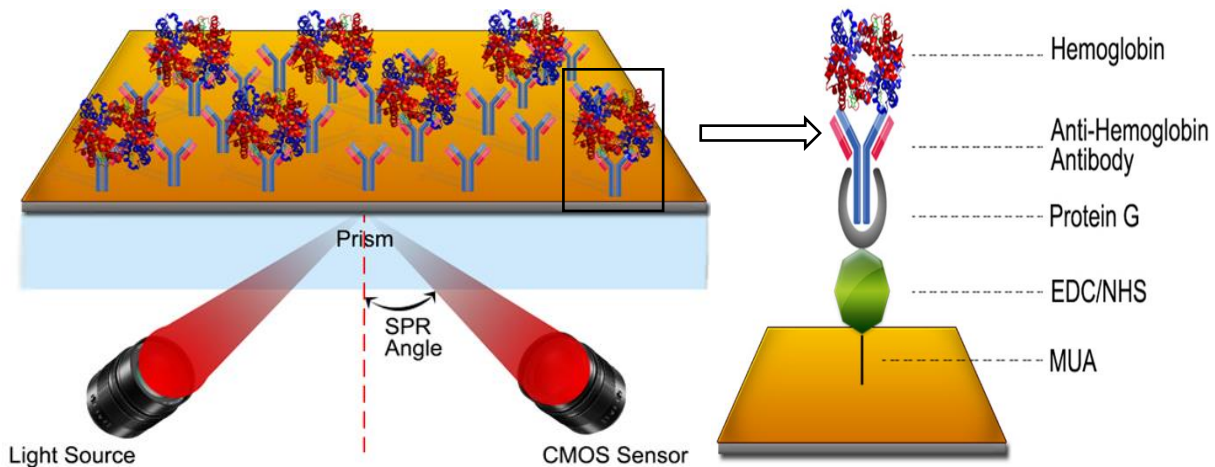


Figure 3.10. Schematic representation of the microfluidic-integrated SPR biosensor.

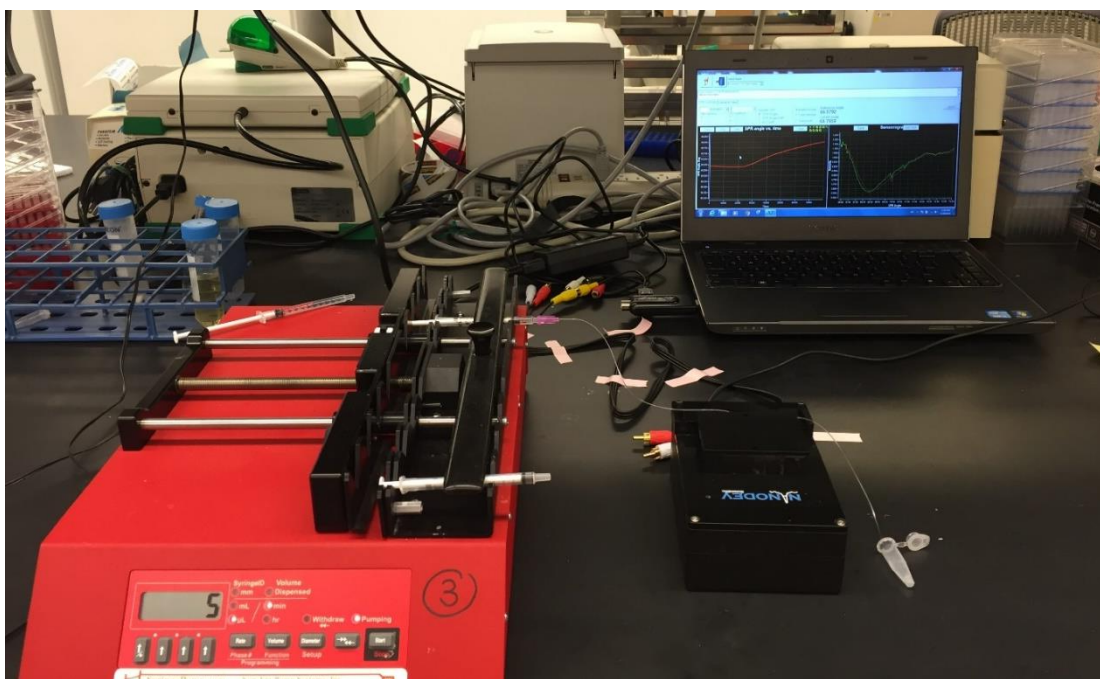


Figure 3.11. The portable microfluidic-integrated SPR biosensor system.



## 4. RESULTS AND DISCUSSION

### 4.1. Characterization of Acrylamide

Acrylamide monomer sample was placed in a sample holder by Fourier transform infrared (FTIR) spectroscopy system and obtained an FTIR spectrum (Figure 4.1). The absorption located in the regions around 3100-3300  $\text{cm}^{-1}$  represents to the asymmetric and symmetric N-H stretching vibrations from acrylamide. The intensity band appearing in the region 2809  $\text{cm}^{-1}$  are assigned to symmetric C-H stretching vibrations. The amide I band (between 1600 and 1700  $\text{cm}^{-1}$ ) is principally related to the C=O stretching vibration and is directly associated with the backbone conformation. The absorption located in the region 1427  $\text{cm}^{-1}$  has been designated to C-N stretching vibrations [107].

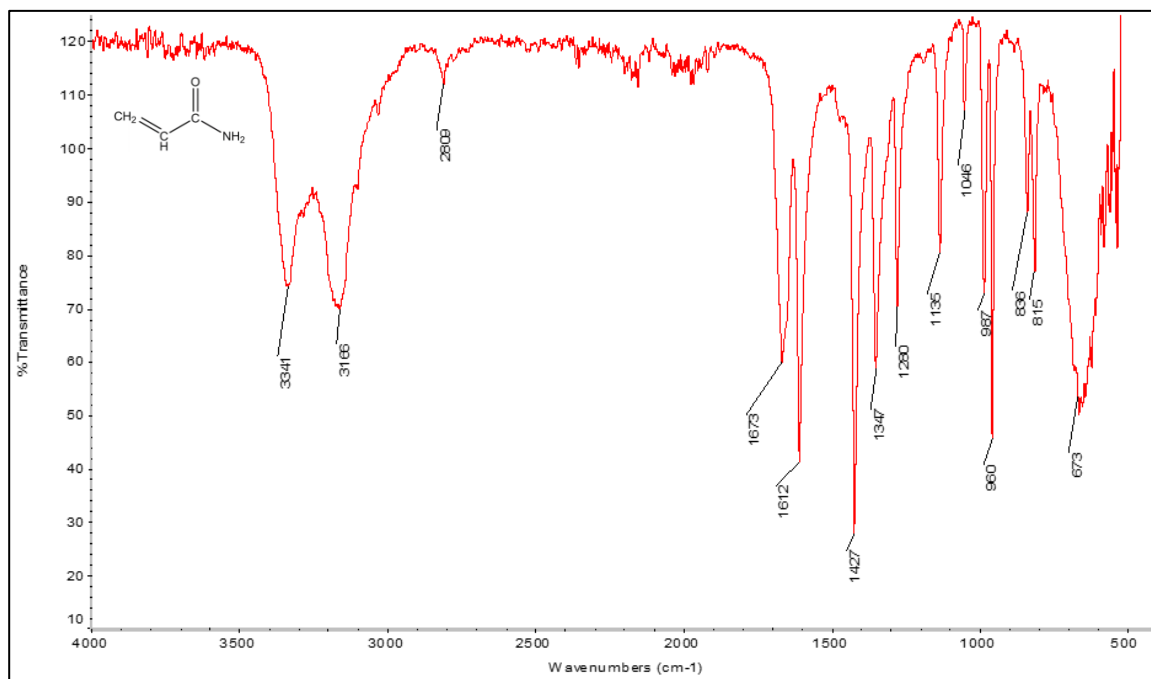


Figure 4.1. The FTIR spectrum of acrylamide monomer.

### 4.2. Preparation of Hemoglobin:Acrylamide Pre-Complex

The hemoglobin:acrylamide (Hb:AAM) pre-complex was prepared with functional monomer, acrylamide and template molecule, hemoglobin. As shown in Figure 4.2, the Hb:AAM pre-complex ratio was chosen as 1  $\mu\text{mol}$ :4 mmol (Hb:AAM). Hb:AAM pre-

complex absorbance intensity increment has ended up at this ratio and polymerization was carried out according to the determined ratio.

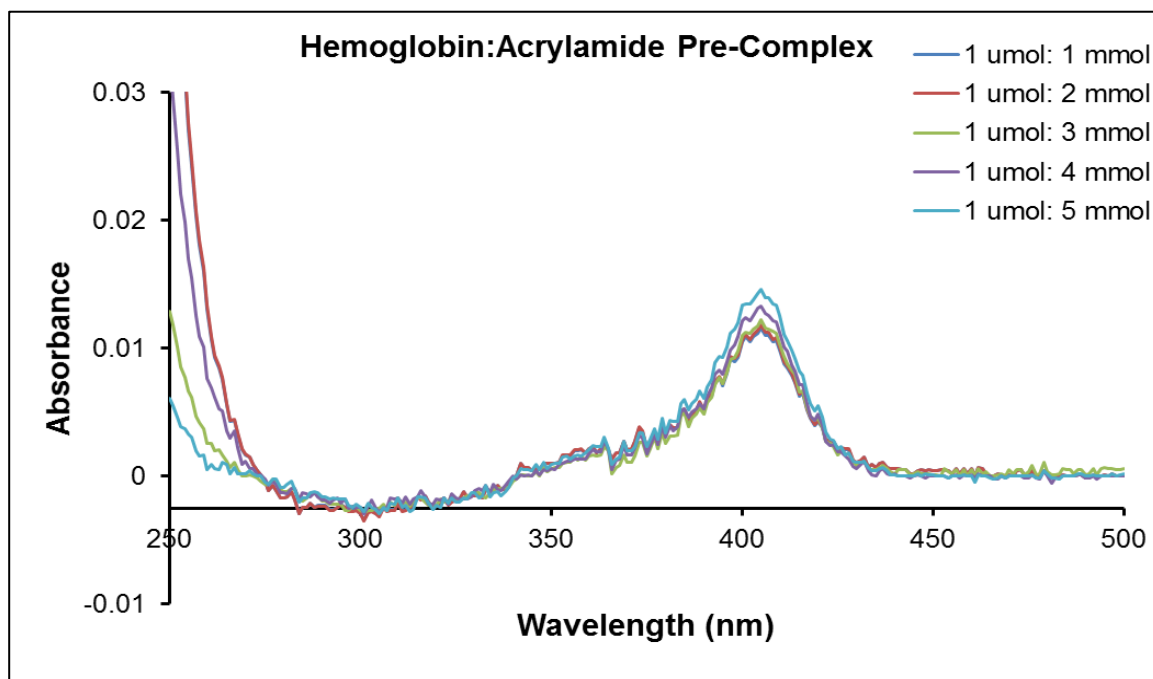


Figure 4.2. The spectrophotometric measurements of hemoglobin:acrylamide pre-complex.

### 4.3. Characterization of SPR Biosensors

#### 4.3.1. FTIR-ATR Spectroscopy Analysis

The hemoglobin imprinted and non-imprinted SPR biosensors were placed in a sample holder by FTIR-ATR spectroscopy system and obtained FTIR spectra (Figure 4.3- Figure 4.4). The absorption located in the regions around  $3100-3300\text{ cm}^{-1}$  represents to the asymmetric and symmetric N-H stretching vibrations from polyacrylamide matrix. The intensity band appears at around  $2900\text{ cm}^{-1}$  are assigned to symmetric C-H stretching vibrations. The amide I bands (between  $1600$  and  $1650\text{ cm}^{-1}$ ) is related to the C=O stretching vibrations. The shifting bands of from  $1647\text{ cm}^{-1}$  to  $1655\text{ cm}^{-1}$  C=O and C-N from  $1448\text{ cm}^{-1}$  to  $1424\text{ cm}^{-1}$  confirmed that the imprinting process succeeded [12].

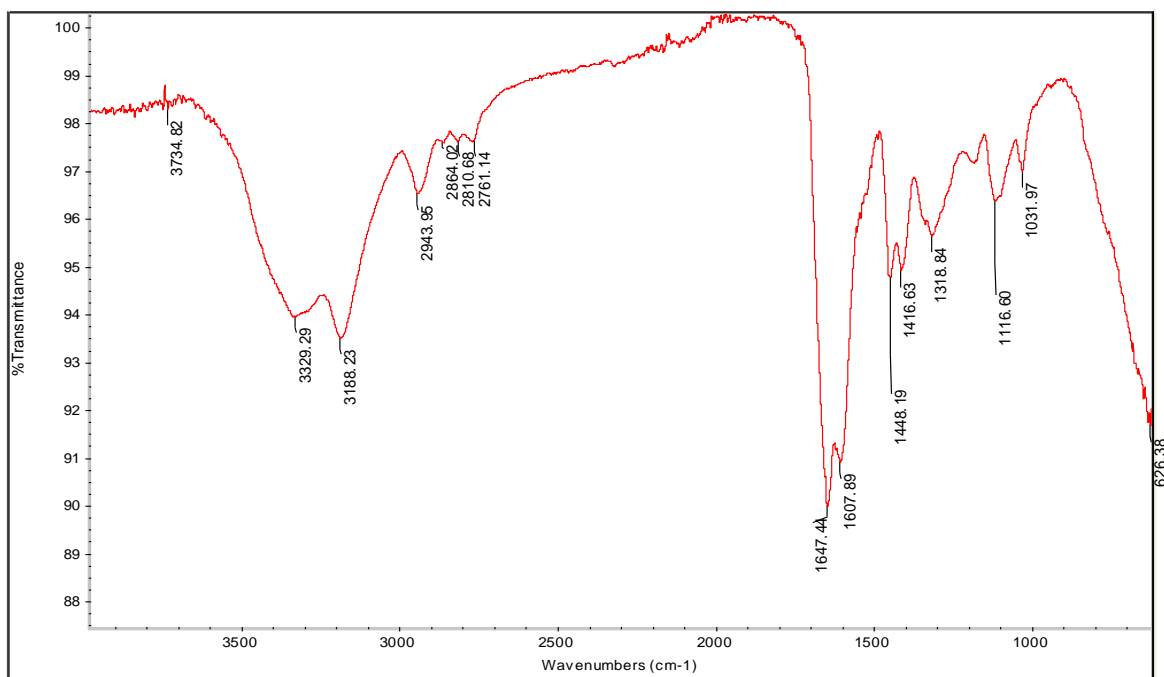


Figure 4.3. The FTIR-ATR spectrum of non-imprinted SPR biosensor.

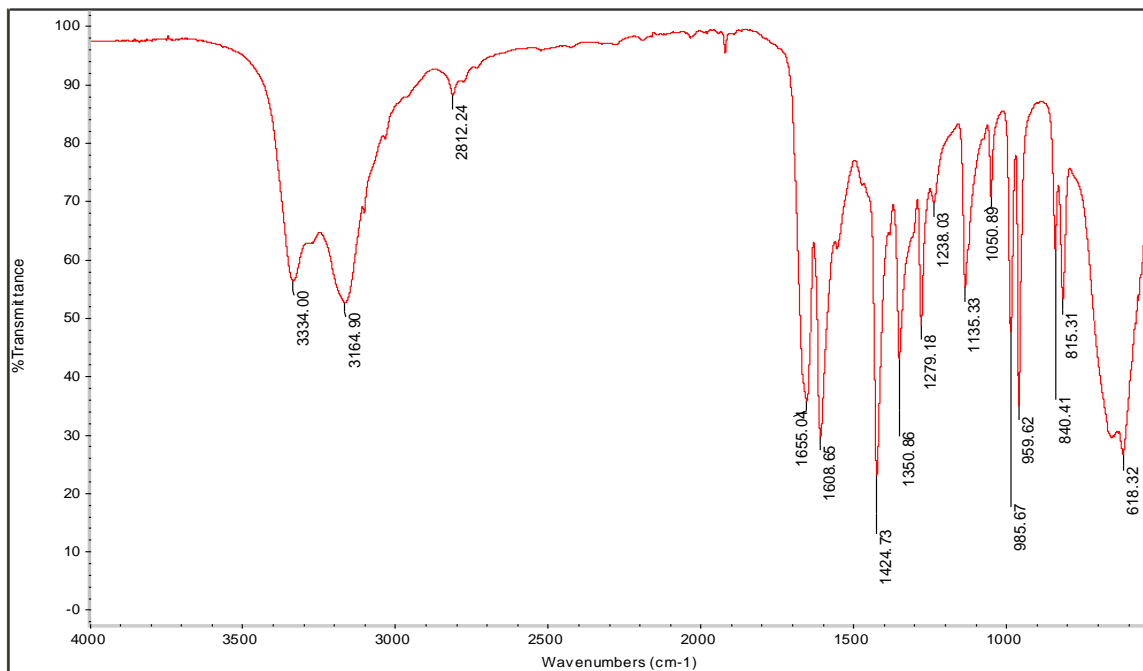


Figure 4.4. The FTIR-ATR spectrum of hemoglobin imprinted SPR biosensor.

### 4.3.2. Atomic Force Microscopy Analysis

AFM analysis was carried out by using Nanomagnetics instrument. As seen in Figures 4.5-4.7, the surface deepness of hemoglobin imprinted SPR biosensor was increased. The AFM images of bare, non-imprinted and hemoglobin imprinted SPR biosensors revealed that the average surface roughness values were increased from 0.54 nm to 1.86 nm that indicated the generation of the polymeric nanofilm. This result also confirmed that the surface roughness was amplified and polymerization was succeeded onto the SPR biosensor. In addition, root mean square (RMS) values were also increased from 0.73 nm to 2.46 nm with imprinting process. The almost homogeneous biosensor surfaces were displayed by AFM images.

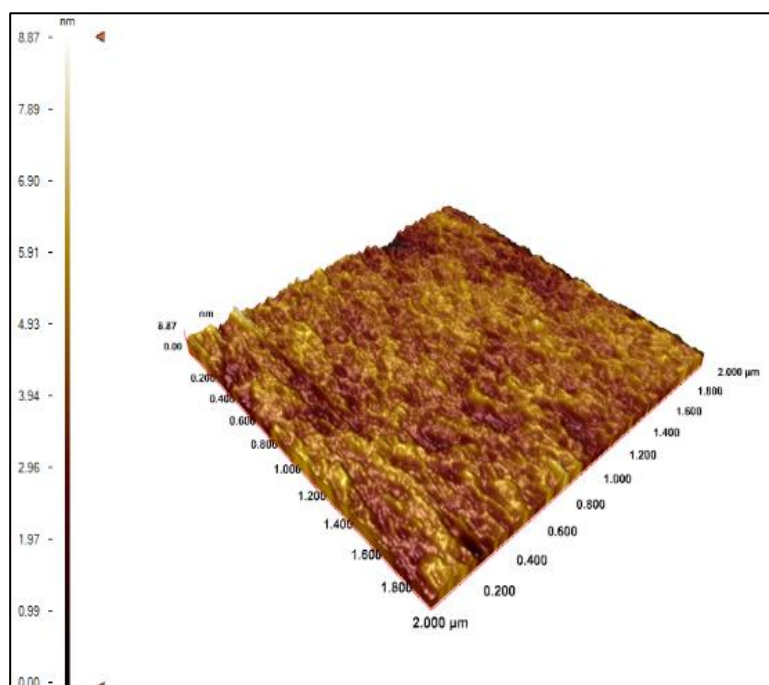


Figure 4.5. The AFM image of bare SPR biosensor.

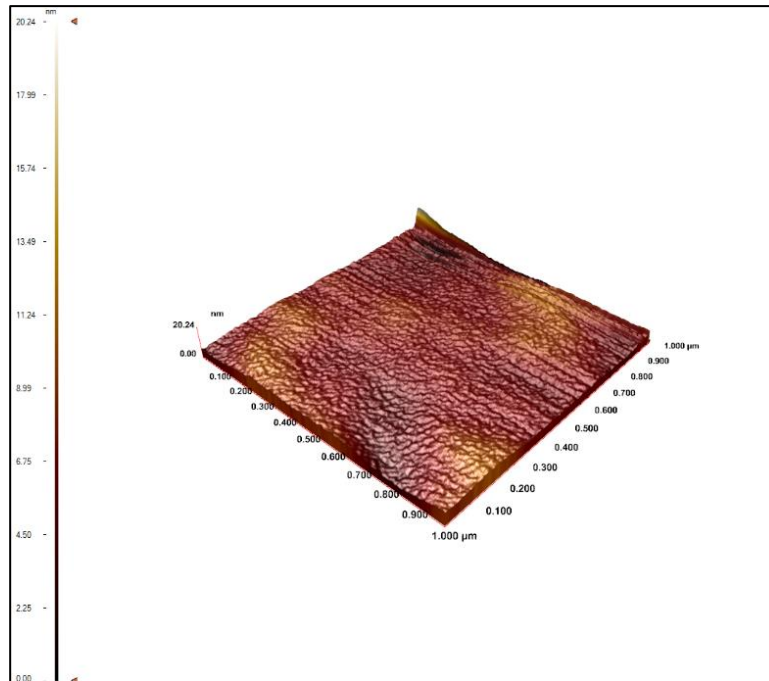


Figure 4.6. The AFM image of non-imprinted SPR biosensor.

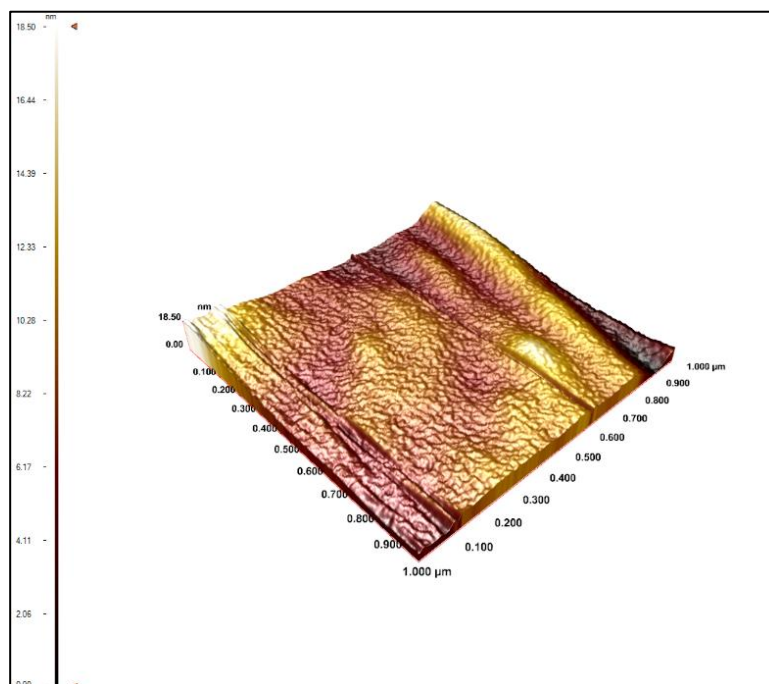


Figure 4.7. The AFM image of hemoglobin imprinted SPR biosensor.

### 4.3.3. Ellipsometry Analysis

Ellipsometry analysis was also accomplished to prove the nanofilm polymerization. Surface thicknesses were calculated as  $88.3 \pm 3.3$  nm and  $87.9 \pm 1.6$  nm for non-imprinted and hemoglobin imprinted SPR biosensors (Figure 4.8 and Figure 4.9). To conclude, it can be assumed that almost homogeneous and monolayer formation of the nanofilm had succeeded.

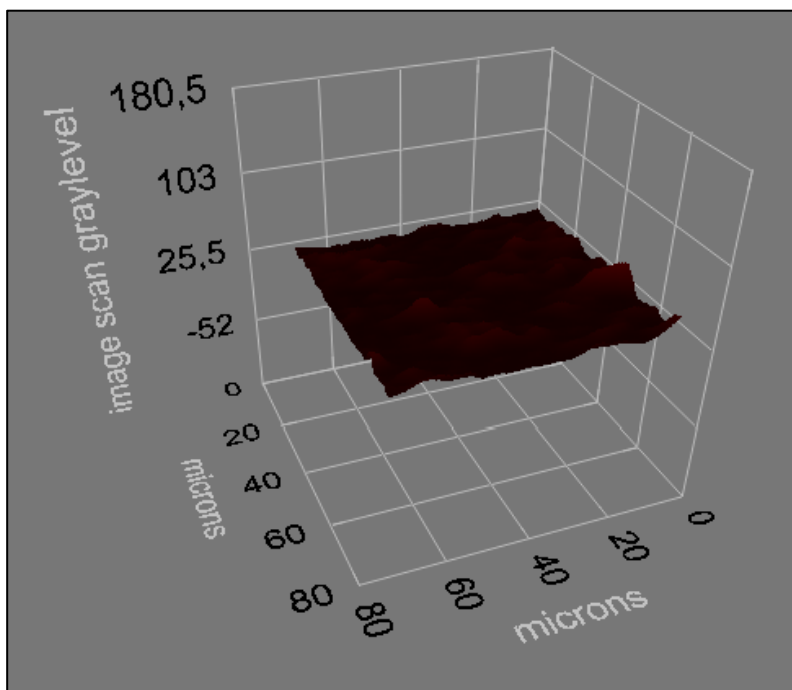


Figure 4.8. The ellipsometer image of non-imprinted SPR biosensor.

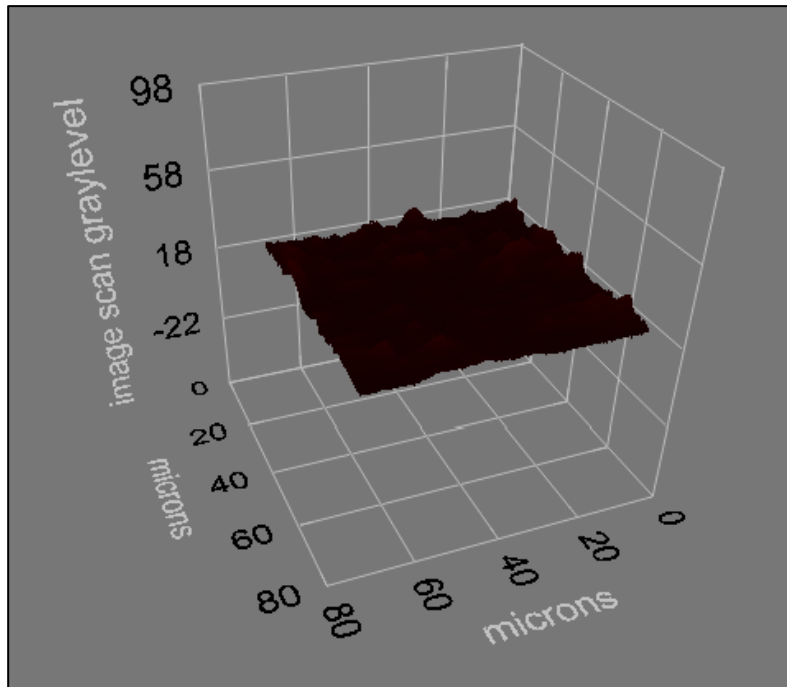


Figure 4.9. The ellipsometer image of hemoglobin imprinted SPR biosensor.

#### 4.3.4. Contact Angle Analysis

The contact angle values of SPR biosensor surfaces were quantified with a KRUSS DSA100 instrument. According to the results, the contact angle value of the hemoglobin imprinted SPR biosensor was decreased from  $64.7 \pm 1.4^\circ$  to  $58.4 \pm 1.0^\circ$  with imprinting process. A significant reduction of the contact angle indicated that the surface hydrophilicity was increased. This can be explained as follows: In the preparation of hemoglobin imprinted SPR biosensors, hydrophilic monomer, acrylamide was used. In addition, hydrophobic property of hemoglobin imprinted SPR biosensor was increased when compared with non-imprinted SPR biosensor because of introduced hemoglobin containing hydrophobic amino acid groups. So, the contact angle of non-imprinted SPR biosensor has  $42.5 \pm 1.6^\circ$ . The images with angles were exhibited in Figure 4.10- 4.12.

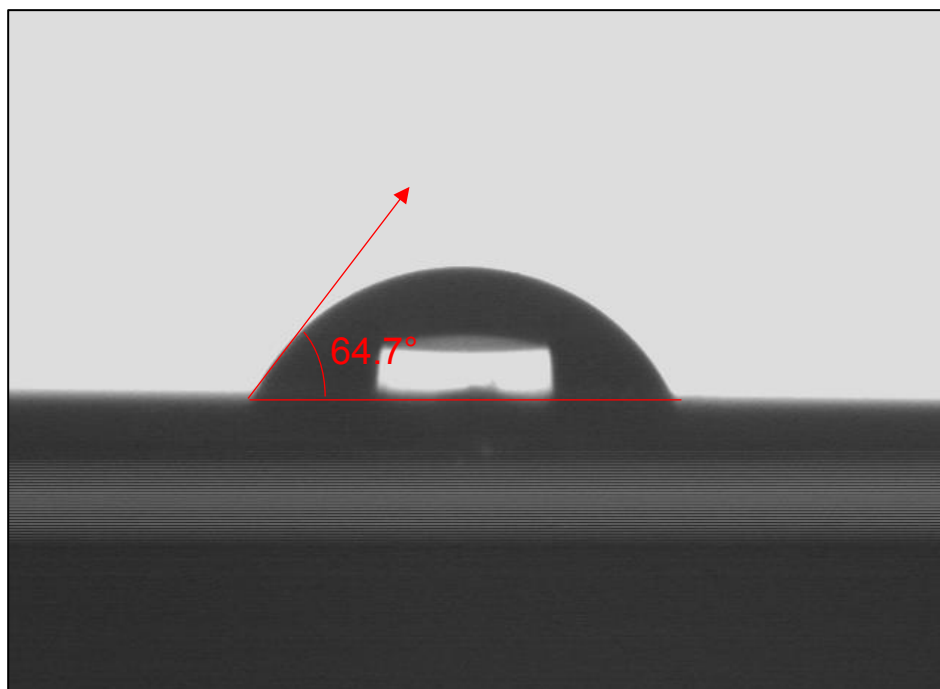


Figure 4.10. The contact angle image of bare SPR biosensor.

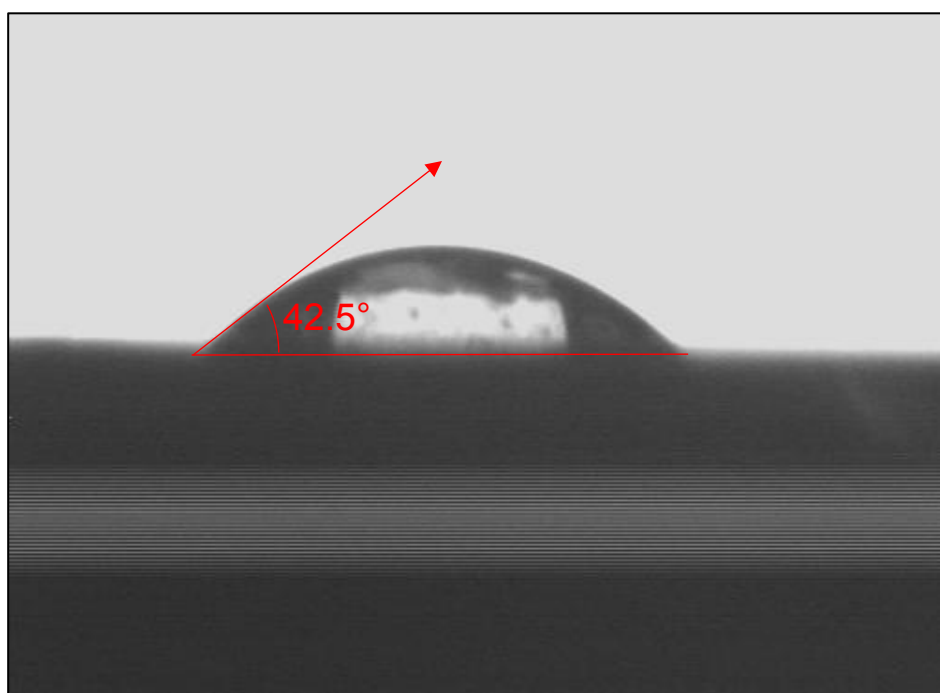


Figure 4.11. The contact angle image of non-imprinted SPR biosensor.



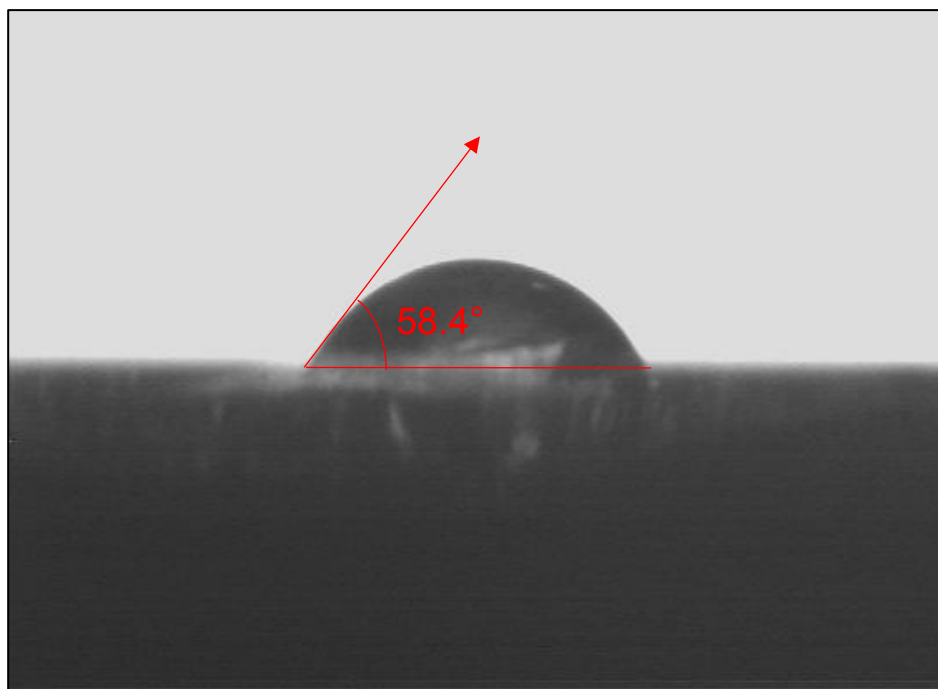


Figure 4.12. The contact angle image of hemoglobin imprinted SPR biosensor.

#### **4.4. Surface Plasmon Resonance Measurements**

Unlike the commonly used method for determination of biomolecules, SPR biosensors can be used without the need for any labelling. The absence of the labelling process saves both time and costs. Also, because of marker molecules interactions with other molecules in the environment can obtain incorrect results. These problems are resolved by the use of SPR biosensors. In addition, the interactions between analyte and SPR biosensor surface can be measure in real-time and directly. These features provide to the characterization of the relationship between analyte and ligand as a quantitative analysis or determination of the kinetic, thermodynamic and concentration parameters as a qualitative analysis [108].

##### **4.4.1. Effect of pH**

The hemoglobin imprinted SPR biosensor was washed with pH solution for 200 sec and hemoglobin solutions in same concentration (0.1 mg/mL) and at different pH (range from 4.0-8.0) were employed to SPR system for 1000 sec. Then, 0.01 M NaCl solution was applied as desorption agent for a 200 sec. After finalizing the analysis, the

hemoglobin imprinted SPR biosensor was continued to wash with desorption agent for 30 min, then with deionized water for 30 min and finally with adsorption agent for 30 min.

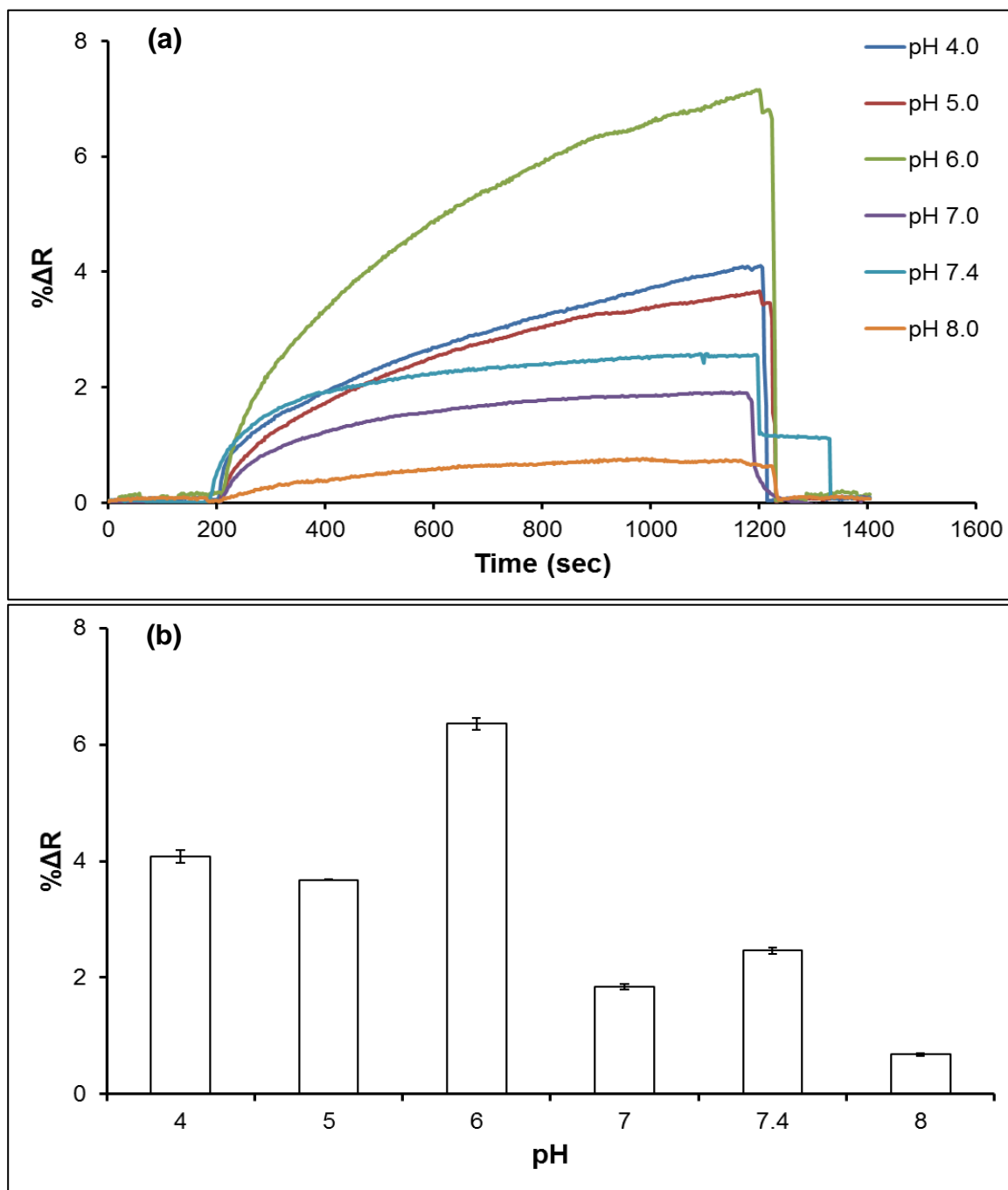


Figure 4.13. The real-time hemoglobin detection with hemoglobin imprinted SPR biosensor at different pH in terms of a sensorgram (a) and a bar graph (b). Experiment condition:  $c_{Hb}=0.1$  mg/mL,  $T=25^{\circ}C$ .

As seen in Figure 4.13 (a-b), the highest response was observed at pH 6.0. Hemoglobin and acrylamide were used as a template and functional monomer. Acrylamide can supply several H-bonding spots for hemoglobin. Thus, the hemoglobin molecule can be polymerized in the polymeric matrix through the H-bond between the acrylamide amide group and the hemoglobin amino and carboxyl groups.

#### 4.4.2. Effect of Hemoglobin Concentration

As seen from Figure 4.14-Figure 4.22, a rise in hemoglobin concentration originated an increase in SPR response. In this SPR system, data converted to the real change in reflectivity,  $\% \Delta R$ , because it is the absolute physical unit of measurement.  $\% \Delta R$  values in resonance frequency arrived at a plateau value in 1200 sec.

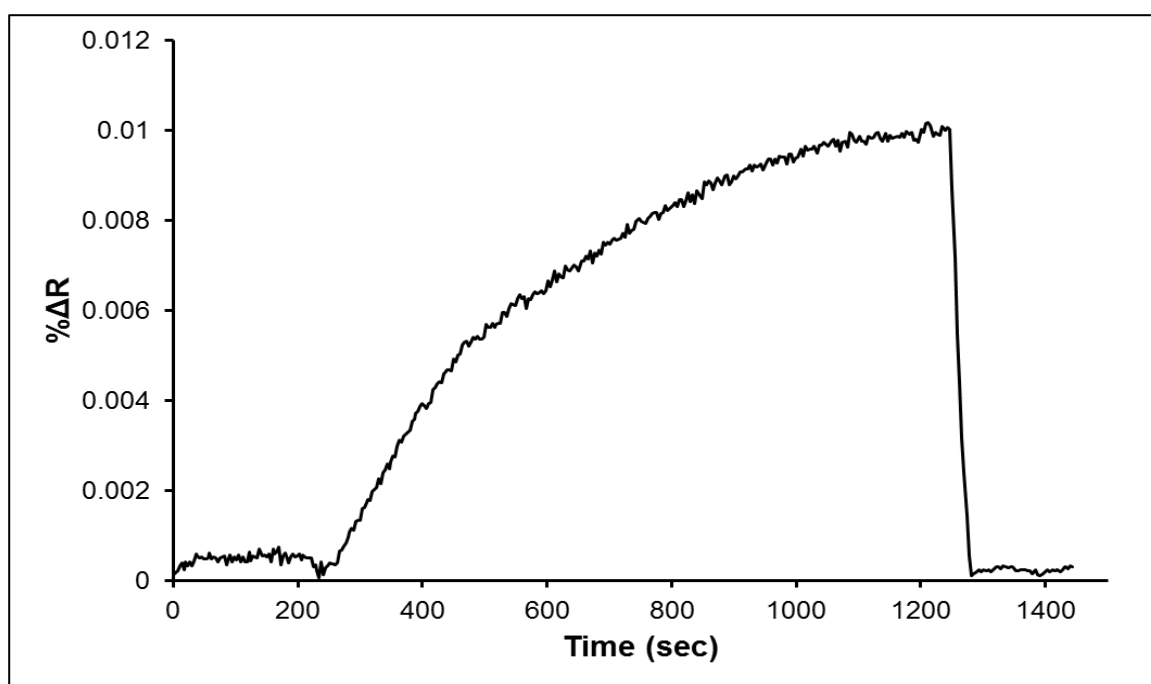


Figure 4.14. The real-time hemoglobin detection with hemoglobin imprinted SPR biosensor. Experiment condition:  $C_{Hb}=0.0005$  mg/mL,  $T=25^{\circ}C$ , pH 6.0.

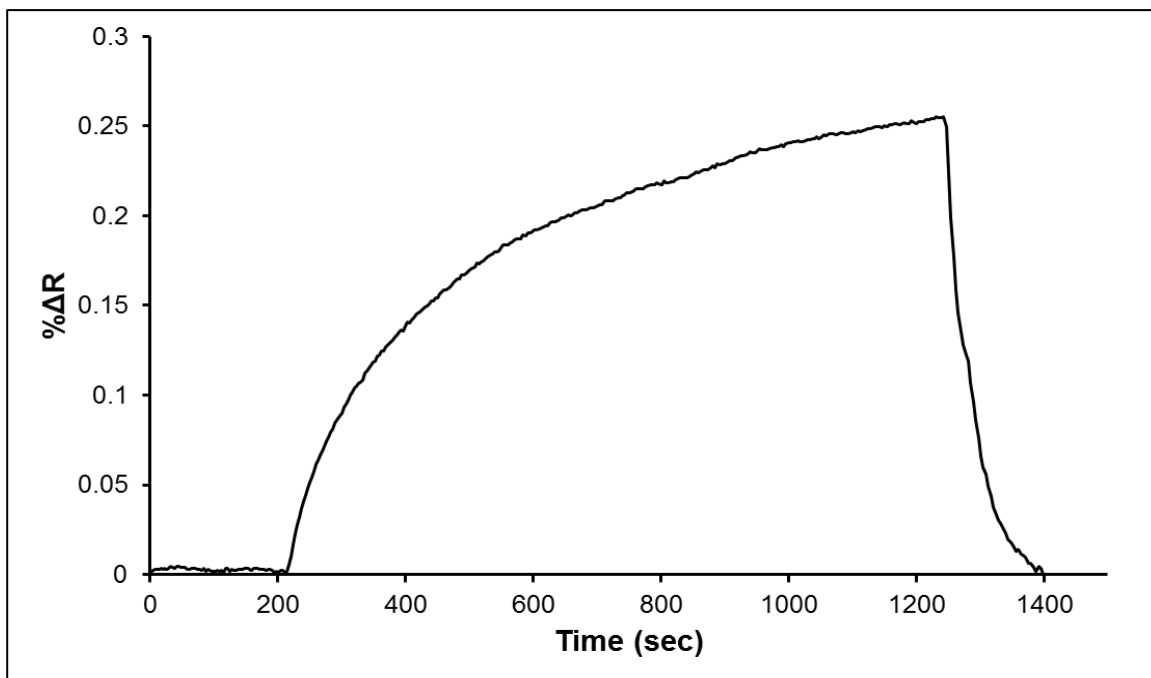


Figure 4.15. The real-time hemoglobin detection with hemoglobin imprinted SPR biosensor. Experiment condition:  $C_{Hb}=0.0015$  mg/mL,  $T=25^{\circ}\text{C}$ , pH 6.0.

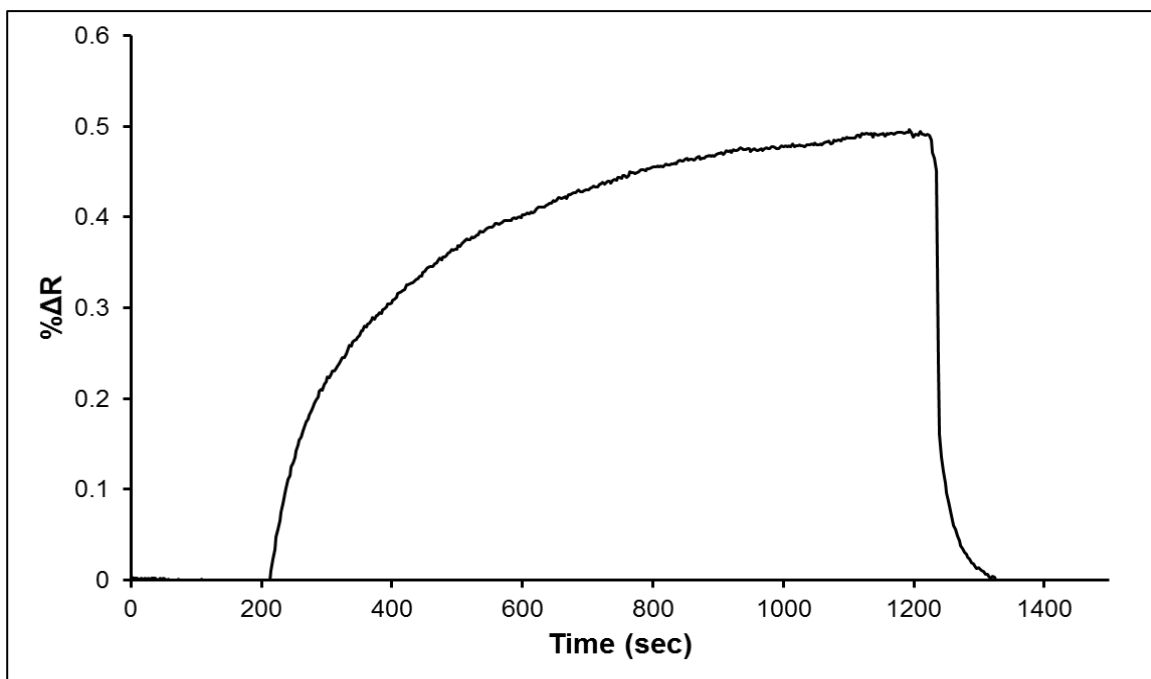


Figure 4.16. The real-time hemoglobin detection with hemoglobin imprinted SPR biosensor. Experiment condition:  $C_{Hb}=0.0035$  mg/mL,  $T=25^{\circ}\text{C}$ , pH 6.0.

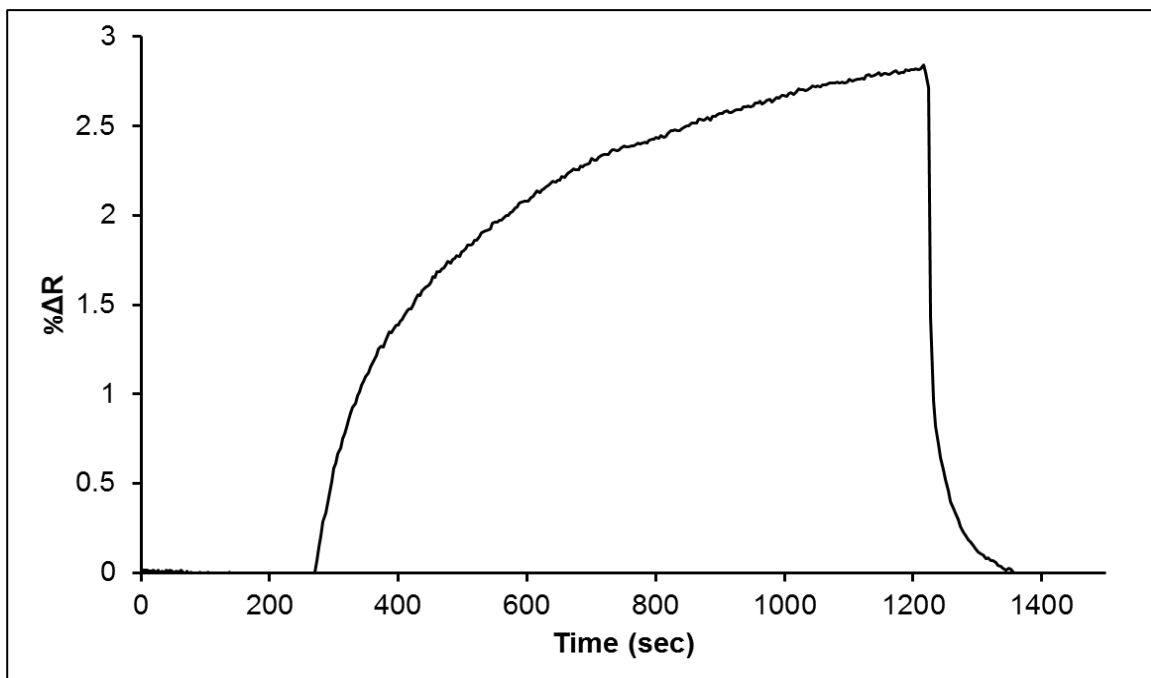


Figure 4.17. The real-time hemoglobin detection with hemoglobin imprinted SPR biosensor. Experiment condition:  $c_{Hb}=0.025$  mg/mL,  $T=25^{\circ}\text{C}$ , pH 6.0.

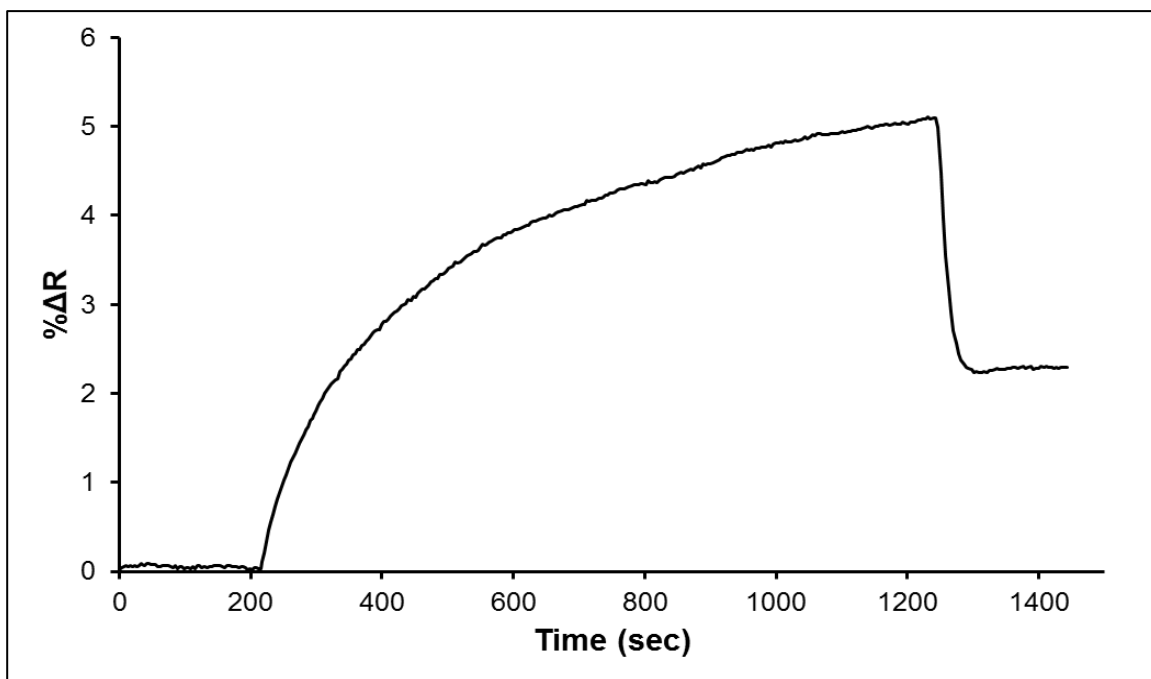


Figure 4.18. The real-time hemoglobin detection with hemoglobin imprinted SPR biosensor. Experiment condition:  $c_{Hb}=0.05$  mg/mL,  $T=25^{\circ}\text{C}$ , pH 6.0.

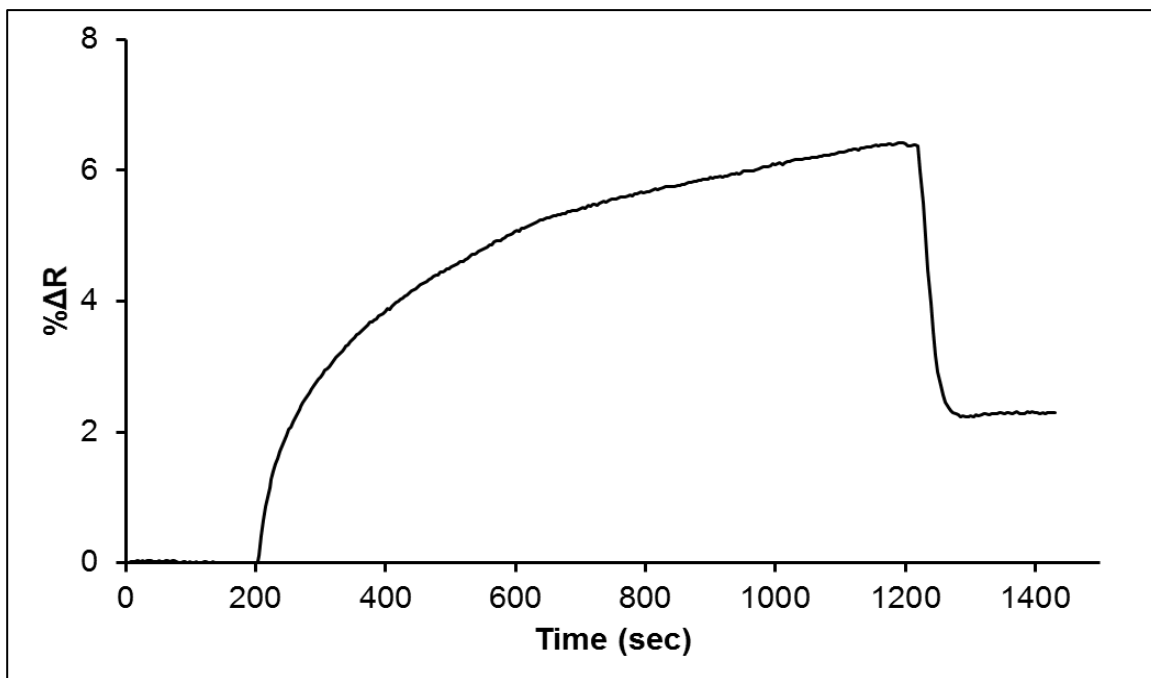


Figure 4.19. The real-time hemoglobin detection with hemoglobin imprinted SPR biosensor. Experiment condition:  $c_{Hb}=0.1$  mg/mL,  $T=25^{\circ}\text{C}$ , pH 6.0.

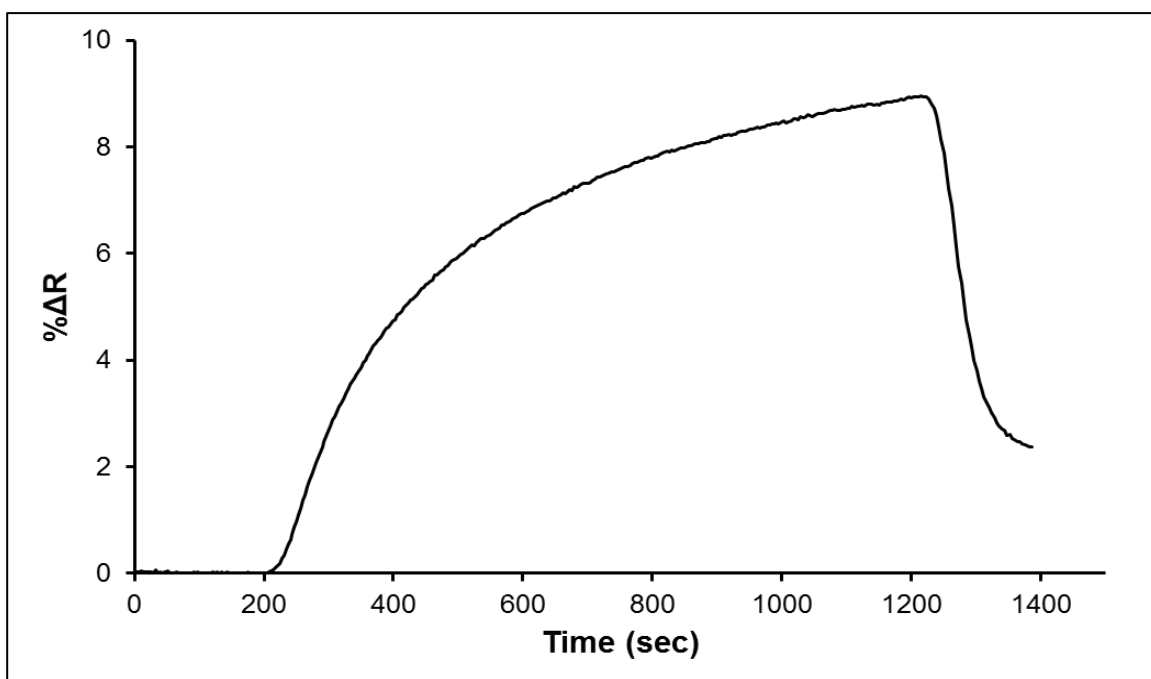


Figure 4.20. The real-time hemoglobin detection with hemoglobin imprinted SPR biosensor. Experiment condition:  $c_{Hb}=0.25$  mg/mL,  $T=25^{\circ}\text{C}$ , pH 6.0.

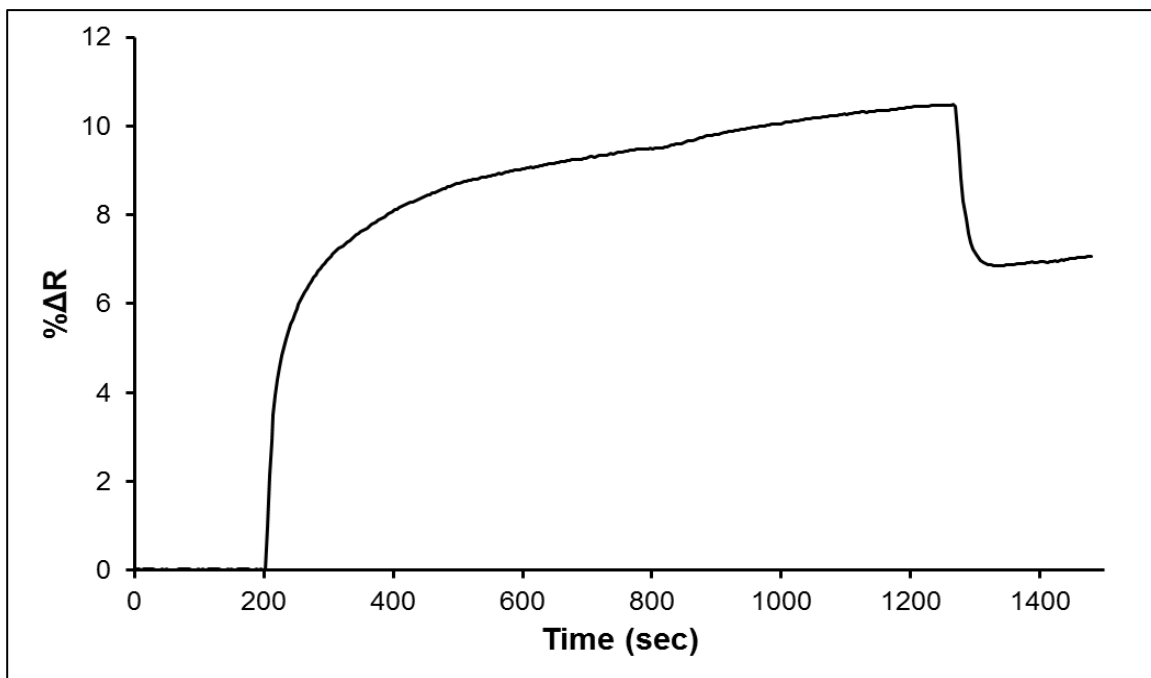


Figure 4.21. The real-time hemoglobin detection with hemoglobin imprinted SPR biosensor. Experiment condition:  $c_{Hb}=0.5$  mg/mL,  $T=25^{\circ}\text{C}$ , pH 6.0.

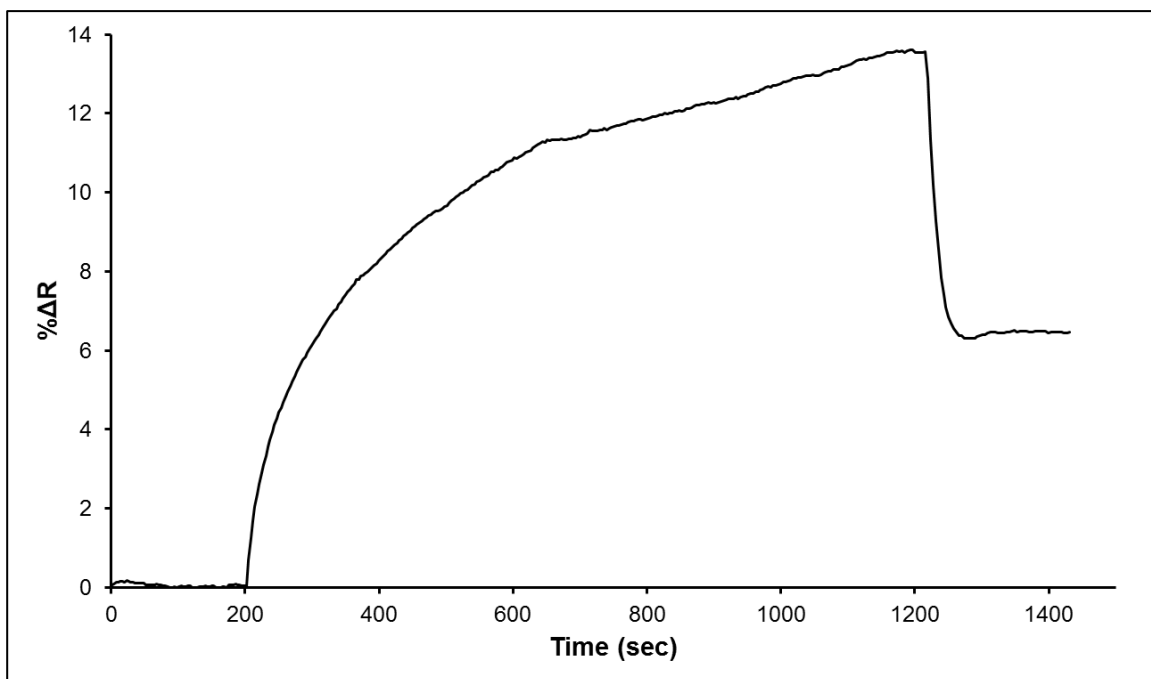


Figure 4.22. The real-time hemoglobin detection with hemoglobin imprinted SPR biosensor. Experiment condition:  $c_{Hb}=1.0$  mg/mL,  $T=25^{\circ}\text{C}$ , pH 6.0.

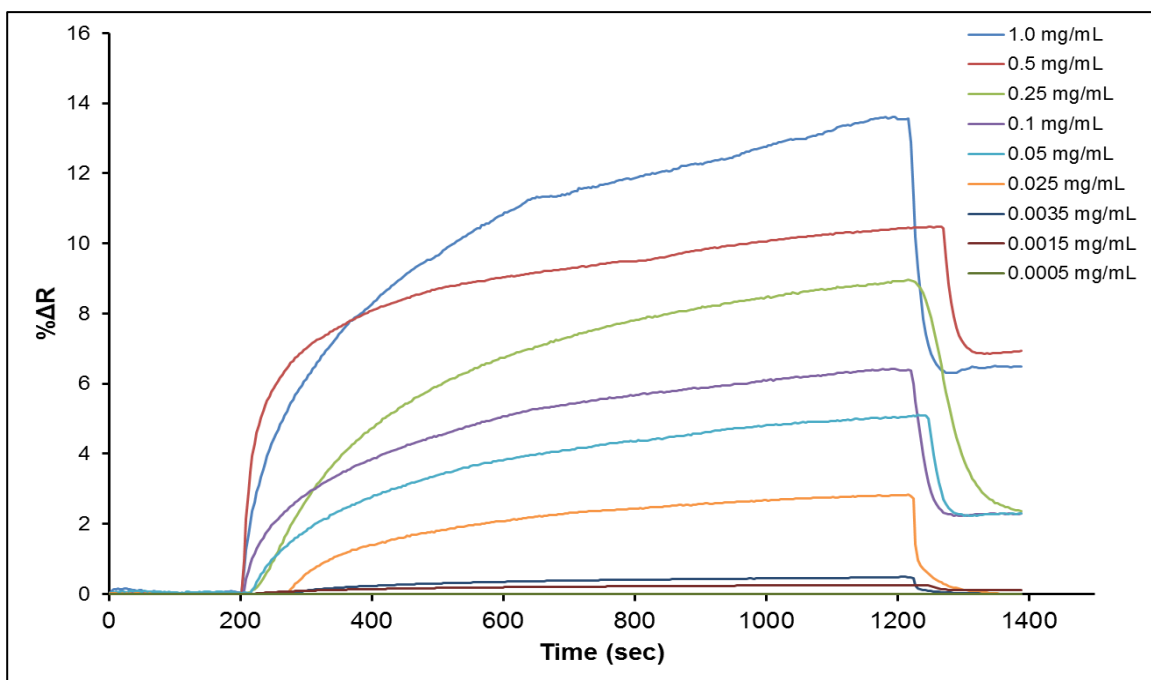


Figure 4.23. The combination of real-time responses of hemoglobin imprinted SPR biosensor. Experiment condition:  $C_{Hb}=0.0005-1.0$  mg/mL,  $T=25^{\circ}C$ , pH 6.0.

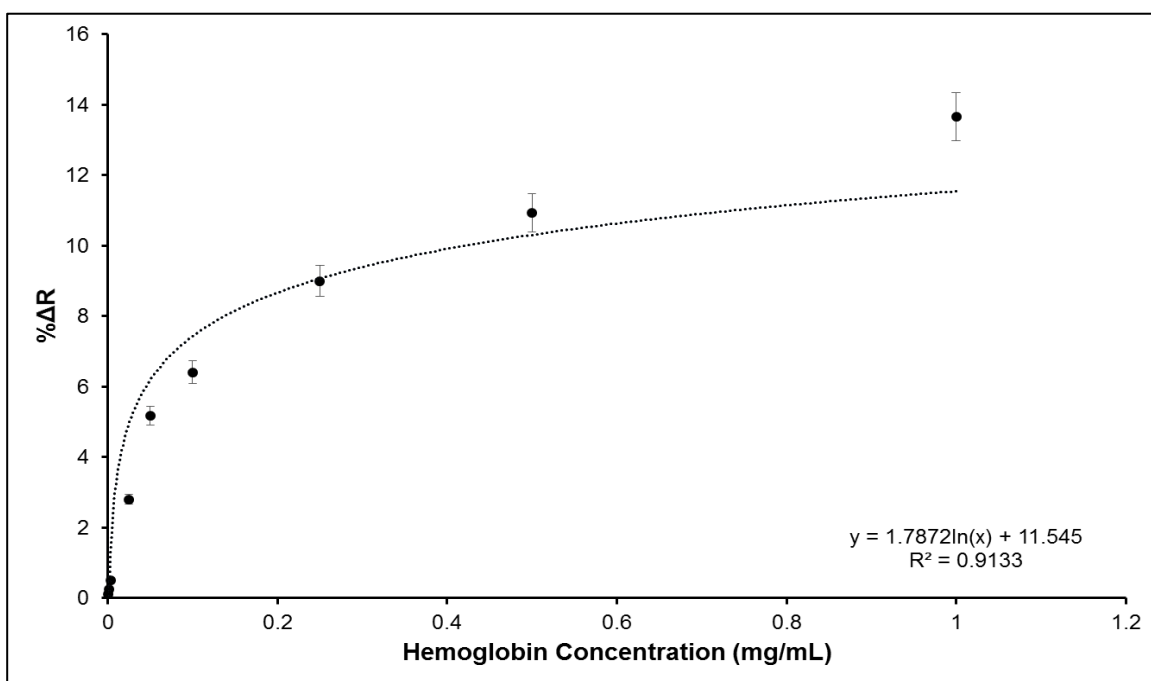


Figure 4.24. The calibration curve of hemoglobin imprinted SPR biosensor response to hemoglobin solutions between 0.0005 mg/mL and 1.0 mg/mL.



The combination of real-time responses of hemoglobin imprinted SPR biosensor was exhibited in Figure 4.23. In Figure 4.24, the relationships between hemoglobin concentration and % $\Delta R$  were also given. As referred before, hemoglobin concentration has been coordinated by diluting with pH 6.0 phosphate buffer in different ratios. In all solutions, hemoglobin imprinted SPR biosensor extended the plateau value in 1200 sec. After 0.01 M NaCl was applied, % $\Delta R$  values cut down to approximately initial value. According to increase in the concentration,  $\Delta R$  values increased, as well. Thus, reduce the concentration also reduced the driving force between hemoglobin solution and hemoglobin imprinted SPR biosensor. Therein, the change in % $\Delta R$  values increased from 0.098 to 13.67 while hemoglobin concentration was increased from 0.0005 mg/mL to 1.0 mg/mL, respectively. When the % $\Delta R$  data which were determined for the concentration between 0.0005-1.0 mg/mL were taken, the curve had an equation  $y = 1.7872\ln x + 11.545$  with  $R^2$  value as 0.91, correspondingly. It means that the hemoglobin imprinted SPR biosensor is talented to detect hemoglobin from sample solutions with 91% precision if it is a range in 0.0005-1.0 mg/mL. Also, the hemoglobin imprinted SPR biosensor is talented to detect hemoglobin from sample solutions with 99% precision if it is a range in 0.0005-0.05 mg/mL and 94% precision if the concentration range is 0.1-1.0 mg/mL.

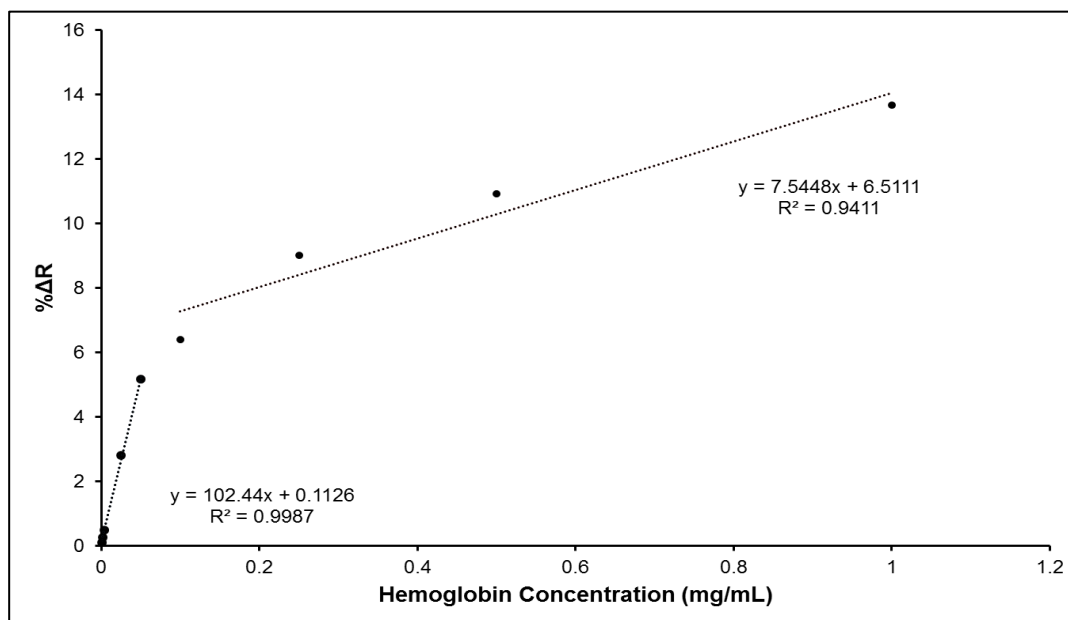


Figure 4.25. The calibration curves of hemoglobin imprinted SPR biosensor response to hemoglobin solutions between 0.0005-0.05 mg/mL (a) and 0.1-1.0 mg/mL (b).

According to the results, a limit of detection (LOD) value was determined. The linear part of the calibration curve gives the LOD value by using  $3S/b$  formula. The LOD value was calculated as 0.00035 mg/mL at the end of the experiment.

#### 4.4.3. Kinetic Studies

##### 4.4.3.1. Equilibrium Analysis

All hemoglobin concentration can be depicted as hemoglobin imprinted SPR biosensor response change,  $\% \Delta R$ , [109]. In the pseudo first order reactions, the hemoglobin concentration is kept constant and the interaction can be defined by Equation 1:

$$\frac{d\Delta R}{dt} = k_a c (\Delta R_{max} - \Delta R) - k_d \Delta R \quad (1)$$

that  $d\Delta R/dt$  is the rate change of the SPR biosensor response,  $\Delta R$  and  $\Delta R_{max}$  are the obtained and maximum response quantified,  $c$  is the hemoglobin concentration,  $k_a$  and  $k_d$  are the association and dissociation rate constants. The association constant,  $K_A$ , can be found as  $K_A = k_a/k_d$ . Generally,  $d\Delta R/dt = 0$  at equilibrium. The equation can be revised as Equation 2:

$$\Delta R_{eq}/c = K_A \Delta R_{max} - K_A \Delta R_{eq} \quad (2)$$

The  $K_A$  value can obtain from a plot of  $\Delta R_{eq}/c$  vs.  $\Delta R_{eq}$  and the dissociation constant,  $K_D$ , can be found as  $1/K_A$ .

Equation 1 can be revised to provide Equation 3:

$$\frac{d\Delta R}{dt} = k_a c \Delta R_{max} - (k_a c + k_d) \Delta R \quad (3)$$

A plot of  $d\Delta R/dt$  against  $\Delta R$  will be a straight line with slope  $-(k_a c + k_d)$ . The initial binding rate is comparable to the hemoglobin concentration. If  $\Delta R_{max}$  is identified, both

$k_a$  and  $k_d$  can be described from an association sensorgram [110]. A preferred method is to quantify the association sensorgram at various hemoglobin concentrations [111]. The forward and back rates are obtained from a plot of  $d\Delta R/dt$  versus  $\Delta R$  supplies a value  $s$  as the slope which associates the forward and back rates as follows as Equation 4:

$$s = k_a c + k_d \quad (4)$$

The plot of  $s$  versus  $c$  will be a straight line and  $k_a$  is obtained from the slope. In principle, the intercept on the ordinate gives  $k_d$  [112]. But the direct determination of the dissociation from saturated binding sites into an adsorption solution flow that contains no hemoglobin is a more accurate way. The dissociation is quantified by Equation 5:

$$\ln(\Delta R_0/\Delta R_t) = k_d(t - t_0) \quad (5)$$

that  $\Delta R_0$  is the initial response at  $t_0$ ;  $\Delta R$  and  $t$  obtain from the dissociation curve [113]. Association kinetics analysis graph was shown in Figure 4.26.

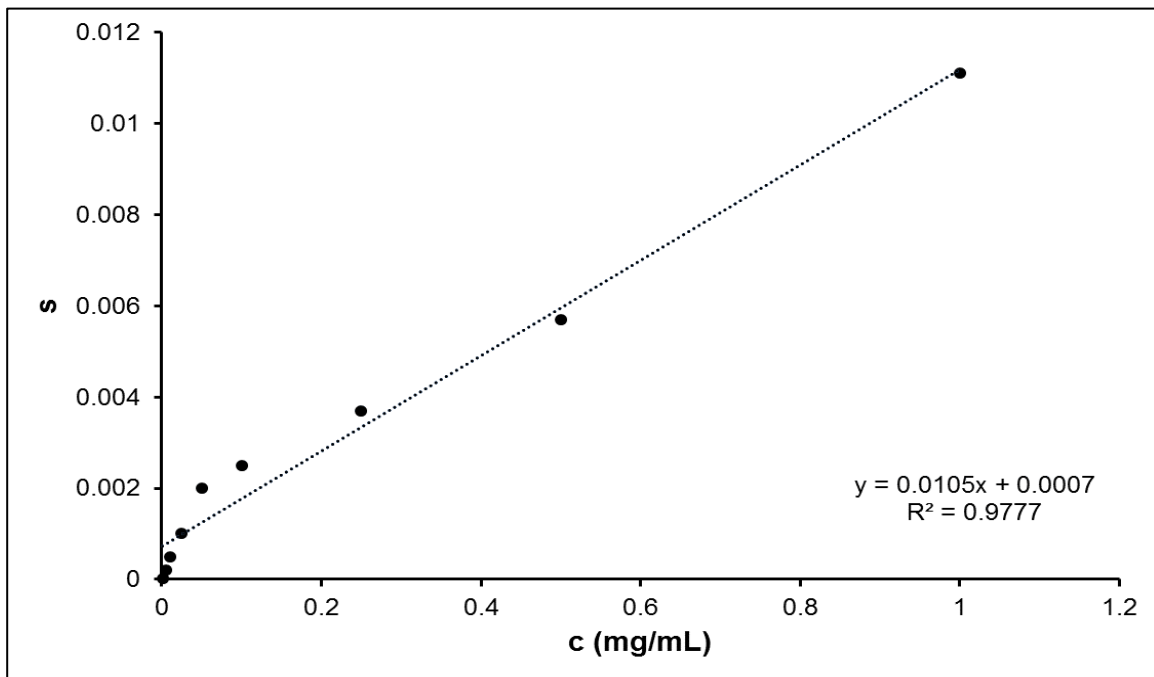


Figure 4.26. Determination of kinetic rate constants: Association kinetics analysis.

Equilibrium analysis that is called as Scatchard is employed to examine the experimental data for reversible host/guest interactions and find the total binding sites the host has in equilibrium condition [114].

$$\Delta R_{ex}/c = K_A(\Delta R_{max} - \Delta R_{eq}) \quad (6)$$

Equilibrium analysis graph was also shown in Figure 4.27.

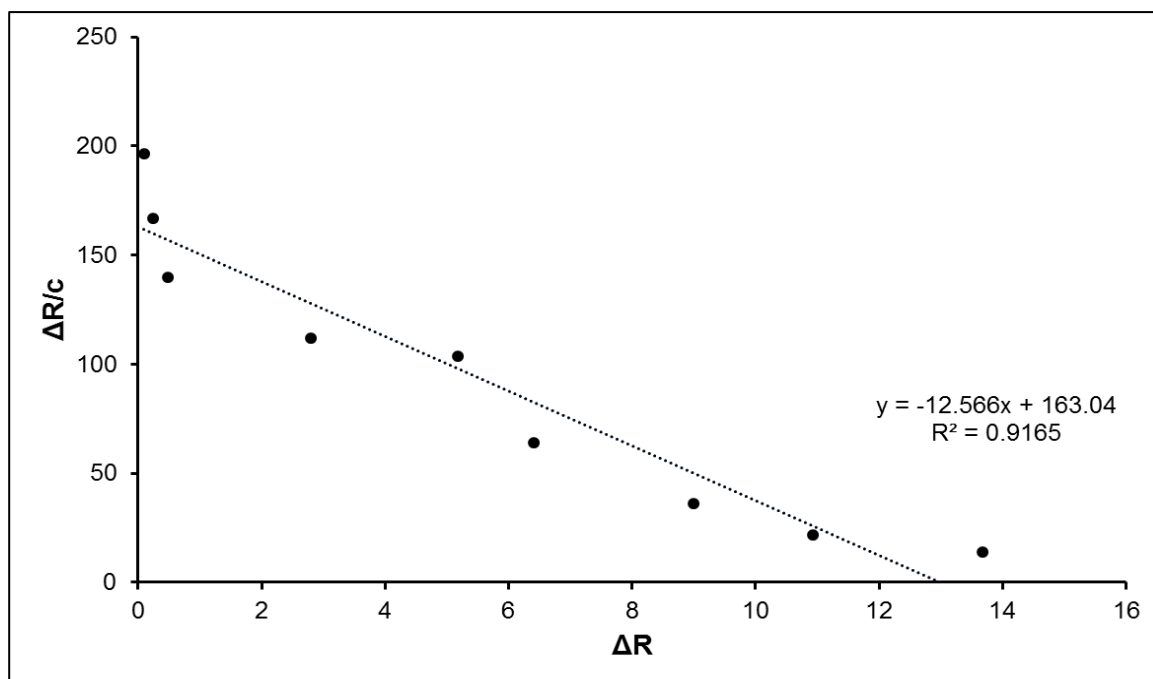


Figure 4.27. Determination of kinetic rate constants: Equilibrium analysis.

Table 4.1. Equilibrium and association kinetics constants.

Equilibrium analysis		Association kinetic analysis	
$\Delta R_{max}$	13	$k_a, \text{mL/mg.s}$	0.011
$K_A, \text{mL/mg}$	12.6	$k_d, 1/s$	0.001
$K_D, \text{mg/mL}$	0.08	$K_A, \text{mL/mg}$	15
$R^2$	0.92	$K_D, \text{mg/mL}$	0.07
		$R^2$	0.98

#### 4.4.3.2. Adsorption Isotherm Models

The adsorption isotherm models can be employed to describe the detection capability, selectivity and surface homogeneity of the molecularly imprinted biosensors [114].

As shown in Equations 7 to 9, the binding between the hemoglobin imprinted SPR biosensor and hemoglobin was defined with three different adsorption isotherm models were studied:

$$\text{Langmuir} \quad \Delta R = \{\Delta R_{max}[c]/K_D + [c]\} \quad (7)$$

$$\text{Freundlich} \quad \Delta R = \Delta R_{max}[c]^{1/n} \quad (8)$$

$$\text{Langmuir–Freundlich} \quad \Delta R = \{\Delta R_{max}[c]^{1/n}/K_D + [c]^{1/n}\} \quad (9)$$

Langmuir adsorption isotherm model bases on the acceptance of a homogeneous distribution of equal energy and also no extra interactions [112]. Freundlich adsorption isotherm model is a suitable heterogeneous interaction. The heterogeneity index,  $1/n$ , ranges between 0 and 1, as heterogeneity decreases,  $1/n$  becomes closer to 1, and

equals to 1 for a homogeneous system [115]. Langmuir-Freundlich adsorption isotherm model is a hybrid model that can be employed to suitable for both systems [114]. This adsorption isotherm model can be fitted to define adsorption of homogeneous and heterogeneous surfaces.

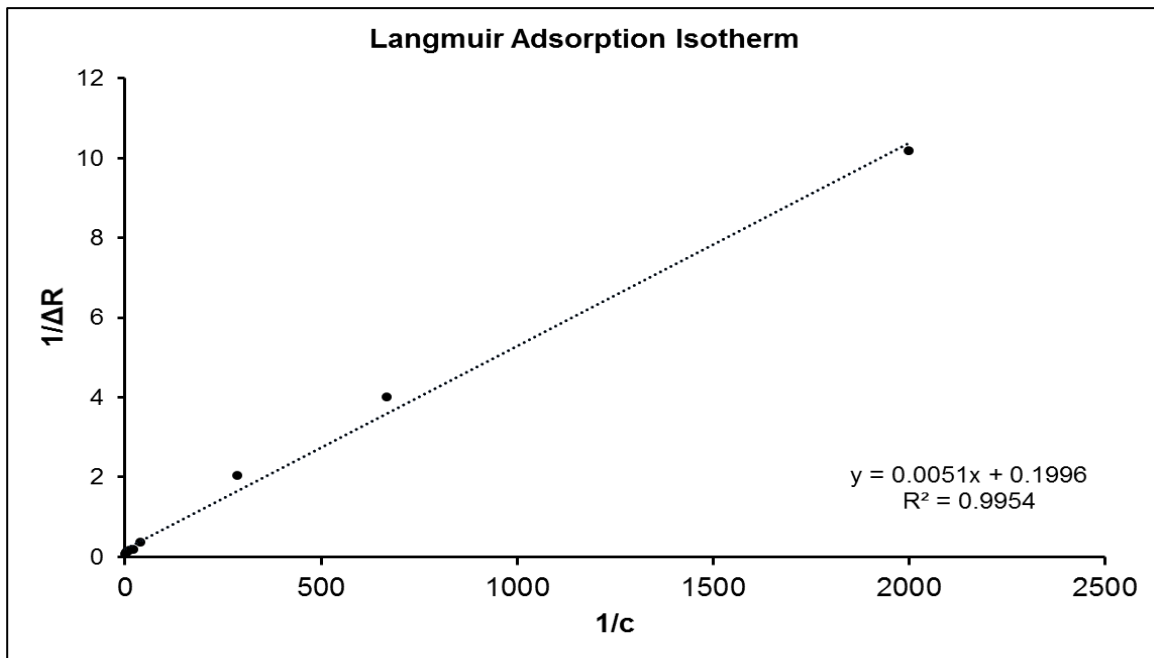


Figure 4.28. Langmuir adsorption isotherm model.

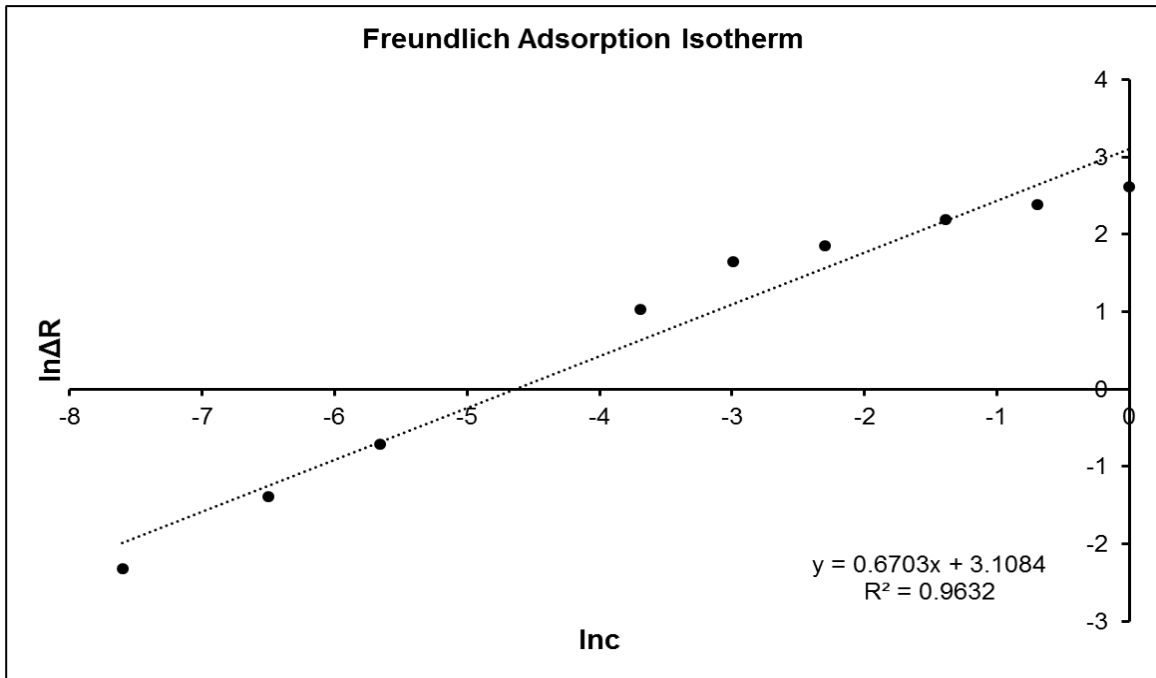


Figure 4.29. Freundlich adsorption isotherm model.

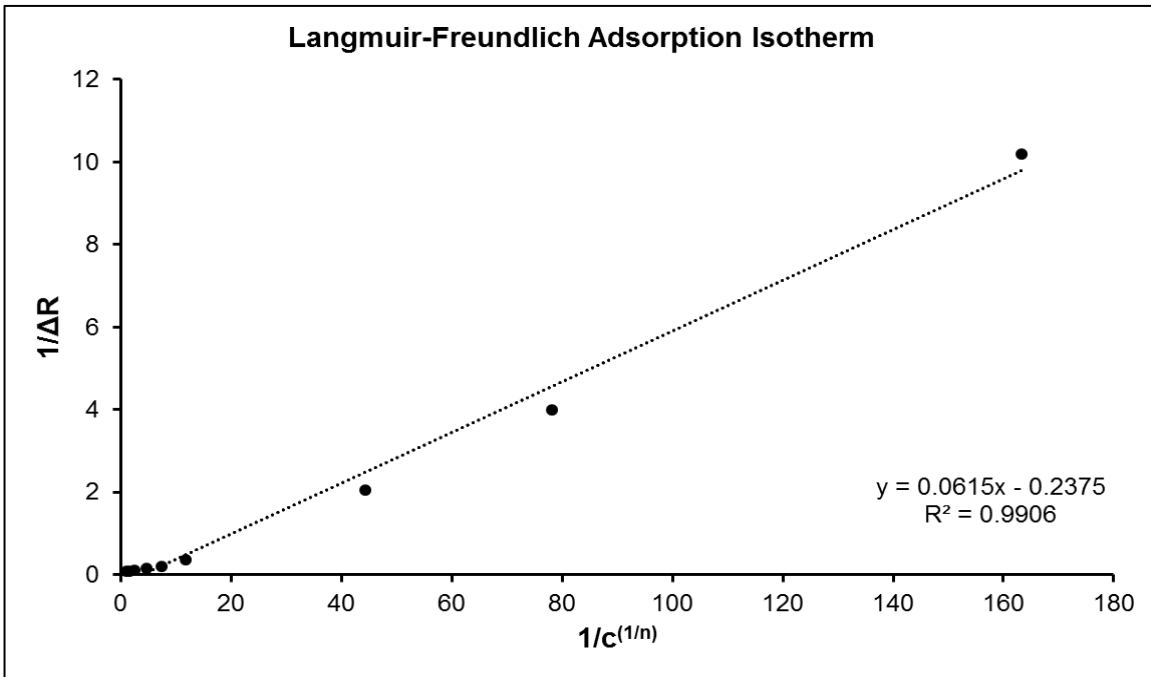


Figure 4.30. Langmuir-Freundlich adsorption isotherm model.

Table 4.2. The comparison of adsorption isotherm models.

Langmuir		Freundlich		Langmuir-Freundlich	
$\Delta R_{max}$	5.01	$\Delta R_{max}$	22.4	$\Delta R_{max}$	4.21
$K_D, \text{mg/mL}$	0.03	$1/n$	0.67	$1/n$	0.67
$K_A, \text{mL/mg}$	39.1	$R^2$	0.96	$K_D, \text{mg/mL}$	0.26
$R^2$	0.99			$K_A, \text{mL/mg}$	3.86
				$R^2$	0.99

All adsorption isotherm models graphs were demonstrated in Figure 4.28-4.30. In addition, the constants for all adsorption isotherm models were displayed in Table 4.2. As seen from there, the most suitable adsorption isotherm model is that Langmuir adsorption isotherm model ( $R^2=0.99$ ). According to the results,  $K_A$  and  $K_D$  values were also found as 39.1 mL/mg and 0.03 mg/mL.

#### 4.4.4. Selectivity Analysis

The selectivity analysis of the hemoglobin imprinted SPR biosensor was carried out by using competing proteins that include lysozyme (Lyz), transferrin (Trf), bovine serum albumin (BSA), and myoglobin (Myb). All protein sample solutions were prepared as 0.1 mg/mL and then applied to the SPR system for selectivity analysis. As expected, the response of the hemoglobin imprinted SPR biosensor was the highest value ( $\% \Delta R=7.15$ ), indicating that the hemoglobin imprinted SPR biosensor displayed good selectivity for the template Hb molecule. Furthermore, Lyz ( $\% \Delta R=4.19$ ) exhibited higher rebinding on the hemoglobin imprinted SPR biosensor than Trf ( $\% \Delta R=1.64$ ), BSA ( $\% \Delta R=0.61$ ), and Myb ( $\% \Delta R=0.40$ ). Compared with BSA (MW=66 kDa), Trf (MW=76 kDa) and Myb (MW=17 kDa), Lyz (MW=14.3 kDa) was much smaller one according to the molecular weights of proteins. This result can be explained by using size, charge



and shape of the proteins. Small proteins can be diffused easily into the cavities and generated non-selective binding. Contrary to the small proteins, the large proteins were easier to be removed from the cavities because of the steric hindrance [116]. As seen from Figure 4.31, the results suggested that the hemoglobin imprinted SPR biosensor had particular detection capability toward hemoglobin because of the imprinting process.

The non-imprinted SPR biosensor (NIP) was also prepared. The non-imprinted SPR biosensor gave a low response to hemoglobin solution ( $\% \Delta R = 0.57$ ). The  $\% \Delta R$  values of the non-imprinted SPR biosensor to Lyz, Trf, BSA, and Myb were also defined as 1.48, 1.00, 0.46 and 0.24, respectively (Figure 4.32). The selectivity coefficients were calculated between Hb and Lyz, Trf, BSA, and Myb as 1.71, 4.36, 11.7 and 17.9 for hemoglobin imprinted SPR biosensor, respectively. In addition, the selectivity coefficients were determined between Hb and Lyz, Trf, BSA, and Myb as 1.39, 0.57, 1.24 and 2.38 for non-imprinted SPR biosensor as well. The relative selectivity coefficients were also calculated as 4.39, 7.65, 9.44 and 7.52 for Lyz, Trf, BSA, and Myb. According to all responses of hemoglobin imprinted and non-imprinted SPR biosensors, the structural memory and specificity were only observed in hemoglobin imprinted SPR biosensor due to the imprinting process.

The selectivity coefficient,  $k$ , is depicted by Equation 10. The relative selectivity coefficient,  $k'$ , is also described by Equation 11 as well.

$$k = \Delta R_{template} / \Delta R_{competitor} \quad (10)$$

$$k' = k_{MIP} / k_{NIP} \quad (11)$$

All selectivity and relative selectivity coefficients of the hemoglobin imprinted and non-imprinted SPR biosensors were shown in Table 4.3.

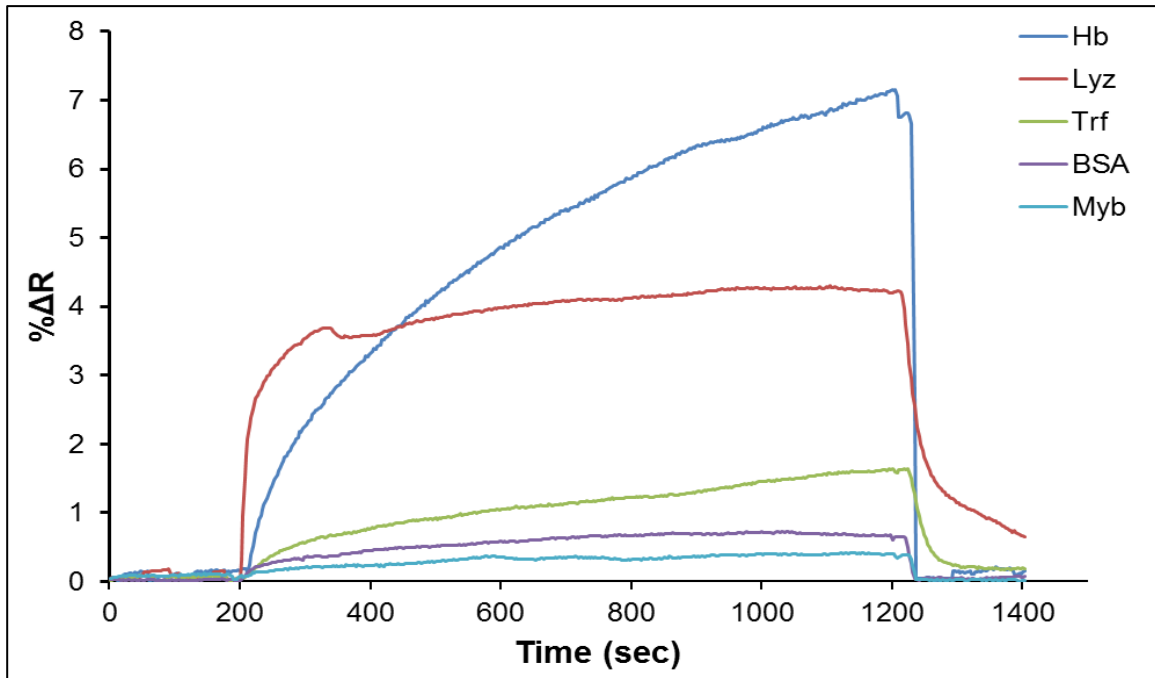


Figure 4.31. The selectivity combination of real-time responses of hemoglobin imprinted SPR biosensor. Experiment condition:  $c_{\text{protein}}=0.1$  mg/mL,  $T=25^{\circ}\text{C}$ , pH 6.0.

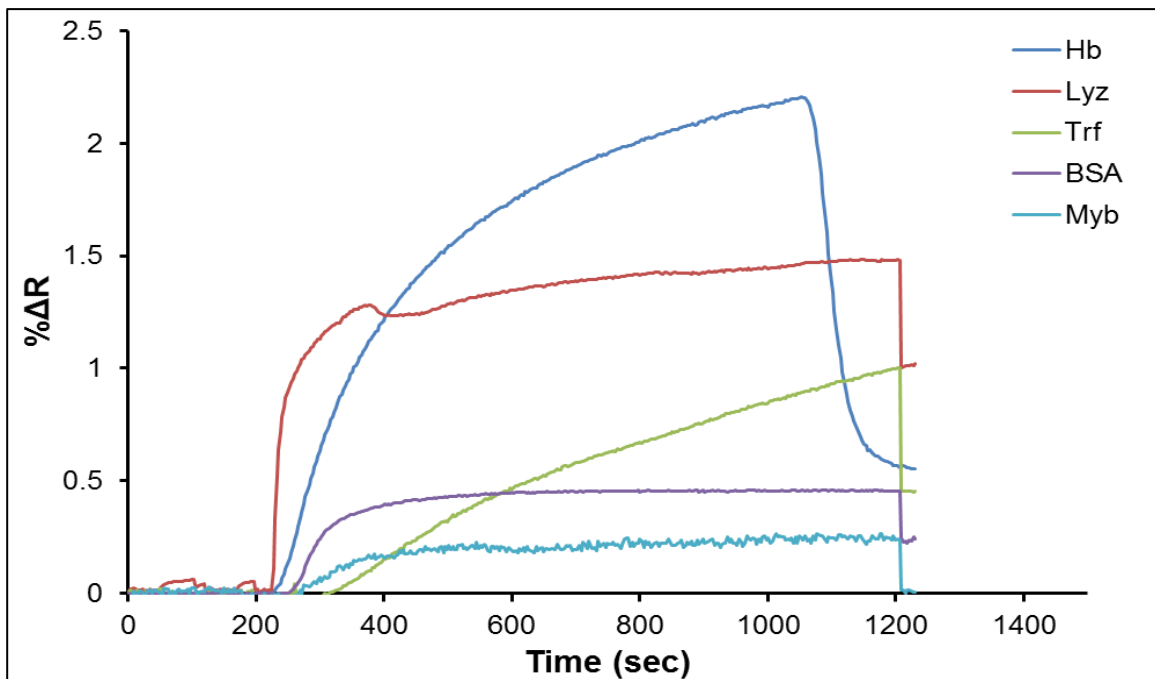


Figure 4.32. The selectivity combination of real-time responses of non-imprinted SPR biosensor. Experiment condition:  $c_{\text{protein}}=0.1$  mg/mL,  $T=25^{\circ}\text{C}$ , pH 6.0.

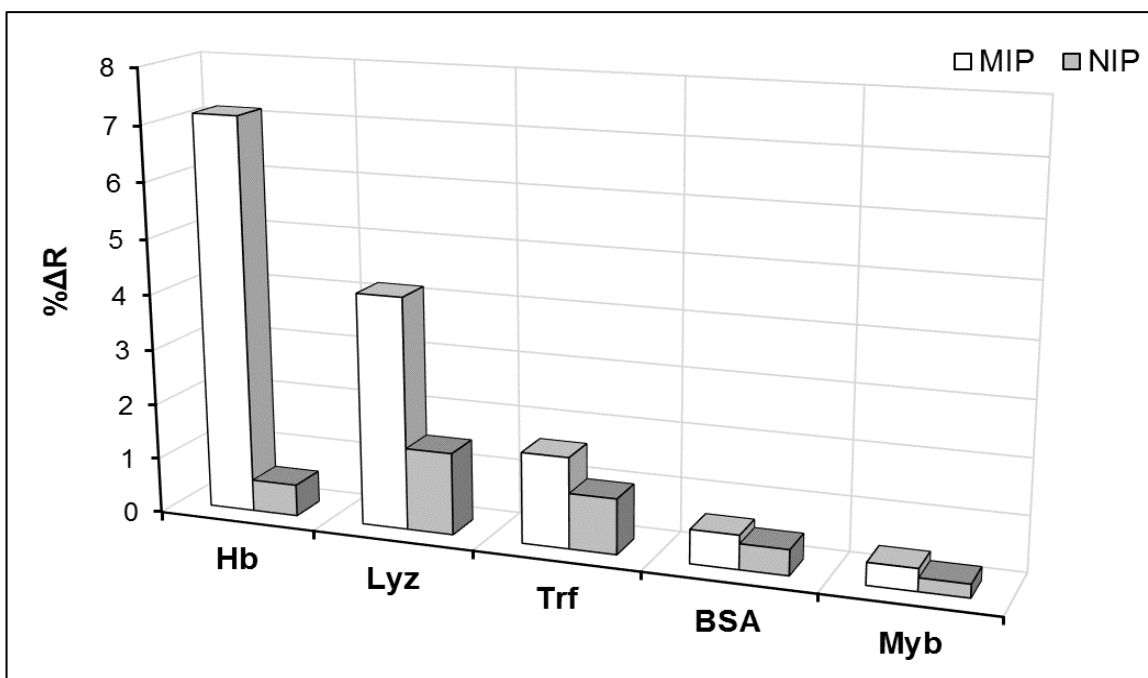


Figure 4.33. The selectivity comparison of hemoglobin imprinted (MIP) and non-imprinted (NIP) SPR biosensors. Experiment condition:  $c_{\text{protein}}=0.1$  mg/mL,  $T=25^{\circ}\text{C}$ , pH 6.0.

Table 4.3. The selectivity and relative selectivity coefficients of hemoglobin imprinted (MIP) and non-imprinted (NIP) SPR biosensors.

Protein	MIP		NIP		$k'$
	$\Delta R$	$k$	$\Delta R$	$k$	
Hb	7.15		0.57		
Lyz	4.19	1.71	1.48	0.39	4.39
Trf	1.64	4.36	1	0.57	7.65
BSA	0.61	11.7	0.46	1.24	9.44
Myb	0.4	17.9	0.24	2.38	7.52

Furthermore, the protein mixtures were prepared by the same concentrations of Lyz-Hb, Trf-Hb, BSA-Hb, and Myb-Hb proteins. As demonstrated in Figure 4.34, the mixture of Lyz and Hb showed the highest response ( $\% \Delta R = 5.69$ ) for hemoglobin imprinted SPR biosensor. The Trf-Hb, BSA-Hb, and Myb-Hb protein mixtures responses were observed as 3.05, 2.44 and 1.17 for hemoglobin imprinted SPR biosensor as well. The non-imprinted SPR biosensor was showed less response with the mixture of Lyz-Hb ( $\% \Delta R = 1.89$ ), Trf-Hb ( $\% \Delta R = 1.92$ ), BSA-Hb ( $\% \Delta R = 1.31$ ), and Myb-Hb ( $\% \Delta R = 1.06$ ).

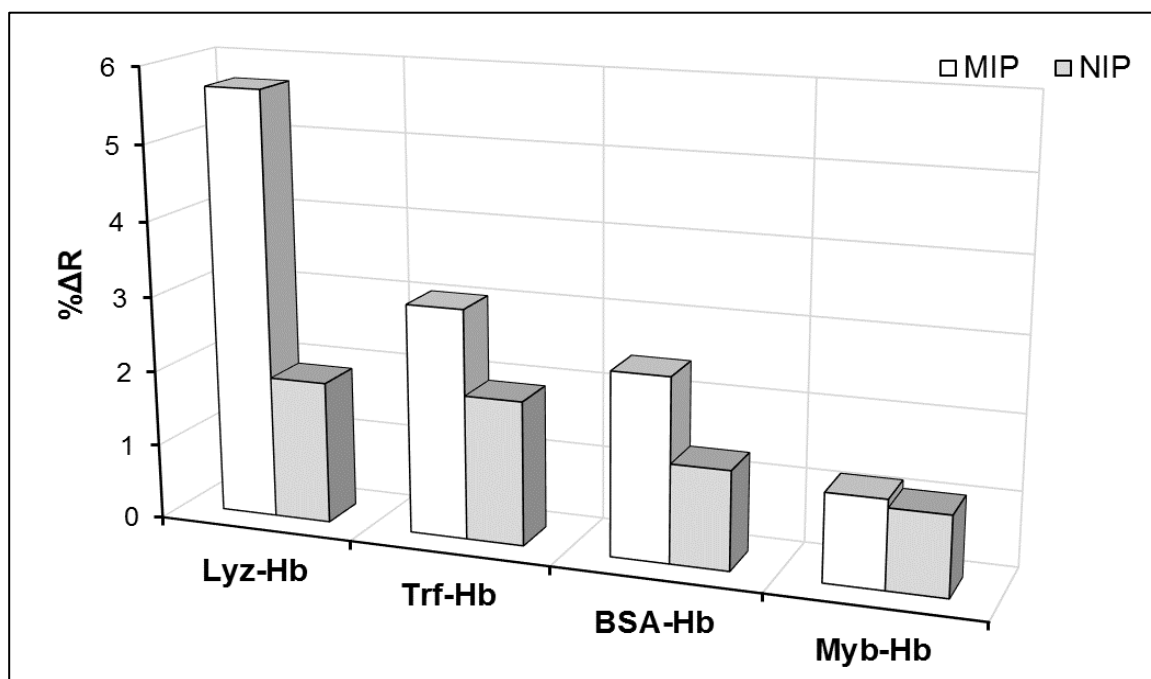


Figure 4.34. Selectivity comparison of hemoglobin imprinted (MIP) and non-imprinted (NIP) SPR biosensors. Experiment condition:  $c_{\text{protein}} = 0.1 \text{ mg/mL}$ ,  $T = 25^\circ\text{C}$ ,  $\text{pH} 6.0$ .

#### 4.4.5. Reusability Analysis

The adsorption-desorption-regeneration cycles were employed as given experimental part to demonstrate the reusability of the hemoglobin imprinted SPR biosensor. As seen in Figure 4.35, the sample solutions were prepared different solutions as 0.05, 0.25, 0.5 and 1.0 mg/mL and then applied to the SPR system consecutively, and the responses of the hemoglobin imprinted SPR biosensor were increased. In addition, the hemoglobin imprinted SPR biosensor was performed with same hemoglobin

concentration (0.1 mg/mL) at different times (0, 3, 27 months) to show storage stability of the hemoglobin imprinted SPR biosensor. The response of the hemoglobin imprinted SPR biosensor was decreased from 6.42 to 6.33 and the performance loss was only 9% in 27 months. According to this result, the hemoglobin imprinted SPR biosensor can be used to detect hemoglobin molecules several times without any loss of performance.

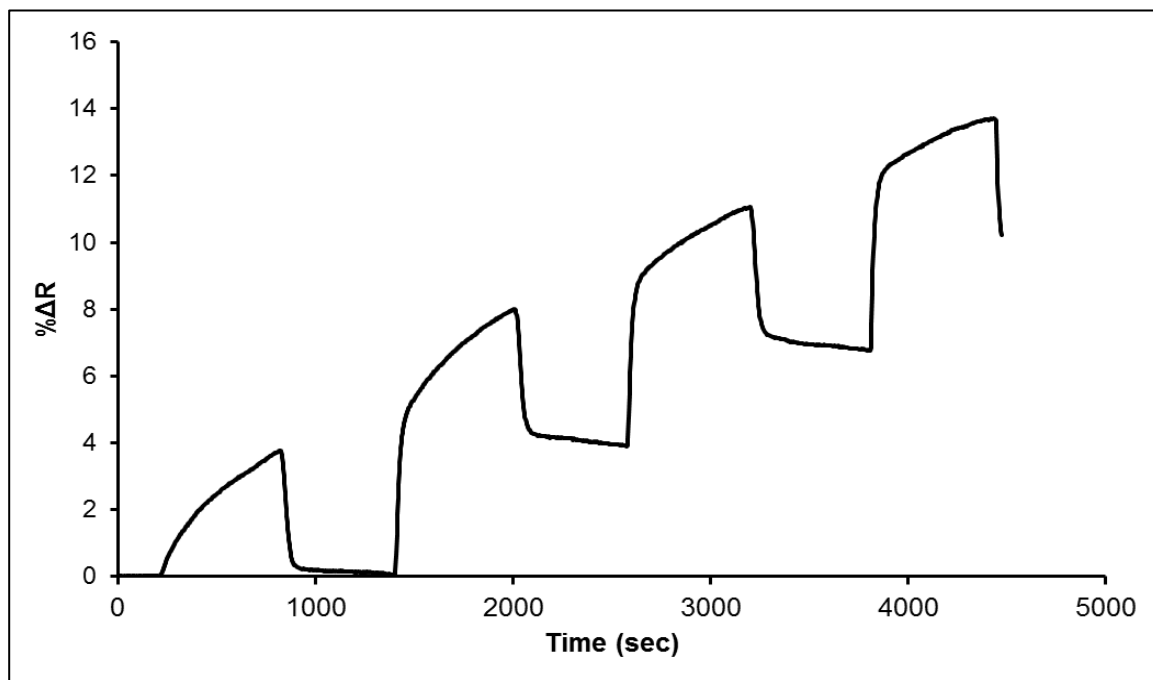


Figure 4.35. Reusability of hemoglobin imprinted SPR biosensor. Experiment condition:  $c_{Hb}=0.05-1.0$  mg/mL,  $T=25^{\circ}\text{C}$ , pH 6.0.

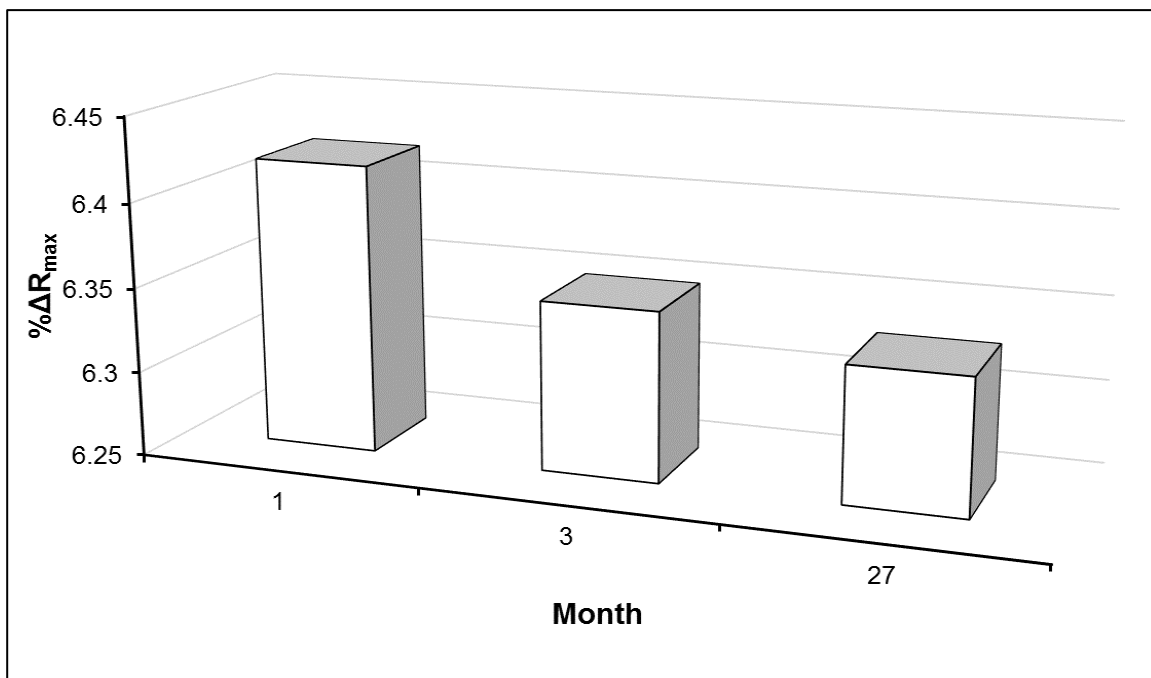


Figure 4.36. Storage stability of hemoglobin imprinted SPR biosensor. Experiment condition:  $c_{\text{Hb}}=0.1$  mg/mL,  $T=25^{\circ}\text{C}$ , pH 6.0.

Table 4.4. The comparison of different systems with this system for hemoglobin detection.

Sensor type	Based on	Detection range	Limit of detection	Selectivity	Reusability	Time	Real sample	Reference
Electrochemical	Magnetic nanoparticles	0.005-0.1 mg/mL	0.001 mg/mL	Lyz, BSA, HRP	Not reported	7 min	Blood	[81]
Fluorescence	Core-shell	0.02-2.0 $\mu$ M	6.3 nM	Lyz, BSA, OB	5 times	15 min	Blood, urine	[82]
Localized surface plasmon resonance	Artificial antibody	0.5-20 $\mu$ g/mL	Not reported	HSA, BSA, Lyz	Not reported	120 min	Not reported	[83]
Differential pulse voltametry	eATRP	$1.10^{-10}$ - $1.10^1$ mg/L	$7.8.10^{-11}$ mg/L	Lyz, BSA, HSA, IgG	3 times	120 min	Bovine blood	[84]
Fluorescence	Gold nanoparticle	0.1-20 $\mu$ mol/L	0.03 $\mu$ mol/L	BSA, BHB, Alb, CE	Not reported	Not reported	Not reported	[85]
Differential pulse voltametry	Cryogel	$1.10^{-8}$ - $1.10^2$ mg/L	$6.7.10^{-9}$ mg/L	Lyz, BSA, HSA	3 times	120 min	Bovine blood	[86]
Electrochemical	SAM	1-20 $\mu$ g/mL	Not reported	Myb	Not reported	Not reported	Not reported	[87]
Localized surface plasmon resonance	PEGlated nanorattle	1-2500 ng/mL	Not reported	HSA, BSA, Myb	Not reported	Not reported	Not reported	[88]
Chemiluminescent	Carbon nanotube	$5.10^{-10}$ - $7.10^{-7}$ mg/mL	$1.5.10^{-10}$ mg/mL	BSA, Lyz	Not reported	Not reported	Waste water	[89]
Electrochemical	Gold nanoparticle	$1.10^{-11}$ - $1.10^{-2}$ mg/mL	Not reported	BSA, EA, Lyz	5 times	Not reported	Not reported	[90]
Electrochemical	Nanoparticle	0.005-0.1 mg/mL	25.8 ng/mL	Lyz, HRP	Not reported	10 min	Not reported	[91]
Electrochemical	Graphene-carbon electrode	$1.10^{-10}$ - $1.10^{-3}$ mg/mL	$3.09.10^{-11}$ mg/mL	BSA, HSA, Lyz, ATP, BI	3 times	120 min	Bovine blood	[92]
Electrochemical	Magnetic nanoparticle	$5.10^{-7}$ - $1.10^{-5}$ mg/mL	$1.184.10^{-8}$ mg/mL	BSA, Lyz, Cyt C, HRP	Not reported	70 min	Not reported	[93]
Electrochemical	Graphene composite	$1.10^{-9}$ - $1.10^{-1}$ mg/mL	$2.10^{-10}$ mg/mL	BSA, Lyz, EA, Pap	Not reported	10 min	Bovine blood	[94]
Surface plasmon resonance-Electrochemical	Thin film	0.0005-5.0 mg/mL	0.000435 mg/mL	BSA, Lyz, Ova	Not reported	25 min	Not reported	[95]
Electrochemi-luminescence	Magnetic nanocomposite	$0.1-4.10^4$ pg/mL	0.023 pg/mL	BSA, CEA, AFP, HCG, HlgG	Not reported	70 min	Human serum	[96]
Phosphorescence	Quantum dot	$1.10^{-7}$ - $5.10^{-6}$ mol/L	$3.8.10^{-8}$ mol/L	Not reported	11 times	15 min	Urine, serum	[97]
Electrochemical	Gold microdendrites	$0.1-4.10^3$ $\mu$ g/mL	0.05 $\mu$ g/mL	BSA, Lyz, Cyt C, Ova	5 times	60 min	Not reported	[98]
Electrochemical	Quantum dot-carbon nanotube	27.8-444 ng/mL	6.73 ng/mL	BSA, Trp, Crp, Glu, Dop, Cys, AA, Ins	Not reported	Not reported	Human blood	[99]
Fluorescence	Quantum dot	0.02-2.1 $\mu$ M	9.4 nM	BSA, Lyz, OB	Not reported	60 min	Bovine blood, urine	[100]
Surface plasmon resonance	Nanofilm	<b>0.0005-1.0 mg/mL</b>	<b>0.00035 mg/mL</b>	<b>Lyz, BSA, Trf, Myb</b>	<b>4 times</b>	<b>23 min</b>	<b>Not reported</b>	<b>Our study</b>

The comparison of the hemoglobin imprinted biosensor systems is summarized in Table 4.4. The table is prepared with different parameters such as sensor type, dynamic range, limit of detection, selectivity, reusability etc. year by year since 2013 and based on MIP database references.

## 4.5. Portable Microfluidic-Integrated SPR Biosensors

### 4.5.1. Surface Chemistry Modification

Each surface modification step was monitored by recording SPR angle shifts on the resonance angle as shown in Figure 4.37. The SPR angle shifted with different surface activators (EDC/NHS, protein G, and antibody) and the baseline was obtained during PBS washing steps after each modification. The sharp angle shift was observed when EDC/NHS couple applied to the portable microfluidic-integrated SPR system. After washing steps, protein G and antibody binding were occurred with angle shifts as well.

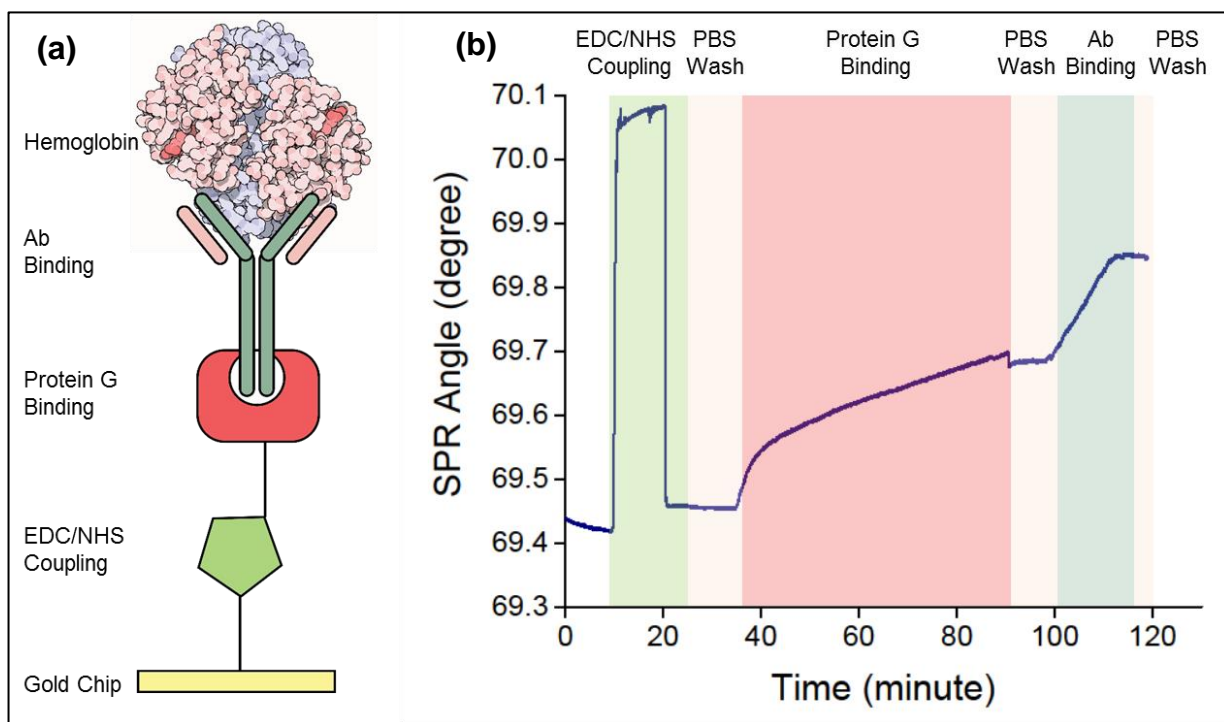


Figure 4.37. Evaluation of surface chemistry steps via real-time monitoring SPR angle changes.

### 4.5.2. SPR Measurements

After antibody immobilization on the chip surfaces, the microfluidic-integrated SPR biosensors were washed with PBS buffer with 5  $\mu\text{L}/\text{min}$  of flow rate before the injecting hemoglobin solutions. Then, the hemoglobin solutions ranging from 5-250  $\mu\text{g}/\text{mL}$  were



applied to the portable SPR monitoring system with 5  $\mu\text{L}/\text{min}$  of flow rate. A complete measurement consists of applying 20 min of PBS buffer, then 30-60 min of hemoglobin solutions injection in PBS to the system and then applying 20 min of PBS buffer at the same flow rate, respectively. All steps including equilibration-detection-washing were approximately completed within 70-100 min.

As demonstrated in Figure 4.38-Figure 4.44, the increments in hemoglobin solution concentration resulted in an amplification in SPR angle shifts. For instance, the representative resonance angle shifts ( $\Delta A$ ) were obtained as 0.06-0.36 degree in the SPR curve upon detection of hemoglobin when 5-250  $\mu\text{g}/\text{mL}$  was applied. The correlation coefficient was obtained as 0.989 between 5-250  $\mu\text{g}/\text{mL}$  of hemoglobin solutions with the  $y=0.0798\ln(x)-0.0862$  equation (Figure 4.45). Namely, the portable microfluidic-integrated SPR biosensor was able to detect hemoglobin with 98.9% precision for 5-250  $\mu\text{g}/\text{mL}$  of hemoglobin concentration ranges.

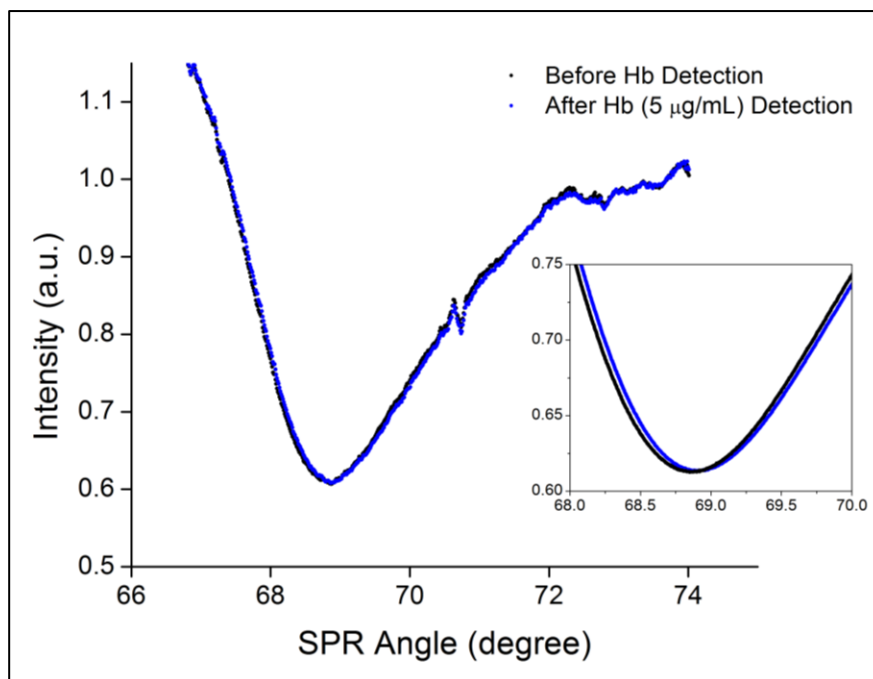


Figure 4.38. The plot of SPR angle shift after the application of 5  $\mu\text{g}/\text{mL}$  hemoglobin to the microfluidic-integrated SPR biosensor.

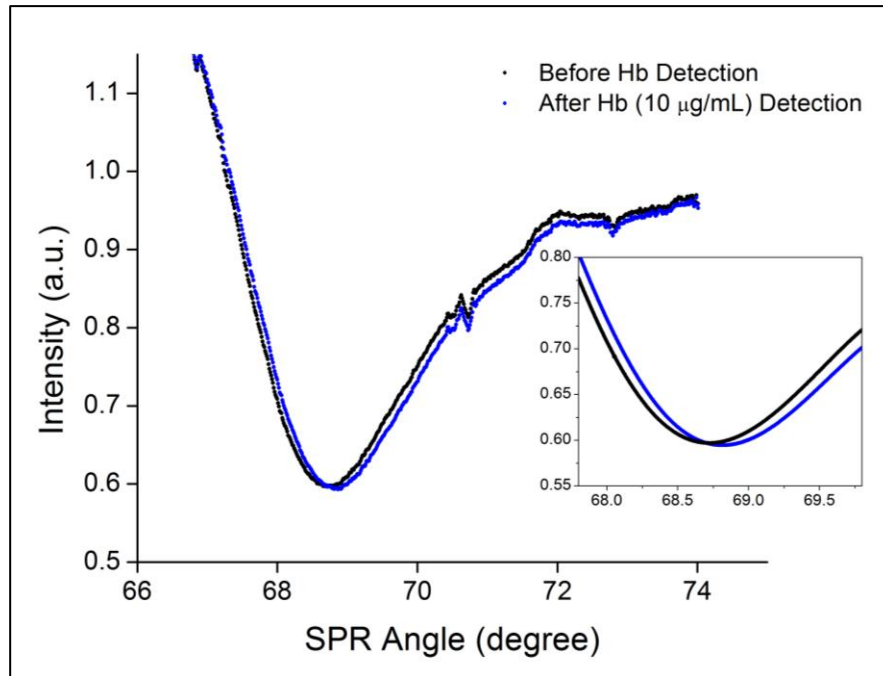


Figure 4.39. The plot of SPR angle shift after the application of 10  $\mu\text{g/mL}$  hemoglobin to the microfluidic-integrated SPR biosensor.

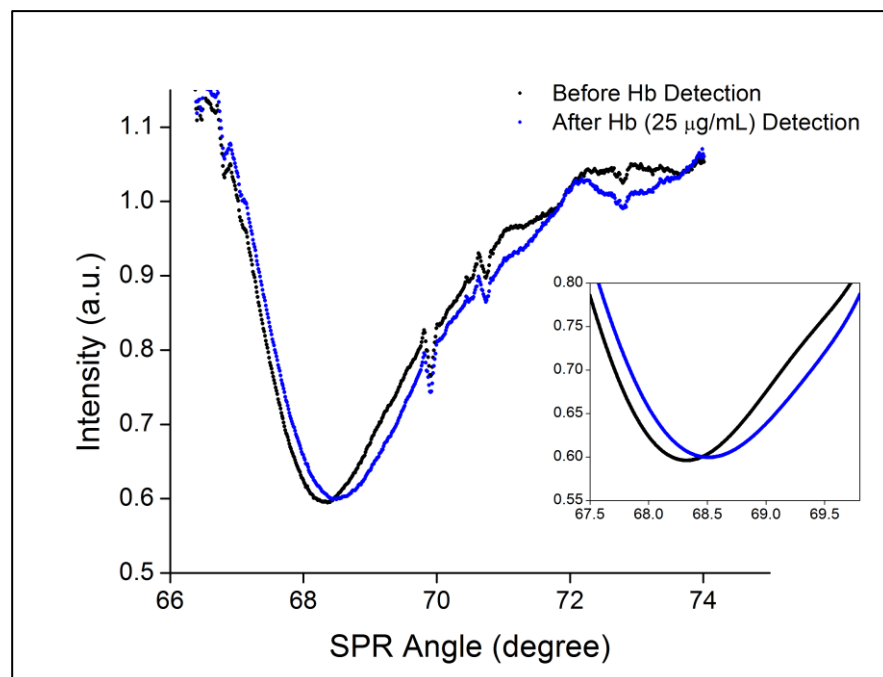


Figure 4.40. The plot of SPR angle shift after the application of 25  $\mu\text{g/mL}$  hemoglobin to the microfluidic-integrated SPR biosensor.

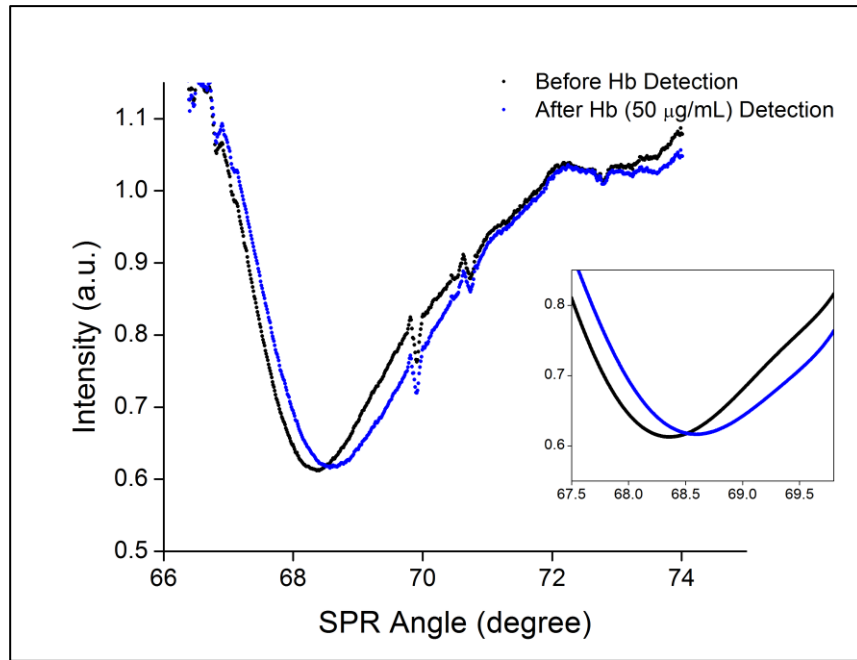


Figure 4.41. The plot of SPR angle shift after the application of 50  $\mu\text{g/mL}$  hemoglobin to the microfluidic-integrated SPR biosensor.

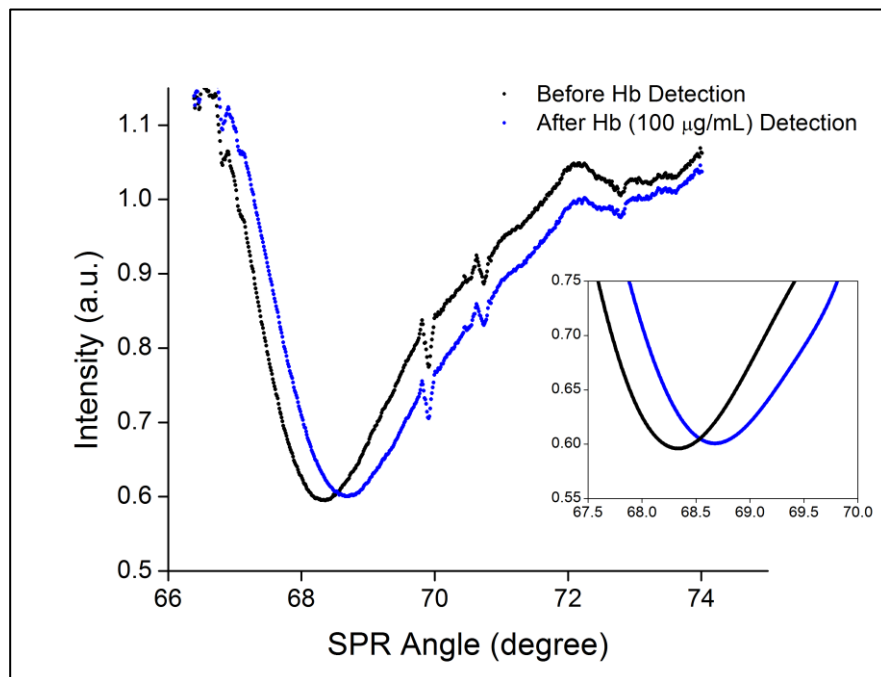


Figure 4.42. The plot of SPR angle shift after the application of 100  $\mu\text{g/mL}$  hemoglobin to the microfluidic-integrated SPR biosensor.

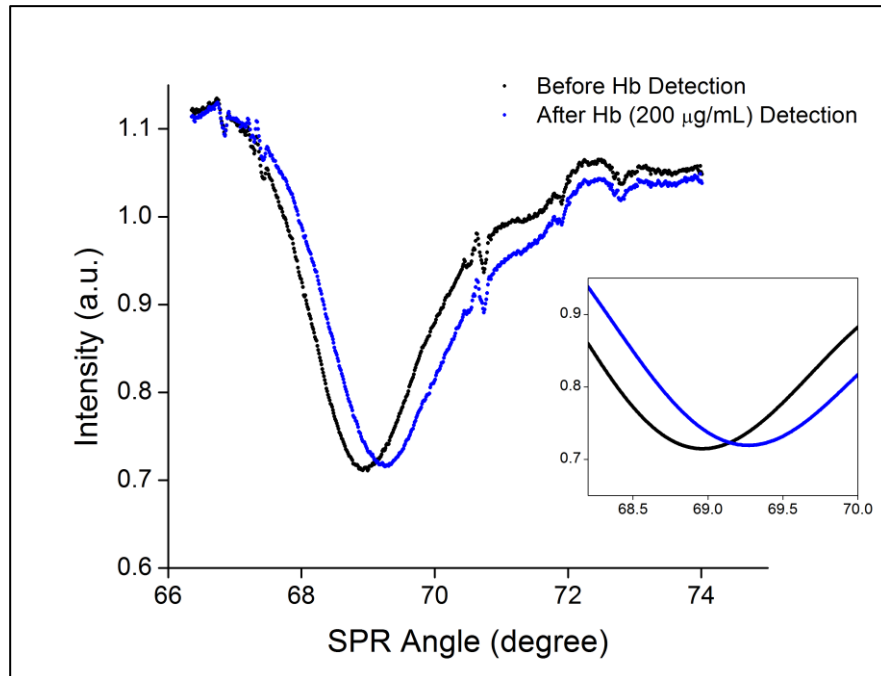


Figure 4.43. The plot of SPR angle shift after the application of 200  $\mu\text{g/mL}$  hemoglobin to the microfluidic-integrated SPR biosensor.

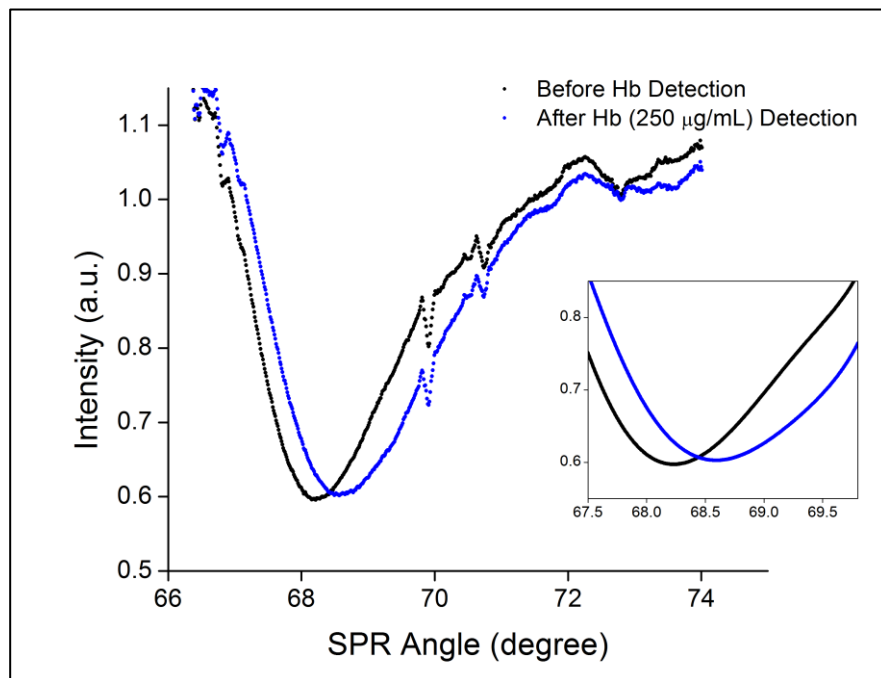


Figure 4.44. The plot of SPR angle shift after the application of 250  $\mu\text{g/mL}$  hemoglobin to the microfluidic-integrated SPR biosensor.

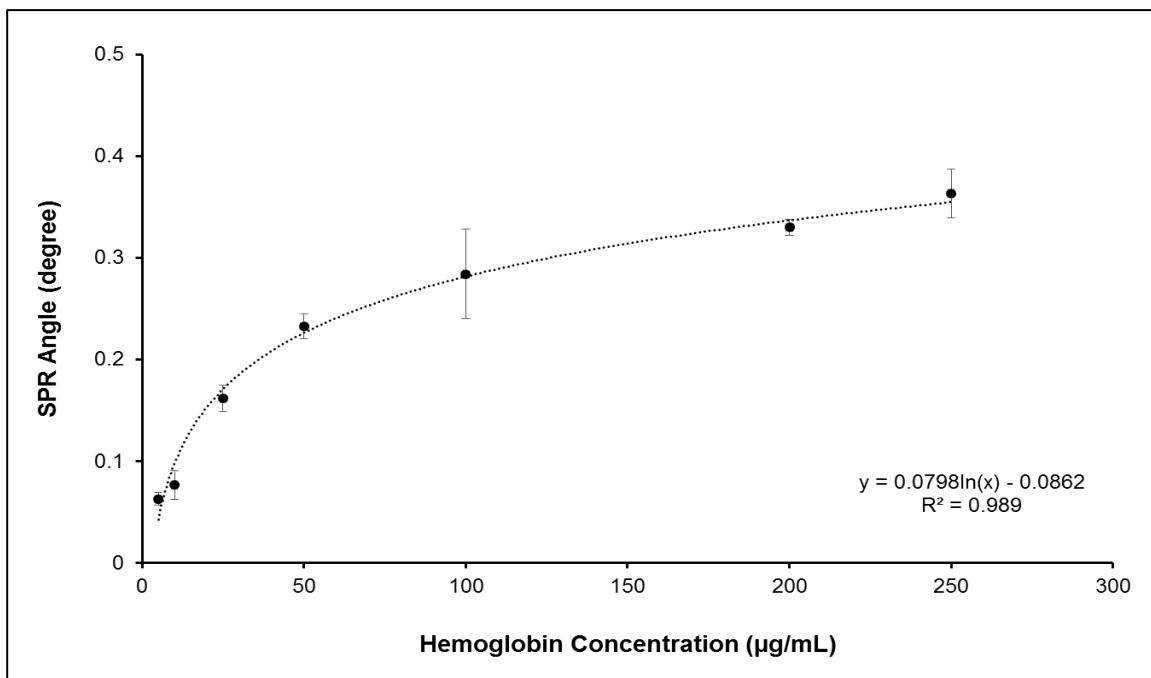


Figure 4.45. The calibration curve for hemoglobin detection onto the microfluidic-integrated SPR biosensor.

#### 4.5.3. Equilibrium Analysis

The equilibrium analysis was investigated to determine the host-guest interactions during SPR measurements. According to the data from Figure 4.46, the maximum resonance angle shift ( $\Delta A_{\max}$ ) was obtained as 0.42 which was close the experimental data. In addition, association ( $K_A$ ) and dissociation ( $K_D$ ) coefficients were calculated as 0.024 mL/ $\mu$ g and 42.6  $\mu$ g/mL with high correlation coefficient ( $R^2= 0.98$ ).

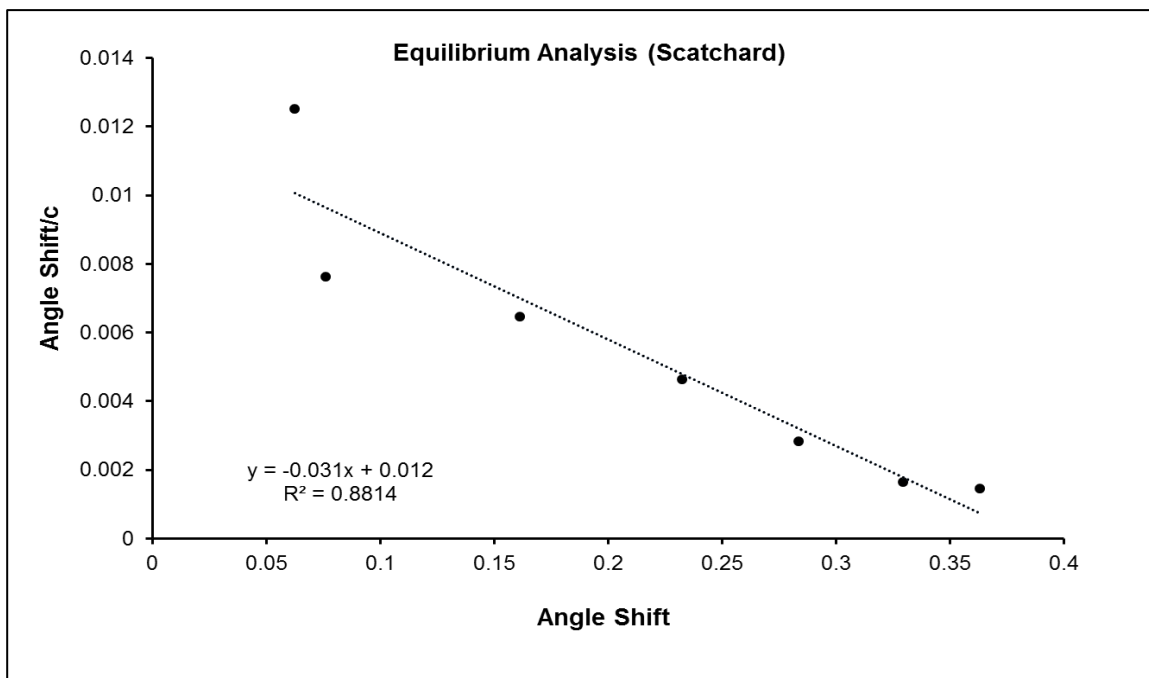


Figure 4.46. Determination of kinetic rate constants: Equilibrium analysis.

#### 4.5.4. Adsorption Isotherm Models

The Langmuir, Freundlich and Langmuir-Freundlich adsorption isotherm model graphs were represented in Figure 47, Figure 48 and Figure 49. The parameters for all isotherm models were presented in Table 4.5. Considering all calculations and results derived from kinetic models, Langmuir adsorption isotherm model provided the fittest adsorption isotherm model to define the interactions between the portable microfluidic-integrated SPR biosensor and the hemoglobin ( $R^2=0.936$ ). The Langmuir equation indicated that the binding of hemoglobin onto the portable microfluidic-integrated SPR biosensor surface was a monolayer.  $K_A$  and  $K_D$  values were also calculated as  $0.044 \text{ mL}/\mu\text{g}$  and  $22.81 \mu\text{g}/\text{mL}$ .

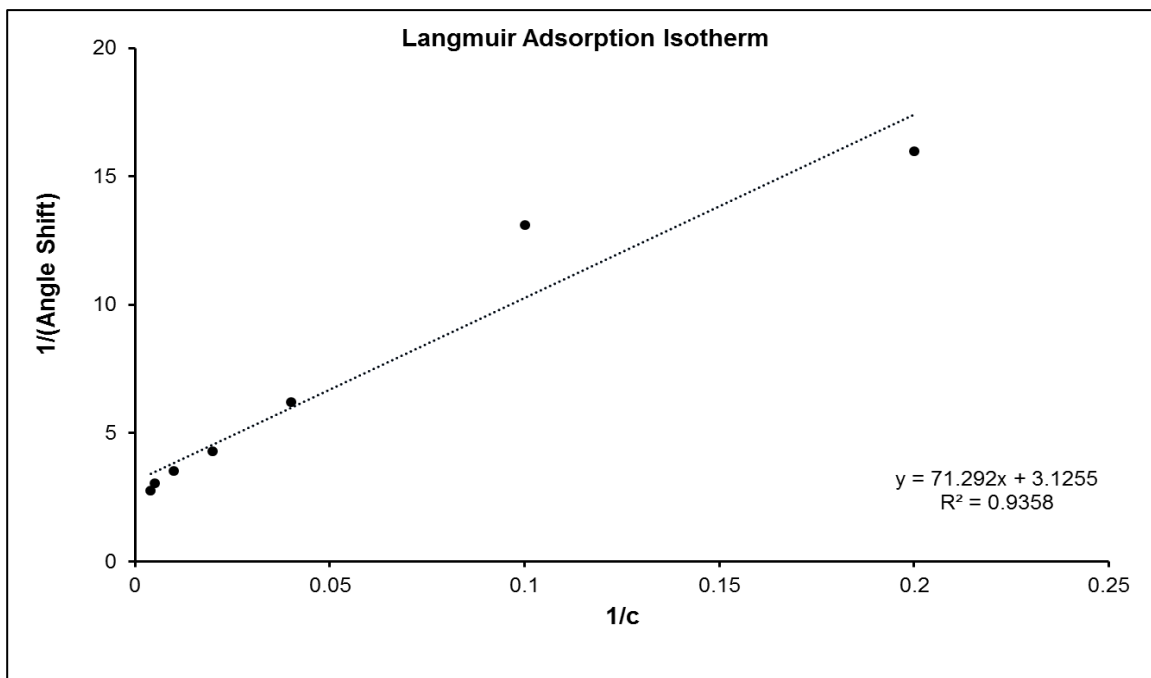


Figure 4.47. Langmuir adsorption isotherm model.

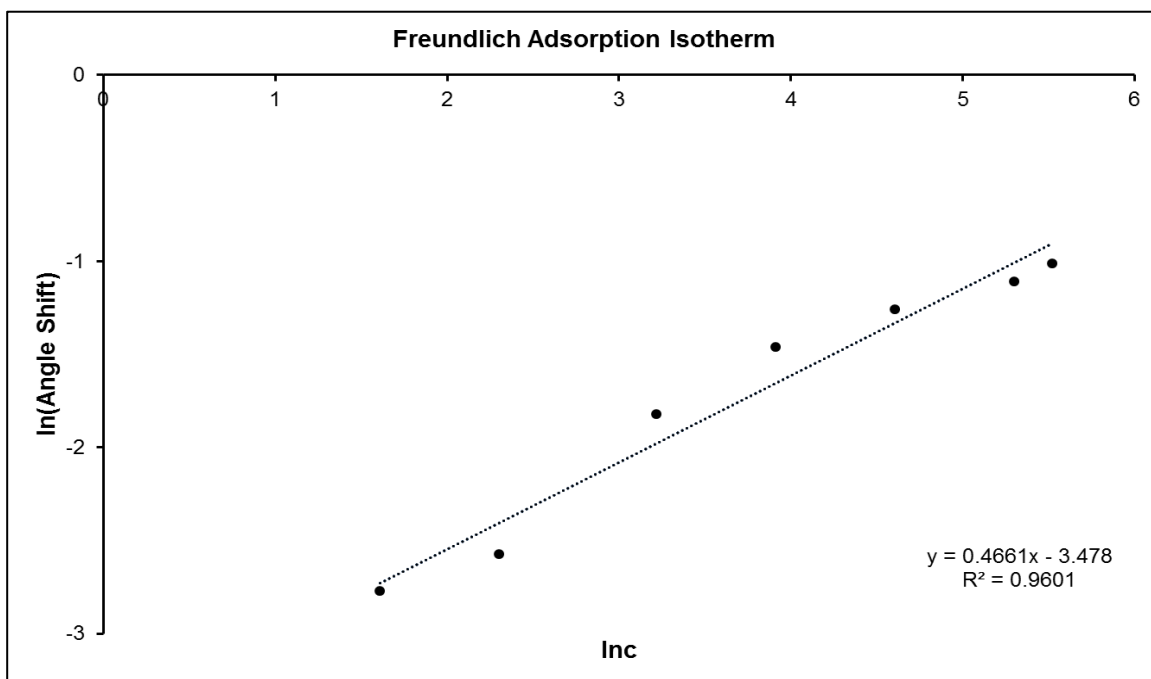


Figure 4.48. Freundlich adsorption isotherm model.

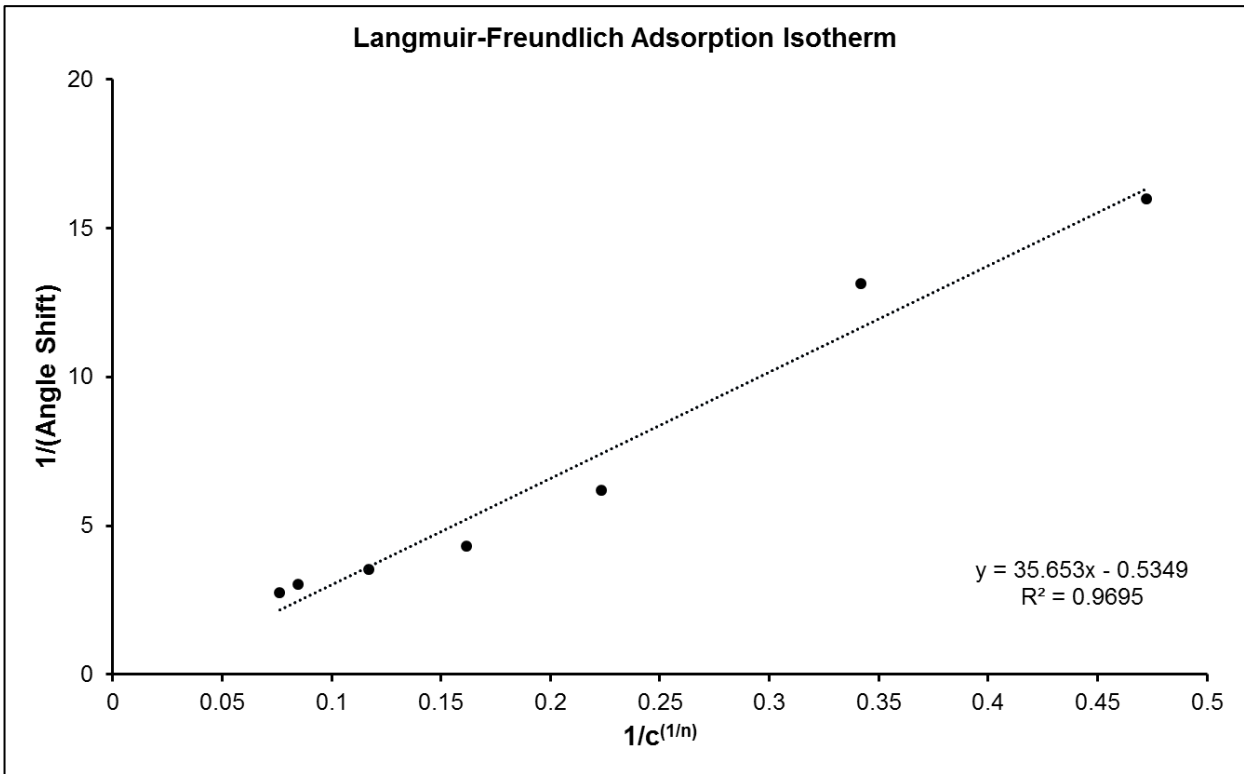


Figure 4.49. Langmuir-Freundlich adsorption isotherm model.

Table 4.5. Comparison of adsorption isotherm models.

Langmuir		Freundlich		Langmuir-Freundlich	
$\Delta A_{max}$	0.32	$\Delta A_{max}$	32.4	$\Delta A_{max}$	1.87
$K_D, \mu\text{g/mL}$	22.8	$1/n$	0.47	$1/n$	0.47
$K_A, \text{mL}/\mu\text{g}$	0.04	$R^2$	0.96	$K_D, \mu\text{g/mL}$	66.7
$R^2$	0.94			$K_A, \text{mL}/\mu\text{g}$	0.02
				$R^2$	0.97



Table 4.6. The comparison of different systems with this system for hemoglobin detection.

Sample load	Detection Conditions	Target	Detection range	Limit of detection	Assay time	Advantages or disadvantages	References
Pump (Flow rate: 60 $\mu$ L/min)	PBS (pH 7.4) and 0.01 M HCl	Hemoglobin	0.2-1.0 $\mu$ M	0.15 $\mu$ M	10 min	Requires multiple washing steps and precise	[117]
Pump (Flow rate: 0.02 mL/min)	PBS (pH 7.4)	Hemoglobin	0.1-25 mg/mL	Not reported	4-8 min	Requires GaAs-based molecular controlled semiconductor	[118]
Pump (Flow rate: 40 $\mu$ L/min)	PBS (pH 7.4)	Apo-hemoglobin	2.5-30.0 $\mu$ M	2 $\mu$ M	500 s	Low dynamic linear range	[119]
Not reported	PBS (pH 7.0)	Hemoglobin	0-250 $\mu$ g/mL	Not reported	2-10 min	Requires ionic strength and content control	[120]
<b>Pump (Flow rate: 5 <math>\mu</math>L/min)</b>	<b>PBS (pH 7.4)</b>	<b>Human hemoglobin</b>	<b>5-250 <math>\mu</math>g/mL</b>	<b>Down to 5 <math>\mu</math>g/mL</b>	<b>30 min</b>	<b>Fully portable setup.</b>	<b>Our Study</b>

Finally, the portable microfluidic-integrated SPR biosensor system was compared with the other studies. The comparison of different systems with this system for hemoglobin detection in Table 4.6. The table is prepared with different parameters such as detection condition, target, assay time, advantages and disadvantages so on.

## 5. CONCLUSION

- The aim of this study is molecularly imprinted nanofilm production onto the surface plasmon resonance biosensor surface to detect hemoglobin protein.
- To increase detection capability of the hemoglobin imprinted SPR biosensor acrylamide monomer was used together with hemoglobin during the imprinting process.
- According to the FTIR spectrum of acrylamide monomer, the absorption located in the regions around 3100-3300  $\text{cm}^{-1}$  represents to the asymmetric and symmetric N-H stretching vibrations from acrylamide. The intensity band appearing in the region 2809  $\text{cm}^{-1}$  are assigned to symmetric C-H stretching vibrations. The amide I band (between 1600 and 1700  $\text{cm}^{-1}$ ) is principally related to the C=O stretching vibration and is directly associated with the backbone conformation. The absorption located in the region 1427  $\text{cm}^{-1}$  has been designated to C-N stretching vibrations (Figure 4.1).
- The hemoglobin:acrylamide pre-complex was prepared and characterized by UV-visible spectroscopy. According to the obtained graph in Figure 4.2, the hemoglobin:acrylamide pre-complex ratio was chosen as 1  $\mu\text{mol}$ :4 mmol (Hb:AAM).
- The hemoglobin imprinted and non-imprinted SPR biosensors were placed in a sample holder by FTIR-ATR spectroscopy system and obtained FTIR spectra (Figure 4.3-Figure 4.4). The absorption located in the regions around 3100-3300  $\text{cm}^{-1}$  represented the asymmetric and symmetric N-H stretching vibrations from polyacrylamide matrix. The intensity band appearing in the region around 2900  $\text{cm}^{-1}$  are assigned to symmetric C-H stretching vibrations. The amide I bands (between 1600 and 1650  $\text{cm}^{-1}$ ) is related to the C=O stretching vibrations. The shifting bands of from 1647  $\text{cm}^{-1}$  to 1655  $\text{cm}^{-1}$  C=O and C-N from 1448  $\text{cm}^{-1}$  to 1424  $\text{cm}^{-1}$  confirmed that the imprinting process succeeded.

- The bare, non-imprinted and hemoglobin imprinted SPR biosensors revealed that the average surface roughness values were raised from 0.54 nm to 1.86 nm that obtained by AFM measurements (Figure 4.5-4.7). In addition, root mean square (RMS) values were also increased from 0.73 nm to 2.46 nm with imprinting process. This result also confirmed that the surface roughness was amplified and polymerization was succeeded onto the SPR biosensor.
- Surface thicknesses were calculated from ellipsometry measurements as  $88.3\pm 3.3$  nm and  $87.9\pm 1.6$  nm for non-imprinted and hemoglobin imprinted SPR biosensors (Figure 4.8 and Figure 4.9). The results showed that the homogeneous and monolayer formation of the nanofilm had succeeded.
- According to contact angle measurements, the contact angle of bare and hemoglobin imprinted SPR biosensors were observed as  $64.7\pm 1.4^\circ$  to  $58.4\pm 1.0^\circ$ . A significant reduction of the contact angle indicated that the surface hydrophilicity was increased. In addition, the contact angle of non-imprinted SPR biosensor has  $42.5\pm 1.6^\circ$ . The contact angle measurements images with angles were demonstrated in Figure 4.10-4.12.
- The hemoglobin imprinted SPR biosensor was performed with hemoglobin solutions in same concentration (0.1 mg/mL) and at different pH (range from 4.0-8.0). As seen in Figure 4.13 (a-b), the highest response was observed at pH 6.0.
- The increase of the hemoglobin imprinted SPR biosensor response in different hemoglobin solutions was shown in Figure 4.14-4.22. The combination of responses of hemoglobin imprinted SPR biosensor was also exhibited in Figure 4.23. According to the results, the change in  $\% \Delta R$  values increased from 0.098 to 13.67 while hemoglobin concentration was raised from 0.0005 mg/mL to 1.0 mg/mL.
- The relationships between hemoglobin concentration and  $\% \Delta R$  were also given in Figure 4.24. When the  $\% \Delta R$  data which were determined for the concentration between 0.0005-1.0 mg/mL were taken, the curve had an equation  $y =$

$1.7872\ln x + 11.545$  with  $R^2$  value as 0.91. It means the hemoglobin imprinted SPR biosensor is talented for hemoglobin detection from sample solutions with 91% precision if it is a range in 0.0005-1.0 mg/mL. Also, the hemoglobin imprinted SPR biosensor is talented to detect hemoglobin from sample solutions with 99% precision if it is a range in 0.0005-0.05 mg/mL and 94% precision if it is a range of 0.1-1.0 mg/mL (Figure 4.25).

- According to the results, limit of detection value was determined as 0.00035 mg/mL with  $3S/b$  formula.
- Equilibrium and association kinetics analysis graphs were also shown in Figure 4.26-4.27. According to the results, high correlation coefficients were obtained with experimental data as 0.92 and 0.98 for equilibrium and association kinetics analysis. In addition, the association and dissociation coefficients were obtained as 12.6 mL/mg and 0.08 mg/mL for equilibrium analysis and 15 mL/mg and 0.07 mg/mL for association kinetic analysis. All coefficients were given in Table 4.1.
- The adsorption isotherm models were demonstrated in Figure 4.28-4.30. In addition, the parameters for all isotherm models were given in Table 4.2. According to the results, the best fitted model to define the interaction between the hemoglobin imprinted SPR biosensor and hemoglobin solution is Langmuir adsorption isotherm model ( $R^2=0.995$ ). The  $K_A$  and  $K_D$  values were also found as 39.1 mL/mg and 0.03 mg/mL.
- The selectivity of the hemoglobin imprinted SPR biosensor was carried out by using lysozyme (Lyz), transferrin (Trf), bovine serum albumin (BSA), and myoglobin (Myb) detections. The Figure 4.31, Lyz ( $\% \Delta R=4.19$ ) exhibited higher rebinding on the hemoglobin imprinted SPR biosensor than Trf ( $\% \Delta R=1.64$ ), BSA ( $\% \Delta R=0.61$ ), and Myb ( $\% \Delta R=0.40$ ).
- The non-imprinted SPR biosensor was also prepared and it gave a low response to hemoglobin solution ( $\% \Delta R=0.57$ ). The  $\% \Delta R$  values of the non-imprinted SPR

biosensor to Lyz, Trf, BSA, and Myb were also defined as 11.48, 1.00, 0.46 and 0.24 (Figure 4.32).

- The selectivity coefficients were calculated between hemoglobin and Lyz, Trf, BSA, and Myb as 1.71, 4.36, 11.7 and 17.9 for hemoglobin imprinted SPR biosensor.
- The selectivity coefficients were determined between hemoglobin and Lyz, Trf, BSA, and Myb as 1.39, 0.57, 1.24 and 2.38 for non-imprinted SPR biosensor as well.
- The relative selectivity coefficients were also calculated as 4.39, 7.65, 9.44 and 7.52 for Lyz, Trf, BSA, and Myb. According to all responses of hemoglobin imprinted and non-imprinted SPR biosensors, the structural memory and specificity were only observed in hemoglobin imprinted SPR biosensor due to the imprinting process.
- The protein mixtures were prepared by the same concentrations of Lyz-Hb, Trf-Hb, BSA-Hb, and Myb-Hb proteins to support selectivity property of the hemoglobin imprinted SPR biosensor. As demonstrated in Figure 4.34, the mixture of Lyz and Hb showed the highest response ( $\% \Delta R = 5.69$ ) for hemoglobin imprinted SPR biosensor. The Trf-Hb, BSA-Hb, and Myb-Hb protein mixtures responses were observed as 3.05, 2.44 and 1.17 for hemoglobin imprinted SPR biosensor as well. The non-imprinted SPR biosensor was showed less response with the mixture of Lyz-Hb ( $\% \Delta R = 1.89$ ), Trf-Hb ( $\% \Delta R = 1.92$ ), BSA-Hb ( $\% \Delta R = 1.31$ ), and Myb-Hb ( $\% \Delta R = 1.06$ ).
- The reusability analysis of the hemoglobin imprinted SPR biosensor, adsorption-desorption-regeneration cycles were performed. As seen in Figure 4.35, the sample solutions were prepared different solutions as 0.05, 0.25, 0.5 and 1.0 mg/mL and then applied to the SPR system consecutively. As indicated, the responses of the hemoglobin imprinted SPR biosensor was increased.

- The storage stability of the hemoglobin imprinted SPR biosensor was performed with same hemoglobin concentration (0.1 mg/mL) at different times (0, 3, 27 months). The % $\Delta R$  of the hemoglobin imprinted SPR biosensor was decreased from 6.42 to 6.33 and the performance loss was only 9% (Figure 4.36) in 27 months.
- To prepare portable microfluidic-integrated SPR biosensors surface modification steps such as EDC/NHS activating, protein G binding, and antibody immobilization was monitored by recording SPR angle shifts on the resonance angle as shown in Figure 4.37.
- As demonstrated in Figure 4.38-4.44, the increments in hemoglobin solution concentration resulted in an amplification in SPR angle shifts onto the portable microfluidic-integrated SPR biosensors. The resonance angle shifts ( $\Delta A$ ) were obtained as 0.06-0.36 degree in the SPR curve upon detection of hemoglobin when 5-250  $\mu\text{g/mL}$  was applied.
- The portable microfluidic-integrated SPR biosensor was able to detect hemoglobin with 98.9% precision for 5-250  $\mu\text{g/mL}$  of hemoglobin concentration ranges with the  $y=0.0798\ln(x)-0.0862$  equation (Figure 4.45).
- The maximum resonance angle shift ( $\Delta A_{\text{max}}$ ) was obtained as 0.42 which was close the experimental data. In addition, association ( $K_A$ ) and dissociation ( $K_D$ ) coefficients were calculated as 0.024 mL/ $\mu\text{g}$  and 42.6  $\mu\text{g/mL}$  with high correlation coefficient ( $R^2= 0.98$ ) for equilibrium analysis (Figure 4.46).
- Considering all calculations and results, Langmuir adsorption isotherm model provided the fittest adsorption isotherm model to define the interactions between the portable microfluidic-integrated SPR biosensor and the hemoglobin molecules (Figure 4.48-4.50). The parameters for all models were presented in Table 4.5.

## 6. REFERENCES

- [1] Altıntaş, E.B., Türkmen, D., Karakoc, V., Denizli, A., Hemoglobin binding from human blood hemolysate with poly(glycidylmethacrylate) beads, *Colloids and Surfaces B: Biointerfaces*, 85, 235–240, **2011**.
- [2] Derazshamshir, A., Baydemir, G., Andac, M., Say, R., Galaev, I.Y., Denizli, A., Molecularly imprinted PHEMA-based cryogel for depletion of hemoglobin from human blood, *Macromolecular Chemistry and Physics*, 211, 657–668, **2010**.
- [3] Angastiniotis, M., Modell, A., Global epidemiology of hemoglobin disorders, *Annals New York Academy of Sciences*, 850, 251–269, **1998**.
- [4] Gao, R., Zhao, S., Hao, Y., Zhang, L., Cui, X., Liu, D., Zhang, M., Tang, Y., Synthesis of magnetic dual-template molecularly imprinted nanoparticles for the specific removal of two high-abundance proteins simultaneously in blood plasma, *Journal of Separation Science*, 38, 3914–3920, **2015**.
- [5] Sun, S., Chen, L., Shi, H., Li, Y., He, X., Magnetic glass carbon electrode, modified with magnetic ferrihydrite nanoparticles coated with molecularly imprinted polymer films for electrochemical determination of bovine hemoglobin, *Journal of Electroanalytical Chemistry*, 734, 18–24, **2014**.
- [6] Zhang, R., Xu, S., Luo, J., Liu, X., Molecularly imprinted photo-sensitive polyglutamic acid nanoparticles for electrochemical sensing of hemoglobin, *Microchimica Acta*, 182, 175–183, **2015**.
- [7] Whitcombe, M.J., Chianella, I., Larcombe, L., Piletsky, S.A., Noble, J., Porter, R., Horgan, A., The rational development of molecularly imprinted polymer-based sensors for protein detection, *Chemical Society Reviews*, 40, 1547–1571, **2011**.
- [8] Du, W., Fu, Q., Zhao, G., Huang, P., Jiao, Y. Y., Wu, H., Luo, Z. M., Chang, C., Dummy-template molecularly imprinted solid phase extraction for selective analysis of ractopamine in pork, *Food Chemistry*, 139, 24–30, **2013**.
- [9] Dibekkaya, H., Saylan, Y., Yilmaz, F., Derazshamshir, A., Denizli, A., Surface plasmon resonance sensors for real-time detection of cyclic citrullinated peptide antibodies, *Journal of Macromolecular Science, Part A: Pure and Applied Chemistry*, 53, 585–594, **2016**.
- [10] Rabieizadeh, M., Kashefiforad, S.M., Naeimpoor, F., Monolithic molecularly imprinted cryogel for lysozyme recognition, *Journal of Separation Science*, 37, 2983–2990, **2014**.

- [11] Kan, X.W., Xing, Z.G., Zhu, A.H., Zhao, Z., Xu, G.L., Li, C., Zhou, H., Molecularly imprinted polymers based electrochemical sensor for bovine hemoglobin recognition, *Sensors and Actuators B Chemical*, 168, 395–401, **2012**.
- [12] Fan, L.L., Zhang, Y., Li, X.J., Luo, L.N., Lu, F.G., Qiu, H.M., Removal of alizarin red from water environment using magnetic chitosan with Alizarin Red as imprinted molecules, *Colloids and Surfaces B*, 91, 250–257, **2012**.
- [13] Tokel, O., Yildiz, U.H., Inci, F., Durmus, N.G., Ekiz, O.O., Turker, B., Cetin, C., Rao, S., Sridhar, K., Natarajan, N., Shafiee, H., Dana, A., Demirci, U., Portable microfluidic integrated plasmonic platform for pathogen detection, *Scientific Reports*, 5, 9152–9161, **2015**.
- [14] Tokel, O., Inci, F., Demirci, U., Advances in plasmonic technologies for point of care applications, *Chemical Reviews*, 114, 5728–5752, **2014**.
- [15] Sommer, G.J., Chang, D.S., Jain, A., Langelier, S.M., Park, J., Rhee, M., Wang, F., Zeitoun, R.I., Burns, M.A., Introduction to microfluidics, *Microfluidics for biological applications*, Springer Science and Business Media, LLC, 1–34, **2008**.
- [16] Whitford, D., Proteins: Structure and function, *John Wiley & Sons Ltd*, The Atrium, Southern Gate, West Sussex, England, 439–479, **2005**.
- [17] Scheller, F.W., Bistolas, N., Liu, S., Jänchen, M., Katterle, M., Wollenberger, U., Thirty years of haemoglobin electrochemistry, *Advances in Colloid and Interface Science*, 116, 111–120, **2005**.
- [18] Fathallah, H., Taher, A., Bazarbachi, A., Atweh, G.F., Differences in response to fetal hemoglobin induction therapy in beta-thalassemia and sickle cell disease, *Blood Cells, Molecules, and Diseases*, 43, 58–62, **2009**.
- [19] Bellelli, A., Brunori, M., Heme Proteins, the Globins, *Encyclopedia of Metalloproteins*, 951–963, **2013**.
- [20] Mader, S.S., Cardiovascular system, Inquiry into life, *The McGraw-Hill Companies*, 239–256, **2002**.
- [21] Hardison, R., Hemoglobins from bacteria to man: Evolution of different patterns of gene expression, *The Journal of Experimental Biology*, 201, 1099–1117, **1998**.
- [22] Lawn, R. M., Fritsch, E.F., Parker, R.C., Blake, G., Maniatis, T., The isolation and characterization of linked  $\delta$ - and  $\beta$ -globin genes from a cloned library of human DNA, *Cell*, 15, 1157–1174, **1978**.
- [23] Brecher, G., Cronkite, E.P., Morphology and enumeration of human blood platelets', *Journal of Applied Physiology*, 3, 365–377, **1950**.



- [24] Modell, B., Darlison, M., Birgens, H., Cario, H., Faustino, P., Giordano, P.C., Gulbis, B., Hopmeier, P., Lena-Russo, D., Romao, L., Theodorsson, E., Epidemiology of haemoglobin disorders in Europe: an overview, *Scandinavian Journal of Clinical and Laboratory Investigation*, 67, 39–69, **2007**.
- [25] Modell, B., Darlison, M., Global epidemiology of haemoglobin disorders and derived service indicators, *Bulletin of the World Health Organization*, 6, 480–487, **2008**.
- [26] Lv, Y.Q., Tan, T.W., Svec, F., Molecular imprinting of proteins in polymers attached to the surface of nanomaterials for selective recognition of biomacromolecules, *Biotechnology Advances*, 31, 1172–1186, **2013**.
- [27] Li, L., Fan, L., Dai, Y., Kan, X., Recognition and determination of bovine hemoglobin using a gold electrode modified with gold nanoparticles and molecularly imprinted self-polymerized dopamine, *Microchimica Acta*, 182, 2477–2483, **2015**.
- [28] Wulff, G., Sarhan, A., Use of polymers with enzyme analogous structures for the resolution of racemates, *Angewandte Chemie International Edition*, 11, 341, **1972**.
- [29] Wulff, G., Gross, T., Schonfeld, R., Enzyme models based on molecularly imprinted polymers with strong esterase activity, *Angewandte Chemie International Edition*, 36, 1962–1964, **1997**.
- [30] Verma, A., Nakade, H., Simard, J.M., Rotello, V.M., Recognition and stabilization of peptide  $\alpha$ -helices using templatable nanoparticle receptors, *Journal of the American Chemical Society*, 126, 10806–10807, **2004**.
- [31] Aubin-Tam, M.E., Hamad-Schifferli, K., Gold nanoparticle-cytochrome c complexes: the effect of nanoparticle ligand charge on protein structure, *Langmuir*, 21, 12080–12084, **2005**.
- [32] Cabaleiro-Lago, C., Quinlan-Pluck, F., Lynch, I., Lindman, S., Minogue, A.M., Thulin, E., Walsh, D.M., Dawson, K.A., Linse, S., Inhibition of amyloid  $\beta$  protein fibrillation by polymeric nanoparticles, *Journal of the American Chemical Society*, 130, 15437–15443, **2008**.
- [33] Hoshino, Y., Urakami, T., Kodama, T., Koide, H., Oku, N., Okahata, Y., Shea, K.J., Design of synthetic polymer nanoparticles that capture and neutralize a toxic peptide, *Small*, 5, 1562–1568, **2009**.
- [34] Haupt, K., Molecularly imprinted polymers: the next generation, *Analytical Chemistry*, 75, 376A–383A, **2003**.

- [35] Zimmerman, S.C., Lemcoff, N.G., Synthetic hosts via molecular imprinting—are universal synthetic antibodies realistically possible? *Chemical Communications*, 1, 5–14, **2004**.
- [36] Mosbach, K., The promise of molecular imprinting, *Scientific American*, 295, 86, **2006**.
- [37] Saylan, Y., Yılmaz, F., Özgür, E., Derazshamshir, A., Yavuz, H., Denizli, A., Molecularly imprinting of macromolecules for sensors applications, *Sensors*, 17, 898–928, **2017**.
- [38] Piletsky, S.A., Turner W.N., Laitenberger, P., Molecularly imprinted polymers in clinical diagnostics-Future potential and existing problems, *Medical Engineering & Physics*, 28, 971–977, **2006**.
- [39] Ikegami, T., Mukawa, T., Nariai, H., Takeuchi, T., Bisphenol A-recognition polymers prepared by covalent molecular imprinting, *Analytica Chimica Acta*, 504, 131–135, **2004**.
- [40] Arshady, R., Mosbach, K., Synthesis of substrate-selective polymers by host-guest polymerization, *Macromolecular Chemistry and Physics*, 182, 687–692, **1981**.
- [41] Curcio, P., Zandanel, C., Wagner, A., Mioskowski, C., Baati, R., Semi-covalent surface molecular imprinting of polymers by one-stage mini-emulsion polymerization: Glucopyranoside as a model analyte, *Macromolecular Bioscience*, 9, 596–604, **2009**.
- [42] Wu, L.Q., Li, Y.Z., Metal ion-mediated molecular-imprinting polymer for indirect recognition of formate, acetate and propionate, *Analytica Chimica Acta*, 517, 145–151, **2004**.
- [43] Ansell, R.J., Characterization of the binding properties of molecularly imprinted polymers, *Advances in Biochemical Engineering/Biotechnology*, Molecularly Imprinted Polymers in Biotechnology, 150, 51–93, **2015**.
- [44] Algieri, C., Drioli, E., Guzzo, L., Donato, L., Bio-mimetic sensors based on molecularly imprinted membranes, *Sensors*, 14, 13863–13912, **2014**.
- [45] Ye, L., Synthetic strategies in molecular imprinting, *Advances in Biochemical Engineering/Biotechnology*, Molecularly Imprinted Polymers in Biotechnology, 150, 1–24, **2015**.
- [46] Ramstroem, O., Andersson, L.I., Mosbach, K., Recognition sites incorporating both pyridinyl and carboxy functionalities prepared by molecular imprinting, *The Journal of Organic Chemistry*, 58, 7562–7464, **1993**.

- [47] Siemann, M., Andersson, L.I., Mosbach, K., Separation and detection of macrolide antibiotics by HPLC using macrolide-imprinted synthetic polymers as stationary phases, *The Journal of Antibiotics*, 50, 89–91, **1997**.
- [48] Yan, H., Row, K.R., Characteristic and synthetic approach of molecularly imprinted polymer, *International Journal of Molecular Sciences*, 7, 155–178, **2006**.
- [49] Santora, B.P., Gagne, M.R., Moloy, K.G., Radu, N.S., Porogen and cross-linking effects on the surface area, pore volume distribution, and morphology of macroporous polymers obtained by bulk polymerization, *Macromolecules*, 34, 658–661, **2001**.
- [50] Yılmaz, E., *Preparation of Molecular Imprinting Based Lysozyme Sensors*, Doktora Tezi, Hacettepe Üniversitesi Fen Bilimleri Enstitüsü, Ankara, **2007**.
- [51] Asliyuca, S., Uzun, L., Rad, A.Y., Unal, S., Say, R., Denizli, A., Molecular imprinting based composite cryogel membranes for purification of anti-hepatitis B surface antibody by fast protein liquid chromatography, *Journal of Chromatography B*, 889, 95–102, **2012**.
- [52] Tamayo, F.G., Turiel, E., Martín-Esteban, A., Molecularly imprinted polymers for solid-phase extraction and solid-phase microextraction: Recent developments and future trends, *Journal of Chromatography A*, 1152, 32–40, **2007**.
- [53] Kimaro, A., Kelly, L.A., Murray, G.M., Molecularly imprinted ionically permeable membrane for uranyl ion, *Chemical Communications*, 1282–1283, **2001**.
- [54] Hilt, J.Z., Byrne, M.E., Configurational biomimesis in drug delivery: molecular imprinting of biologically significant molecules, *Advanced Drug Delivery Reviews*, 56, 1599–1620, **2004**.
- [55] Haijia, S., Ying, Z., Jia, L., Tianwei, T., Biosorption of Ni<sup>2+</sup> by the surface molecular imprinting adsorbent, *Process Biochemistry*, 41, 1422–1426, **2006**.
- [56] Kubo, A., Shinmori, H., Takeuchi, T., Atrazine-imprinted microspheres prepared using a microfluidic device, *Chemistry letters*, 35, 588–589, **2006**.
- [57] Cieplak, M., Kutner, W., Artificial biosensors: How can molecular imprinting mimic biorecognition? *Trends in Biotechnology*, 34, 922–941, **2016**.
- [58] <http://mipdatabase.com/>, May, **2017**.
- [59] <http://www.sciencedirect.com/science/search>, May, **2017**.
- [60] Goode, J.A., Rushworth, J.V.H., Millner, P.A., Biosensor regeneration: A review of common techniques and outcomes, *Langmuir*, 31, 6267–6276, **2015**.

- [61] Verma, N., Bhardwaj, A., Biosensor technology for pesticides—A review, *Applied Biochemistry Biotechnology*, 175, 3093–3119, **2015**.
- [62] Altintas, Z., Tothill, I., Biomarkers and biosensors for the early diagnosis of lung cancer, *Sensors and Actuators B Chemical*, 188, 988– 998, **2013**.
- [63] Chen, X., Jia, X., Han, J., Ma, J., Ma, Z., Electrochemical immunosensor for simultaneous detection of multiplex cancer biomarkers based on graphene nanocomposites, *Biosensors and Bioelectronics*, 50, 356–361, **2013**.
- [64] Rusling, J.F., Nanomaterials-based electrochemical immunosensors for proteins, *The Chemical Record*, 12,164–176, **2012**.
- [65] Yang, T., Wang, S., Jin, H., Bao, W., Huang, S., Wang, J., An electrochemical impedance sensor for the label-free ultrasensitive detection of interleukin-antigen, *Sensors and Actuators B Chemical*, 178, 310–315, **2013**.
- [66] Yilmaz, E., Majidi, D., Ozgur, E., Denizli, A., Whole cell imprinting based Escherichia coli sensors: A study for SPR and QCM, *Sensors and Actuators B Chemical*, 209, 714–721, **2015**.
- [67] Sener, G., Ozgur, E., Yilmaz, E., Uzun, L., Say, R., Denizli, A., Quartz crystal microbalance based nanosensor for lysozyme detection with lysozyme imprinted nanoparticles, *Biosensors and Bioelectronics*, 26, 815–821, **2010**.
- [68] Suri, C.R., Immunosensors for pesticide monitoring, *Advances in Biosensors, Perspectives in Biosensors*, Elsevier Science, Amsterdam, 5, 161-176, **2003**.
- [69] Sciacca, B., François, A., Hoffmann, P., Monroe, T.M., Multiplexing of radiative-surface plasmon resonance for the detection of gastric cancer biomarkers in a single optical fiber, *Sensors and Actuators B Chemical*, 183, 454–458, **2013**.
- [70] Saylan, Y., Yilmaz, F., Derazshamshir, A., Yilmaz, E., Denizli, A., Synthesis of hydrophobic nanoparticles for real-time lysozyme detection using surface plasmon resonance sensor, *Journal of Molecular Recognition*, e2631, 1–7, **2017**.
- [71] Osman, B., Uzun, L., Beşirli, N., Denizli, A., Microcontact imprinted surface plasmon resonance sensor for myoglobin detection, *Materials Science and Engineering: C*, 33, 3609–3614, **2013**.
- [72] Wood, R.W., On a remarkable case of uneven distribution of light in a diffraction grating spectrum, *Proceedings of the Physical Society of London*, 18, 396–402, **1902**.

- [73] Kretschmann, H.R.E., Radiative decay of non-radiative surface plasmons excited by light, *Zeitschrift für Naturforschung A*, 2135–2136, **1968**.
- [74] Otto, A., Excitation of surface plasma waves in silver by the method of frustrated total reflection, *Zeitschrift für Physik*, 398–410, **1968**.
- [75] Liedberg, B., Nylander, C., Lunström, I., Surface plasmon resonance for gas detection and biosensing, *Sensors and Actuators*, 4, 299–304, **1983**.
- [76] Owen, V., Real-time optical immunosensors—a commercial reality, *Biosensors and Bioelectronics*, 12, i–ii, **1997**.
- [77] Helmerhorst, E., Chandler, D.J., Nussio, M., Mamotte, C.D., Real-time and label-free bio-sensing of molecular interactions by surface plasmon resonance: A laboratory medicine perspective, *Clinical Biochemistry Reviews*, 33, 161–174, **2012**.
- [78] Earp, R.L., Dessy, R.E., Commercial biosensors: applications to clinical, bioprocess, and environmental samples, *Surface Plasmon Resonance*, John Wiley and Sons, New York, 23, 1–27, **1996**.
- [79] Yılmaz, F., Saylan, Y., Akgönüllü, S., Çimen, D., Derazshamshir, A., Bereli, N., Denizli, A., Surface plasmon resonance based nanosensors for detection of triazinic pesticides in agricultural foods, *Nanotechnology in the agri-food industry, New Pesticides and Soil Sensors*, Elsevier, Cambridge, 19, 679–718, **2017**.
- [80] <https://shared-resources.dhvi.duke.edu/dhvi-core-facilities/dhvi-bia-core>, May, **2017**.
- [81] Sun, B., Ni, X., Cao, Y., Cao, G., Electrochemical sensor based on magnetic molecularly imprinted nanoparticles modified magnetic electrode for determination of Hb, *Biosensors and Bioelectronics*, 91, 354–358, **2017**.
- [82] Hongzhi, L., Shoufang, X., Functional monomer-template-QDs sandwich structure for mesoporous structured bovine hemoglobin imprinted ratiometric fluorescence sensor, *Talanta*, 165, 482–488, **2017**.
- [83] Hu, R., Luan, J., Kharasch, E.D., Singamaneni, S., Morrissey, J.J., Aromatic functionality of target proteins influences monomer selection for creating artificial antibodies on plasmonic biosensors, *ACS Applied Materials and Interfaces*, 9, 145–151, **2017**.
- [84] Sun, Y., Du, H., Lan, Y., Wang, W., Liang, Y., Feng, C., Yang, M., Preparation of hemoglobin (Hb) imprinted polymer by Hb catalyzed eATRP and its application in biosensor, *Biosensors and Bioelectronics*, 77, 894–900, **2016**.

- [85] Li, H., Wei, X., Zhang, Y., Xu, Y., Lu, K., Li, C., Yan, Y., Rapid and sensitive detection of hemoglobin with gold nanoparticles based fluorescence sensor in aqueous solution, *Journal of Alloys and Compounds*, 685, 820–827, **2016**.
- [86] Sun, Y., Lan, Y., Yang, L., Kong, F., Du, H., Feng, C., Preparation of hemoglobin imprinted polymers based on graphene and protein removal assisted by electric potential, *RSC Advances*, 6, 61897–61906, **2016**.
- [87] Yu, Y., Zhang, Q., Chang, C.C., Liu, Y., Yang, Z., Guo, Y., Wang, Y., Galanakis, D.K., Levon, K., Rafailovich, M., Design of a molecular imprinting biosensor with multi-scale roughness for detection across a broad spectrum of biomolecules, *Analyst*, 141, 5607–5618, **2016**.
- [88] Luan, J., Liu, K.K., Tadepalli, S., Jiang, Q., Morrissey, J.J., Kharasch, E.D., Singamaneni, S., PEGylated artificial antibodies: Plasmonic biosensors with improved selectivity, *ACS Applied and Materials Interfaces*, 8, 23509–23516, **2016**.
- [89] Duan, H., Wang, X., Wang, Y., Li, J., Luo, C., Bioreceptor multi-walled carbonnanotubes@Fe<sub>3</sub>O<sub>4</sub>@SiO<sub>2</sub>–surface molecular imprinted polymer in an ultrasensitive chemiluminescent biosensor for bovine hemoglobin, *RSC Advances*, 5, 88492–88500, **2015**.
- [90] Li, L., Fan, L., Dai, Y., Kan, X., Recognition and determination of bovine hemoglobin using a gold electrode modified with gold nanoparticles and molecularly imprinted self-polymerized dopamine, *Microchimica Acta*, 182, 2477–2483, **2015**.
- [91] Zhang, R., Xu, S., Luo, J., Liu, X., Molecularly imprinted photo-sensitive polyglutamic acid nanoparticles for electrochemical sensing of hemoglobin, *Microchimica Acta*, 182, 175–183, **2015**.
- [92] Wang, Z., Li, F., Xia, J., Xia, L., Zhang, F., Bi, S., Shi, G., Xia, Y., Liu, J., Li, Y., Xia, L., An ionic liquid-modified graphene based molecular imprinting electrochemical sensor for sensitive detection of bovine hemoglobin, *Biosensors and Bioelectronics*, 61, 391–396, **2014**.
- [93] Sun, S., Chen, L., Shi, H., Li, Y., He, X., Magnetic glass carbon electrode, modified with magnetic ferriferous oxide nanoparticles coated with molecularly imprinted polymer films for electrochemical determination of bovine hemoglobin, *Journal of Electroanalytical Chemistry*, 734, 18–24, **2014**.
- [94] Luo, J., Jiang, S., Liu, X., Electrochemical sensor for bovine hemoglobin based on a novel graphene-molecular imprinted polymers composite as recognition element, *Sensors and Actuators B Chemical*, 203, 782–789, **2014**.

- [95] Yang, W., Qingwen, Z., Yamin, R., Lijing, J., Tianxin, W., Molecularly imprinted polymer thin film based surface plasmon resonance sensor to detect hemoglobin, *Chemical Research in Chinese Universities*, 30, 42–48, **2014**.
- [96] Zhou, J., Gana, N., Hub, F., Li, T., Zhou, H., Li, X., Zheng, L., A single antibody sandwich electrochemiluminescence immunosensor based on protein magnetic molecularly imprinted polymers mimicking capture probes, *Sensors and Actuators B Chemical*, 186, 300–307, **2013**.
- [97] Tan, L., Kang, C., Xu, S., Tang, Y., Selective room temperature phosphorescence sensing of target protein using Mn-doped ZnS QDs-embedded molecularly imprinted polymer, *Biosensors and Bioelectronics*, 48, 216–223, **2013**.
- [98] Li, Y., Li, Y., Hong, M., Bin, Q., Lin, Z., Lin, Z., Cai, Z., Chen, G., Highly sensitive protein molecularly imprinted electro-chemical sensor based on gold microdendrites electrode and prussian blue mediated amplification, *Biosensors and Bioelectronics*, 42, 612–617, **2013**.
- [99] Li, D.Y., He, X.W., Chen, Y., Li, W.Y., Zhang, Y.K., Novel hybrid structure silica/CdTe/molecularly imprinted polymer: Synthesis, specific recognition, and quantitative fluorescence detection of bovine hemoglobin, *ACS Applied and Materials Interfaces*, 5, 12609–12616, **2013**.
- [100] Prasad, B.B., Prasad, A., Prasad Tiwari, M., Quantum dots-multiwalled carbon nanotubes nanoconjugate-modified pencil graphite electrode for ultratrace analysis of hemoglobin in dilute human blood samples, *Talanta*, 109, 52–60, **2013**.
- [101] Gravesen, P., Branbjerg, J., Jensen, O.S., Microfluidics-a review, *Journal of Micromechanics and Microengineering*, 3, 168, **1993**.
- [102] Terry, S.C., Jerman, J.H., Angell, J.B., A gas chromatographic air analyzer fabricated on a silicon wafer, *IEEE Transactions on Electron Devices*, 26, 1880–1886, **1979**.
- [103] Petersen, K.E., Fabrication of an integrated, planar silicon ink-jet structure, *IEEE Transactions on Electron Devices*, 26, 1918–1920, **1979**.
- [104] Manz, A., Graber, N., Widmer, H.M., Miniaturized total chemical analysis systems: A novel concept for chemical sensing, *Sensors and Actuators B Chemical*, 1, 244–248, **1990**.
- [105] Kumar, S., Kumar, S., Ali, A., Anand, P., Agrawal, V.V., John, R., Maji, S., Malhotra, B.D., Microfluidic-Integrated Biosensors: Prospects for Point-of-Care Diagnostics, *Biotechnology Journal*, 8, 1267–1279, **2013**.

- [106] Tabeling, P., An introduction to microfabrication, *Introduction to Microfluidics*, Oxford University Press, 244–280, **2005**.
- [107] Craciun, G., Ighigeanu, D., Manaila, E., Stelescu, M.D., Synthesis and characterization of poly(acrylamide-co-acrylic acid) flocculant obtained by electron beam irradiation, *Materials Research*, 18, 984–993, **2015**.
- [108] Mariani, S., Minunni, M., Surface plasmon resonance applications in clinical analysis, *Analytical and Bioanalytical Chemistry*, 406, 2303–2323, **2014**.
- [109] Sener, G., Uzun, L., Say, R., Denizli, A., Use of molecular imprinted nanoparticles as biorecognition element on surface plasmon resonance sensor, *Sensors and Actuators B Chemical*, 160, 791–799, **2011**.
- [110] Lin, L.P., Huang, L.S., Lin, C.W., Lee, C.K., Chen, J.L., Hsu, S.M., Lin, S., Determination of binding constant of DNA-binding drug to target DNA by surface plasmon resonance biosensor technology, *Current Drug Target*, 5, 61–72, **2005**.
- [111] Li, X., Husson, S.M., Adsorption of dansylated amino acids on molecularly imprinted surfaces: A surface plasmon resonance study, *Biosensors and Bioelectronics*, 22, 336–348, **2006**.
- [112] Wei, X., Samadi, A., Husson, S.M., Synthesis and characterization of molecularly imprinted polymers for chromatographic separations, *Separation Science and Technology*, 40, 109–129, **2005**.
- [113] Krishnamoorthy, G., Carlen, E.T., Van Der Berg, A., Scafsfoot, R.B.M., Surface plasmon resonance imaging based multiplex biosensor: Integration of biomolecular screening detection and kinetics estimation, *Sensors and Actuators B Chemical*, 148, 511–521, **2010**.
- [114] Saylan, Y., Akgönüllü, S., Çimen, D., Derazshamshir, A., Bereli, N., Yılmaz, F., Denizli, A., Development of surface plasmon resonance sensors based on molecularly imprinted nanofilms for sensitive and selective detection of pesticides, *Sensors and Actuators B Chemical*, 241, 446–454, **2017**.
- [115] Umpleby, R.J., Baxter, S.C., Chen, Y., Shah, R.N., Shimizu, K.D., Characterization of molecularly imprinted polymers with the Langmuir-Freundlich isotherm, *Analytical Chemistry*, 73, 4584–4591, **2001**.
- [116] Li, W., Sun, Y., Yang, C., Yan, X., Guo, H., Fu, G., Fabrication of surface protein-imprinted nanoparticles using a metal chelating monomer via aqueous precipitation polymerization, *ACS Applied Materials and Interfaces*, 7, 27188–27196, **2015**.



- [117] Yang, Y., Long, Y., Li, Z., Li, N., Li, K., Liu, F., Real-time molecular recognition between protein and photosensitizer of photodynamic therapy by quartz crystal microbalance sensor, *Analytical Biochemistry*, 392, 22–27, **2009**.
- [118] Tatikonda, A.K., Tkachev, M., Naaman, R., A highly sensitive hybrid organic–inorganic sensor for continuous monitoring of hemoglobin, *Biosensors and Bioelectronics*, 45, 201–205, **2013**.
- [119] Briand, A.V., Thilakarathne, V., Kasi, R.M., Kumar, C.V., Novel surface plasmon resonance sensor for the detection of heme at biological levels via highly selective recognition by apo-hemoglobin, *Talanta*, 99, 113–118, **2012**.
- [120] Wang, Y., Zhou, Y., Sokolov, J., Rigas, B., Levon, K., Rafailovich, M., A potentiometric protein sensor built with surface molecular imprinting method, *Biosensors and Bioelectronics*, 24, 162–166, **2008**.

## 7. CURRICULUM VITAE

### Credentials

Name, Surname : Yeşeren Saylan  
Place of Birth : Ordu  
Marital Status : Single  
E-mail : yeseren@hacettepe.edu.tr  
Address : Hacettepe University, Department of Chemistry, 06800, Çankaya,  
Ankara, Turkey

### Education

B.Sc. : 2003-2008, Hacettepe University, Department of Chemistry, Ankara,  
Turkey  
M.Sc. : 2008-2011, Hacettepe University, Department of Chemistry, Ankara,  
Turkey  
Ph.D. : 2012-2017, Hacettepe University, Department of Chemistry, Ankara,  
Turkey

### Foreign Languages

English : Advanced  
German : Intermediate

### Work Experience

Hacettepe University, Department of Chemistry, Ankara, Turkey, 2010-Continue.  
Stanford University, School of Medicine, Palo Alto, California, US, 2015-2016.

## **Areas of Experiences**

Biosensor, microfluidic, protein detection, surface plasmon resonance.

## **Projects and Budes**

-

## **Publications**

Molecularly Imprinted Plasmonic Biosensors for Hemoglobin Detection, 30 October-2 November 2016, IEEE Sensors, Orlando, Florida, US.

## **Oral and Poster Presentation**

Preparation and Characterization of Surface Plasmon Resonance Based Molecularly Imprinted Biosensors for Detection of Hemoglobin, Turkey, 10-12 June 2015, 2<sup>nd</sup> International Congress on Biosensors, İzmir, Turkey. (Poster)



HACETTEPE UNIVERSITY  
GRADUATE SCHOOL OF SCIENCE AND ENGINEERING  
THESIS/DISSERTATION ORIGINALITY REPORT

HACETTEPE UNIVERSITY  
GRADUATE SCHOOL OF SCIENCE AND ENGINEERING  
TO THE DEPARTMENT OF CHEMISTRY

Date: 20/06/2017

Thesis Title / Topic: Preparation of Hemoglobin Imprinted Surface Plasmon Resonance Biosensors

According to the originality report obtained by myself/my thesis advisor by using the *Turnitin* plagiarism detection software and by applying the filtering options stated below on 20/06/2017 for the total of 90 pages including the a) Title Page, b) Introduction, c) Main Chapters, d) Conclusion sections of my thesis entitled as above, the similarity index of my thesis is 9 %.

Filtering options applied:

1. Bibliography/Works Cited excluded
2. Quotes excluded / ~~included~~
3. Match size up to 5 words excluded

I declare that I have carefully read Hacettepe University Graduate School of Science and Engineering Guidelines for Obtaining and Using Thesis Originality Reports; that according to the maximum similarity index values specified in the Guidelines, my thesis does not include any form of plagiarism; that in any future detection of possible infringement of the regulations I accept all legal responsibility; and that all the information I have provided is correct to the best of my knowledge.

I respectfully submit this for approval.

20.06.2017  
Date and Signature

Name Surname: Yeşeren Saylan

Student No: N11246454


Department: Chemistry

Program: Biochemistry

Status:  Masters  Ph.D.  Integrated Ph.D.

**ADVISOR APPROVAL**

APPROVED.

  
(Prof. Dr. Adil Denizli)